Amanda Stefanie Jabur de Assis

ENHANCING ABIOTIC STRESS RESILIENCE IN *ERUCA SATIVA*: THE SYNERGISTIC ROLE OF EXTREMOPHILIC MICROBIAL INOCULANTS AND CRYSTALLINE ZINC OXIDE

Sorocaba

2026

Amanda Stefanie Jabur de Assis

ENHANCING ABIOTIC STRESS RESILIENCE IN *ERUCA SATIVA*: THE SYNERGISTIC ROLE OF EXTREMOPHILIC MICROBIAL INOCULANTS AND CRYSTALLINE ZINC OXIDE

Tese apresentada ao Programa de Pós-Graduação em Biotecnologia e Monitoramento Ambiental como requisito para a obtenção do título de Doutora em Biotecnologia e Monitoramento Ambiental.

Orientação Prof.ª Dr.ª Iolanda Cristina Silveira Duarte

Financiamento: Coordenação de Aperfeiçoamento de Pessoal de Nível Superior - CAPES

Sorocaba

2026

de Assis, Amanda Stefanie Jabur

Enhancing abiotic stress resilience in Eruca sativa: the synegistic role of extremophilic microbial inoculants and crystalline zinc oxide / Amanda Stefanie Jabur de Assis -- 2026.
108f.

Tese de Doutorado - Universidade Federal de São Carlos, campus Sorocaba, Sorocaba
Orientador (a): Iolanda Cristina Silveira Duarte
Banca Examinadora: Giovanni Pimenta Mambrini, Paula Juliane Barbosa de Oliveira, Paulo José de Sousa Maia, Renata Fracácio Francisco
Bibliografia

1. Microbial seed priming. 2. Abiotic stress. 3. Zinc Oxide. I. de Assis, Amanda Stefanie Jabur. II. Título.

Ficha catalográfica desenvolvida pela Secretaria Geral de Informática (SIn)

DADOS FORNECIDOS PELO AUTOR

Bibliotecário responsável: Maria Aparecida de Lourdes Mariano - CRB/8 6979

UNIVERSIDADE FEDERAL DE SÃO CARLOS

Centro de Ciências e Tecnologias Para a Sustentabilidade
Programa de Pós-Graduação em Biotecnologia e Monitoramento Ambiental

COMPROVANTE DE DEFESA

A Comissão de Pós-Graduação do Programa de Pós-Graduação em Biotecnologia e Monitoramento Ambiental, da Universidade Federal de São Carlos, declara, por meio deste, a realização da seguinte Defesa de Doutorado:

Candidata: Amanda Stefanie Jabur de Assis

Título do Trabalho: ENHANCING ABIOTIC STRESS RESILIENCE IN ERUCA SATIVA: THE SYNERGISTIC ROLE OF EXTREMOPHILIC MICROBIAL INOCULANTS AND CRYSTALLINE ZINC OXIDE

Dia: 20/02/2026
Horário: 14:00
Local: Sorocaba, SP

Banca Examinadora:

Iolanda Cristina Silveira Duarte, presidente titular interno, UFSCar - Universidade Federal de São Carlos, presencialmente, Aprovou o candidato

Giovanni Pimenta Mambrini, membro titular interno, UFSCar - Universidade Federal de São Carlos, presencialmente, Aprovou o candidato

Paulo José de Sousa Maia, membro titular interno, UFSCar - Universidade Federal de São Carlos, presencialmente, Aprovou o candidato

Renata Fracácio Francisco, membro titular externo, UNESP - Universidade Estadual Paulista Júlio de Mesquita Filho, presencialmente, Aprovou o candidato

Paula Juliane Barbosa de Oliveira, membro titular externo, Compostec - Compostec Soluções Agroambientais Ltda, a distância, Aprovou o candidato

Resultado Final: Aprovado

Título Definitivo do Trabalho: ENHANCING ABIOTIC STRESS RESILIENCE IN ERUCA SATIVA: THE SYNERGISTIC ROLE OF EXTREMOPHILIC MICROBIAL INOCULANTS AND CRYSTALLINE ZINC OXIDE

Obs: o resultado da defesa ainda não foi homologado pela CPG do PPG.

O(a) candidato(a) só fará jus ao título de mestre(a)/doutor(a), quando o diploma estiver em fase de emissão. O documento apto para comprovar a obtenção de título acadêmico é o Diploma ou o Certificado de Conclusão de Curso (enquanto o diploma estiver em fase de emissão).

AGRADECIMENTOS

Agradeço, primeiramente, a Deus, que esteve comigo em cada passo desta caminhada, sustentando-me nos momentos difíceis e celebrando comigo cada conquista, assim como todos aqueles entes queridos que hoje estão junto dele e que, de alguma forma, continuam presentes em minha vida.

Aos meus pais, deixo minha eterna gratidão por todo o suporte financeiro, psicológico e físico, por acreditarem em mim sempre, e por tornarem possível, até mesmo com as próprias mãos, a construção da estufa que viabilizou este trabalho.

À minha irmã, Juliana, agradeço por compartilhar comigo seus conhecimentos na área agronômica, contribuindo de forma essencial para o desenvolvimento desta pesquisa.

Ao meu parceiro de vida, Guilherme, agradeço por todo o apoio emocional e profissional, pela compreensão nos dias longos e difíceis, por me encorajar a seguir em frente e por caminhar ao meu lado em cada etapa dessa jornada.

À minha orientadora, Iolanda, minha profunda admiração e gratidão por me acompanhar desde o mestrado, por acolher minhas infinitas ideias, por sua dedicação, generosidade e por ser uma fonte constante de inspiração acadêmica e pessoal.

Aos meus amigos e amigas que estiveram comigo ao longo desses anos — Maria, Liliane, Beatriz, Giovanni Miraveti e, em especial, a Juliana — agradeço pela amizade, pelo companheirismo e pela parceria no laboratório, que tornaram essa trajetória mais leve e significativa.

Por fim, agradeço a todos aqueles que, direta ou indiretamente, contribuíram para que este sonho se tornasse realidade. Cada gesto, palavra de incentivo e ajuda oferecida foi fundamental para a conclusão deste trabalho.

RESUMO

ASSIS, Amanda Stefanie Jabur de. Enhancing abiotic stress resilience in eruca sativa: the synergistic role of extremophilic microbial inoculants and crystalline zinc oxide. 2026. Tese (Doutorado em Biotecnologia e Monitoramento Ambiental) – Universidade Federal de São Carlos, Sorocaba, 2026.

Estresses abióticos como salinidade, déficit hídrico e elevada radiação solar constituem importantes limitações para o estabelecimento de plantas e a produtividade agrícola. Micro-organismos extremófilos, adaptados a ambientes severos, apresentam características fisiológicas que podem ser exploradas para a mitigação desses estresses em plantas. Esta tese investiga o potencial de microrganismos extremófilos isolados de painéis fotovoltaicos em melhorar o desempenho vegetal de plântulas de rúcula (*Eruca sativa*) sob estresse abiótico, com ênfase na interação desses micro-organismos com óxido de zinco (ZnO) cristalino. Inicialmente, foi avaliada a resistência à radiação ultravioleta de isolados bacterianos e leveduras provenientes de painéis fotovoltaicos, evidenciando perfis contrastantes de tolerância, com destaque para *Rhodotorula mucilaginosa* como altamente resistente à radiação UV. Em seguida, cepas com melhores desempenhos foram aplicadas a sementes de *Eruca sativa* para avaliar seus efeitos sobre a porcentagem e a velocidade de germinação sob estresse salino e osmótico, na presença ou ausência de ZnO. Por fim, foram analisados os efeitos da inoculação microbiana de *Arthrobacter koreensis* e de ZnO sobre o crescimento de plântulas e as respostas aos estresses abióticos (comprimentos, alocação de biomassa, área foliar). Os resultados demonstram que microrganismos extremófilos podem melhorar a germinação e o desempenho de plântulas sob estresse abiótico de forma dependente da cepa e do contexto ambiental. A suplementação com ZnO ampliou consistentemente os efeitos microbianos, especialmente sob condições de estresse severo. Em vez de promover crescimento uniforme, a inoculação microbiana contribuiu para maior estabilidade do crescimento e tolerância ao estresse. Este trabalho destaca o potencial da combinação de microrganismos extremófilos e cofatores inorgânicos como uma estratégia sustentável para melhorar o estabelecimento de plantas em ambientes agrícolas sujeitos a estresses ambientais.

Palavras-chave: condicionamento microbiano, óxido de zinco, *Eruca sativa*

ABSTRACT

ASSIS, Amanda Stefanie Jabur de. Enhancing abiotic stress resilience in eruca sativa: the synergistic role of extremophilic microbial inoculants and crystalline zinc oxide. 2026. Tese (PhD in Biotechnology and Environmental Monitoring) – Universidade Federal de São Carlos, Sorocaba, 2026.

Abiotic stresses such as salinity, water deficit, and high solar radiation constitute important limitations for plant establishment and agricultural productivity. Extremophilic microorganisms, adapted to harsh environments, have physiological characteristics that can be exploited to mitigate these stresses in plants. This thesis investigates the potential of extremophilic microorganisms isolated from photovoltaic panels to improve the plant performance of arugula (*Eruca sativa*) seedlings under abiotic stress, with emphasis on the interaction of these microorganisms with crystalline zinc oxide (ZnO). Initially, the ultraviolet radiation resistance of bacterial and yeast isolates from photovoltaic panels was evaluated, showing contrasting tolerance profiles, with *Rhodotorula mucilaginosa* standing out as highly resistant to UV radiation. Next, strains with better performance were applied to Eruca sativa seeds to evaluate their effects on the percentage and speed of germination under saline and osmotic stress, in the presence or absence of ZnO. Finally, the effects of microbial inoculation with *Arthrobacter koreensis* and ZnO on seedling growth and responses to abiotic stresses (lengths, biomass allocation, leaf area) were analyzed. The results demonstrate that extremophilic microorganisms can improve germination and seedling performance under abiotic stress in a strain- and environmental context-dependent manner. Supplementation with ZnO consistently amplified the microbial effects, especially under severe stress conditions. Instead of promoting uniform growth, microbial inoculation contributed to greater growth stability and stress tolerance. This work highlights the potential of combining extremophilic microorganisms and inorganic cofactors as a sustainable strategy to improve plant establishment in agricultural environments subject to environmental stresses.

Keywords: microbial priming, zinc oxide, *Eruca sativa*

SUMÁRIO

1 INTRODUCTION

Context and Motivation

Agricultural productivity is increasingly constrained by abiotic stresses associated with global climate change, land degradation, and the expansion of cultivation into marginal environments (Kajla et al. 2015; Pereira 2016). Among these stressors, salinity, water deficit, and excessive solar radiation represent major limitations to seed germination, early seedling establishment, and plant growth, directly affecting crop performance and yield stability. These challenges are particularly relevant during the initial stages of plant development, when seeds and seedlings exhibit high physiological sensitivity to environmental fluctuations (Jovović et al. 2018; Garbeles et al. 2024; Nowicki et al. 2025).

Conventional strategies to mitigate abiotic stress in agriculture—such as chemical fertilizers and irrigation management—often present economic, environmental, or logistical limitations. Consequently, there is a growing demand for sustainable and biologically based approaches capable of enhancing plant resilience under adverse conditions (Cushman et al. 2022; Teiba et al. 2024; Okon 2025). In this context, plant growth-promoting microorganisms (PGPMs) and inorganic biostimulants have emerged as promising alternatives, offering environmentally friendly solutions that can improve stress tolerance while reducing chemical inputs.

Microorganisms adapted to extreme environments constitute a particularly attractive but still underexplored biological resource. Extremophilic and extremotolerant microorganisms have evolved robust physiological and molecular mechanisms to cope with intense radiation, desiccation, thermal fluctuations, and oxidative stress (Angelakis et al. 2024; Marzban and Tesei 2025). These adaptive traits—such as efficient DNA repair systems, antioxidant production, extracellular polymeric substance (EPS) synthesis, and pigment accumulation—are directly relevant to plant stress mitigation, especially during early developmental stages (Moura et al. 2021; Yarzábal Rodríguez et al. 2024; Gloster and Toksoy Öner 2025).

Photovoltaic panels represent artificial extreme environments characterized by continuous exposure to high solar radiation, pronounced temperature oscillations, and limited water availability (Porcar et al. 2018; Tanner et al. 2020). Recent studies have demonstrated that these surfaces host diverse microbial communities dominated by extremophilic taxa, resembling those

found in desert and high-irradiance ecosystems (Dorado-Morales et al. 2016; Moura et al. 2021). However, despite increasing ecological interest, the biotechnological potential of microorganisms isolated from photovoltaic panels remains largely unexplored, particularly in agricultural applications.

Simultaneously, advances in nanotechnology have introduced inorganic materials such as zinc oxide (ZnO) as potential tools for improving plant stress tolerance (Singh et al. 2022; Wang et al. 2023). Zinc is an essential micronutrient involved in antioxidant defense, membrane stability, and enzyme activation. ZnO materials, especially when applied during seed priming, can modulate oxidative balance and enhance early plant vigor under salinity and drought stress (Mazhar et al. 2022; El-Shazoly et al. 2025; Kumar et al. 2025). Nevertheless, the interaction between ZnO materials and beneficial microorganisms, as well as their combined effects under multiple abiotic stresses, remains insufficiently understood.

Within this framework, the present thesis investigates the hypothesis that extremophilic microorganisms isolated from photovoltaic panels can function as effective biostimulants for plants exposed to abiotic stress, particularly when combined with crystalline zinc oxide. By adopting a stepwise experimental approach—from microbial UV resistance to seed germination and early seedling growth—this work aims to elucidate how microbial origin, stress intensity, radiation exposure, and inorganic cofactors interact to shape plant performance.

2 ARTIGO 1

UV Resistance of Microbes from Photovoltaic Panels

ABSTRACT

Photovoltaic panels represent extreme microbial habitats characterized by intense UV radiation, temperatures fluctuations and limited moisture. These selective pressures tend to favor radiation and desiccation-tolerant microorganisms similar to those from desert and high-altitude ecosystems. In this study, we evaluated the tolerance of bacterial and yeast strains isolated from photovoltaic panels in Sorocaba, Brazil, to UV-C and environmental UV radiation, representing to our knowledge, the first exhibited distinct survival profiles. The yeast *Rhodotorula mucilaginosa* (PSR 34) showed the highest tolerance, surviving UV-C exposures up to 600 J/m², with a survival rate of approximately 85% at this dose, likely due to protective pigmentation. In contrast, bacterial isolates like *Microbacterium hydrothermale* and *Arthrobacter koreensis* exhibited limited UV-C tolerance, with survival rates dropping below 20% at doses above 280 J/m². Other bacterial strains showed moderate resilience under environmental conditions, maintaining viability up to 400 kJ/m² with a 50-60% survival rate. These findings highlight the diversity of microbial strategies for coping with high-irradiance environments and provide a basis for exploring UV-resistant strains as potential biotechnological tools, particularly in agricultural systems subjected to elevated solar radiation.

Keywords: UV resistance, photovoltaic panels, extremophiles, photoprotection.

2.1 INTRODUCTION

The surfaces of photovoltaic panels, continuously exposed to intense solar irradiation, pronounce temperature fluctuations and limited water availability (Tanner et al. 2020; Moura et al. 2021). These physicochemical constraints resemble those found in desert and high-altitude ecosystems and impose strong selective pressures that favor microorganisms equipped with mechanism for radiation and desiccation tolerance. Previous studies consistently report the predominance of genera such *Hymenobacter*, *Deinococcus* and *Sphingomonas* on photovoltaic panels across diverse climatic regions, suggesting convergent biochemical strategies, including the synthesis of carotenoid pigments, efficient DNA repair systems and biofilm formation, with

mitigate oxidative damage and enhance persistence on sun-exposed surfaces (Dorado-Morales et al. 2016; Tanner et al. 2018; Tanner et al. 2019).

Beyond their ecological relevance, UV-resistant microorganisms have increasingly attracted interest for biotechnological applications. In agriculture systems, intense sunlight and UV exposure can limit the survival of beneficial microbes used for plant promotion. Microorganisms capable of withstanding high irradiance may offer advantages by persisting on leaf and soil surfaces and contributing to plant development though phytohormone production, nutrient mobilization, pathogens suppression or other plant-beneficial traits (Blake et al. 2021; Prisa et al. 2023). Their ability tolerance UV radiation may therefore broaden the applicability of microbial inoculants in environments where solar intensity is a major abiotic stress (Chandran et al. 2020; Ajijah et al. 2023).

Moura et al. (2021) previously isolated a diverse set of bacterial and yeast strains from photovoltaic panels in southeastern Brazil, identifying several taxa with putative UV-resistant characteristics. The strains included organisms such as *Microbacterium hydrotermale, Rhodotorula mucilaginosa, Arthrobacter koreensis, Gordonia sp.* and *Kocuria sp.*, highlighting a rich microbial diversity on the panels. The objective of the present study was to evaluate the tolerance of some of these microbial isolates to UV-C and environmental UV radiation by assessing their survival thresholds under controlled exposures. According to our best knowledge, this research is the first to examine irradiation tolerance in microorganisms isolated from photovoltaic panels, marking a novel step in understanding how they respond to varied radiation stresses. This initial research establishes a foundation for further biotechnological exploration, as the potential applications of these UV-resistant microorganisms in agriculture will be tested in subsequent experiments by our research group, including applications in promoting plant growth and supporting seed germination.

2.2 EXPERIMENTAL PROCEDURES

Isolation and Identification

Microorganisms were isolated from seven photovoltaic modules (PSR) located in Sorocaba, southeastern Brazil (-23°28'55", -47°22'19.9") sampled during the winter season, as previously described by Moura et al. (2021). The sampling site is characterized by a tropical climate and during the collection period, the average ambient temperature was 19 °C with relative humidity of

72%, while the panel surface temperature reached an average of 43 °C. Solar irradiance on the panels was measured at 311.5 W/m². Isolates were obtained by swabbing the panel surfaces and plating on varying culture media. Taxonomic identification was performed via 16S rRNA sequencing for bacteria and ITS sequencing for yeasts. The strains selected for this study represent the dominant genera found on the panels: *Microbacterium hydrothermale* (PSR 33), *Rhodotorula mucilaginosa* (PSR 34), *Arthrobacter koreensis* (PSR 37), *Gordonia* sp. (PSR 46), and *Kocuria* sp. (PSR 51).

Inoculum Preparation

Bacterial strains were cultivated in liquid Brain Heart Infusion (BHI) medium (pH 7.4) at 30 ± 0.5 °C with agitation at 150 rpm for 48 hours. The yeast strain *R. mucilaginosa* was grown in liquid YPD medium (pH 6.5) at 25 ± 0.5 °C under identical agitation conditions. Cells were harvested by centrifugation when cultures reached the stationary phase (Optical Density at 600 nm [OD600] ≈ 1.0 abs) and washed twice with sterile 0.85% (w/v) NaCl solution to remove residual medium. Pellets were resuspended in saline to a standardized density of OD600 ~1.0 abs (10^8 CFU/mL) prior to irradiation.

UV-C and Environmental-UV Irradiation Setup

For irradiation assays, 10 µL aliquots of serial dilutions (ranging from 10^{-1} to 10^{-5}) were spotted onto Tryptic Soy Agar (TSA) for bacteria and Sabouraud-Dextrose Agar for yeast. Petri dish lids were removed during all irradiation procedures to prevent UV filtering and ensure accurate dosimetry.

UV-C Exposure

Irradiation was performed in a laminar flow hood equipped with a Philips TUV-20W lamp (emission peak at 254 nm). The distance between the lamp source and the agar surface was fixed at 30 cm. Irradiance was calibrated using a Vilber Lourmat RMX-3W radiometer with a UV-C photocell (CX-254), resulting in a flux of 0.1208 W/m². Doses ranged from 0 to 600 J/m².

Simulated Environmental-UV

Plates were exposed to a broad-spectrum source (Vilber Lourmat simulator) emitting 85.7% UV-A and 11% UV-B. The irradiance at the plate surface was inferred as 51.47 W/m² for UV-A and 35.55 W/m² for UV-B using specific photocells (CX-365 and CX-312). Doses ranged from 0

to 400 kJ/m². Temperature was maintained at 25 °C to decouple thermal stress from radiation effects.

Experimental Design and Statistical Analysis

All experiments were performed with three independent biological replicates (separate cultures) and two technical replicates per dilution. After incubation, plates yielding 30–300 colonies were counted. The concentration of viable cells (CFU/mL) was calculated considering the aliquot volume and dilution factor. Survival fractions were determined as the ratio between the CFU/mL of the irradiated samples and the mean CFU/mL of the non-irradiated control (dose 0), following the methodology described by (Pulschen et al. 2015). Data were log-transformed to meet normality assumptions and analyzed using one-way ANOVA, followed by Tukey's post hoc test, to compare survival differences among isolates at the maximum radiation doses. Differences were considered statistically significant at $p < 0.05$.

Data were analyzed using custom scripts written in Python. The assumption of normality was verified prior to analysis. Differences between groups were evaluated using one-way ANOVA implemented in the SciPy library, followed by Tukey's HSD post-hoc test using the Statsmodels library. All figures were plotted using Seaborn and Matplotlib software 3.10.7.

2.3 RESULTS

UV-C Tolerance of Microbial Isolates

The microbial isolates exhibited significantly different tolerance profiles to UV-C radiation at the discriminative dose of 280 J/m² (ANOVA, $F = 399.17$; $p < 0.001$; Supplementary Tables S1 and S2). The yeast strain *R. mucilaginosa* (PSR 34) demonstrated superior resistance compared to all bacterial isolates. While the yeast maintained high viability, the bacterial strains *M. hydrothermale* (PSR 33) and *A. koreensis* (PSR 37) showed a sharp decline, with survival fractions significantly lower than the yeast (Tukey's HSD, $p < 0.001$). *Kocuria* sp. (PSR 51) and *Gordonia* sp. (PSR 46) displayed intermediate tolerance but were still significantly more sensitive than the yeast isolate (Fig. 1).

Figure 1. Survival curves of microbial isolates exposed to increasing doses of UV-C radiation (254 nm). Data represents the mean of three independent biological replicates ± standard deviation (SD). Statistical analysis (ANOVA followed by Tukey's test) was performed at the dose of 280 J/m².

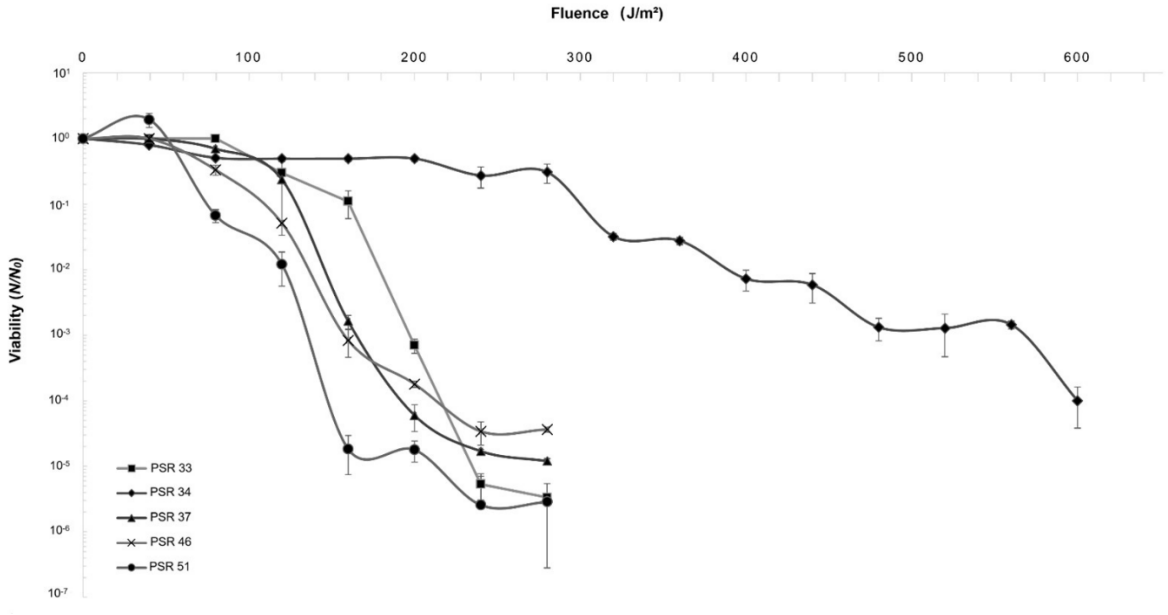

Environmental-UV Tolerance

Under simulated solar conditions (UV-A + UV-B), the difference in survival strategies was further accentuated. At the maximum cumulative dose of 400 kJ/m², statistical analysis revealed significant variation among the isolates ($p < 0.001$; Supplementary Tables S3 and S4). *R. mucilaginosa* (PSR 34) remained highly resilient, showing no significant loss of viability (survival > 80%). In contrast, *M. hydrothermale* and *A. koreensis* experienced a reduction in viability of over 3 log units (survival < 0.1%). The Gram-positive bacteria *Kocuria* sp. and *Gordonia* sp. maintained moderate viability (50–60% survival), statistically distinct from both the sensitive bacteria and the highly resistant yeast (Fig. 2).

Figure 2. Survival profiles of microbial isolates under simulated Ambient-UV radiation (UV-A + UV-B). Note the dose scale in kJ/m². Data represent mean ± SD of three biological replicates.

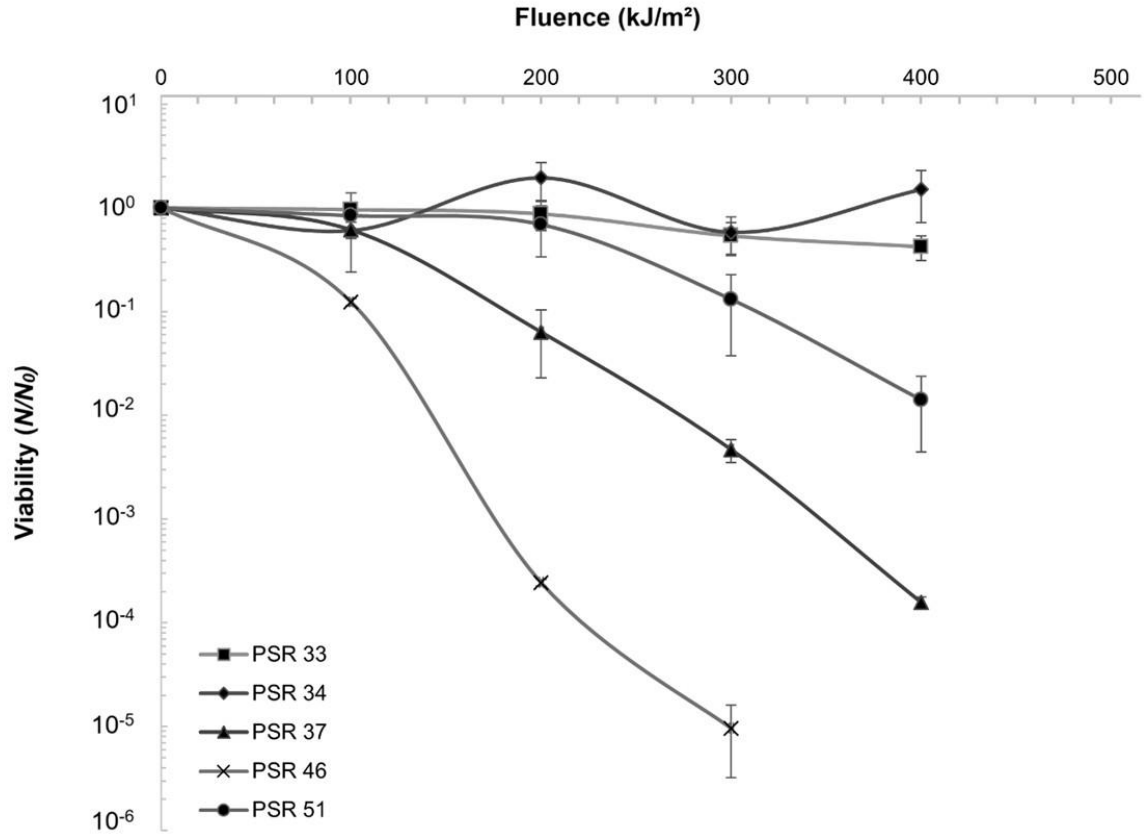

2.4 DISCUSSION

Mechanisms of Yeast Resistance

The superior tolerance of *R. mucilaginosa* (PSR 34) to both UV-C and broad-spectrum environmental-UV ($p < 0.001$) is likely attributable to intrinsic cellular defenses, particularly pigmentation. This strain exhibits distinct pink coloration, characteristic of carotenoid production (e.g., torularhodin and beta-carotene) within the genus *Rhodotorula*. As reported for extremophilic yeasts from high-altitude and high-irradiance environments, carotenoids act as potent antioxidants by quenching singlet oxygen and other reactive oxygen species generated by UV exposure, thereby mitigating oxidative damage to DNA and membrane lipids (Libkind et al. 2009; Moliné et al. 2010; Maldonade et al. 2012; Tkáčová et al. 2017).

In addition, the eukaryotic cellular organization of yeasts may provide further protective layers, including efficient DNA repair pathways such as nucleotide excision repair and photoreactivation, which are often enhanced in organisms adapted to intense solar radiation. Notably, the survival levels observed for PSR 34 under high UV fluence are comparable to those

reported for the radioresistant bacterium *Deinococcus radiodurans* under similar irradiation regimes, underscoring the remarkable radiation tolerance of this yeast, albeit achieved through distinct cellular and molecular strategies (Minton 1994; Pulschen et al. 2015).

Bacterial Vulnerability and Biofilm Hyphotesis

In sharp contrast, the bacterial isolates *M. hydrothermale* and *A. koreensis* exhibited high sensitivity to direct UV irradiation in our *in vitro* assays, with viability declining to below 0.1% at the highest doses tested. This observation contrasts with previous studies of photovoltaic panel microbiomes, which identified *Arthrobacter* and *Microbacterium* as dominant and apparently radiation-tolerant genera (Dorado-Morales et al. 2016; Tanner et al. 2018; Hernández-Fernández et al. 2022). Rather than contradicting these reports, our findings suggest that the persistence of these taxa in situ may depend primarily on extrinsic ecological protection mechanisms rather than on intrinsic cellular resistance.

On photovoltaic panels, these bacteria are likely embedded within multi-species biofilms or associated with dust particles, both of which can substantially reduce UV penetration (de Carvalho 2017; Yin et al. 2019; Labadie et al. 2024). Supporting this interpretation, recent experimental and modeling studies have demonstrated that the extracellular polymeric substances (EPS) matrix of biofilms can significantly attenuate UV-C transmission, generating microenvironments that enable the survival of otherwise UV-sensitive microorganisms (Torkzadeh et al. 2021; Braga et al. 2023). In our experimental design, cells were washed and analyzed as planktonic suspensions, thereby removing these protective structures and revealing their intrinsic sensitivity to direct UV exposure.

Intermediate Tolerance and Gram-Positive Traits

The Actinobacteria representatives *Kocuria sp*. and *Gordonia sp*. displayed an intermediate resistance phenotype, significantly distinct from both the rapid inactivation observed in sensitive bacteria and the high survival of the yeast. This moderate tolerance may be associated with physiological traits typical of Gram-positive bacteria. Their thick peptidoglycan cell wall confers structural robustness and may offer partial protection against oxidative stress and desiccation, stressors commonly associated with high solar irradiance (Dorado-Morales et al. 2016b; Ramijan et al. 2018; Guesmi et al. 2021).

Additionally, the relatively high guanine–cytosine (GC) content characteristic of these genera has been correlated with enhanced genomic stability and the presence of efficient DNA repair systems, features advantageous in mutagenic environments (Wu et al. 2012; Weissman et al. 2019). Nevertheless, despite these adaptations, their survival remained significantly lower than that of *R. mucilaginosa*, reinforcing the notion that, for these prokaryotes, individual resistance mechanisms may be insufficient and that their persistence on photovoltaic panels likely relies on community-level protection.

Implications for Biotechnology

Given its pronounced UV tolerance, *R. mucilaginosa* (PSR 34) emerges as a promising candidate for biotechnological applications, particularly in the development of resilient bioinoculants for the phyllosphere of crops cultivated under high-insolation conditions (Moliné et al. 2010; Villarreal et al. 2016; Garcia-Cortes et al. 2021). In contrast to the bacterial strains evaluated here, whose survival appears dependent on community-based shielding mechanisms such as biofilm formation, the yeast's intrinsic robustness supports its potential deployment as a single-strain inoculant. This feature is advantageous from a production and regulatory standpoint, as single-organism formulations are generally easier to standardize and apply.

Moreover, our findings raise the hypothesis that *R. mucilaginosa* may act as a "shelter provider" within microbial communities, potentially facilitating the persistence of more UV-sensitive taxa (Sen et al. 2019; Li et al. 2022). Future studies exploring co-culture systems and spatial organization on leaf surfaces and other exposed substrates will be essential to determine whether this yeast can confer physical or chemical protection to associated bacterial populations, thereby enhancing microbiome stability under high-radiation environments (Muthukrishanan et al. 2024).

2.5 CONCLUSIONS

In conclusion, this study demonstrates a clear and statistically significant stratification of UV resistance among microorganisms isolated from photovoltaic panels. The yeast isolate *R. mucilaginosa* (PSR 34) exhibited markedly higher tolerance to both germicidal UV-C and simulated environmental UV radiation than all bacterial strains evaluated. This enhanced resilience

is consistent with intrinsic cellular adaptations commonly associated with radiation-tolerant yeasts, including carotenoid pigmentation and efficient DNA repair systems.

In contrast, the pronounced sensitivity of *M. hydrothermale* and *A. koreensis* under planktonic conditions suggests that their persistence on photovoltaic panels is unlikely to rely on individual cellular resistance alone, but rather on community-level protection mechanisms such as biofilm formation or physical shielding by dust particles. Collectively, these findings contribute to a deeper understanding of microbial survival strategies in artificial dryland environments and identify *R. mucilaginosa* as a promising candidate for biotechnological applications, particularly as a UV-resistant bioinoculant for agricultural systems exposed to high solar irradiation.

Supplementary Material to

UV Resistance of Microbes from Photovoltaic Panels

Table S1. One-way ANOVA summary for microbial survival under UV-C radiation (280 nm)

Source of variation	***F-value***	***p-value***
Strain	399.17	5.57×10^{-11}

Table S2. Tukey's HSD post hoc test for microbial resistance under UV-C radiation (280 nm)

Group 1	**Group 2**	***Mean difference***	***Adjusted p-value***	***Lower CI***	***Upper CI***	***Significant***
PSR 33	PSR 34	4.9525	<0.001	4.4637	5.4413	Yes
PSR 33	PSR 37	0.5594	0.0239	0.0706	1.0482	Yes
PSR 33	PSR 46	1.0404	0.0003	0.5516	1.5292	Yes
PSR 33	PSR 51	−0.1015	0.9557	−0.5903	0.3873	No
PSR 34	PSR 37	−4.3931	<0.001	−4.8819	−3.9043	Yes

PSR 34	PSR 46	−3.9121	<0.001	−4.4009	−3.4233	Yes
PSR 34	PSR 51	−5.0540	<0.001	−5.5428	−4.5652	Yes
PSR 37	PSR 46	0.4810	0.0542	−0.0078	0.9698	No
PSR 37	PSR 51	−0.6609	0.0085	−1.1497	−0.1721	Yes
PSR 46	PSR 51	−1.1419	0.0001	−1.6307	−0.6531	Yes

Table S3. One-way ANOVA summary for microbial survival under ambient UV radiation (400 nm)

Source of variation	***F-value***	***p-value***
Strain	701.56	3.38×10^{-12}

Table S4. Tukey's HSD post hoc test for microbial resistance under ambient UV radiation (400 nm)

Group 1	**Group 2**	***Mean difference***	***Adjusted p-value***	***Lower CI***	***Upper CI***	***Significant***
PSR 33	PSR 34	0.5245	0.0202	0.0792	0.9699	Yes
PSR 33	PSR 37	−3.4235	<0.001	−3.8689	−2.9782	Yes
PSR 33	PSR 46	−5.6160	<0.001	−6.0614	−5.1707	Yes
PSR 33	PSR 51	−1.5321	<0.001	−1.9774	−1.0867	Yes
PSR 34	PSR 37	−3.9480	<0.001	−4.3934	−3.5027	Yes
PSR 34	PSR 46	−6.1405	<0.001	−6.5859	−5.6952	Yes
PSR 34	PSR 51	−2.0566	<0.001	−2.5020	−1.6112	Yes
PSR 37	PSR 46	−2.1925	<0.001	−2.6379	−1.7471	Yes
PSR 37	PSR 51	1.8914	<0.001	1.4461	2.3368	Yes
PSR 46	PSR 51	4.0839	<0.001	3.6386	4.5293	Yes

3 ARTIGO 2

Extremophilic microorganisms from photovoltaic panels enhance seed germination under salinity and osmotic stress in the presence of Crystalline Zinc Oxide

ABSTRACT

Salinity and water deficit are major abiotic constraints limiting seed germination and early plant establishment. This study evaluated whether extremophilic microorganisms isolated from photovoltaic panels can improve the germination performance of *Eruca sativa* seeds under saline and osmotic stress, applied alone or in combination with zinc oxide (ZnO) crystals. Seeds were inoculated with *Microbacterium hydrothermale* (PSR 33), *Rhodotorula mucilaginosa* (PSR 34), *Arthrobacter koreensis (PSR 37)*, or *Kocuria sp.* (PSR 51), with or without ZnO supplementation, and exposed to increasing salinity (0, 50, and 150 mM NaCl) or osmotic stress (0, −0.5, and −1.5 MPa PEG 6000). Germination percentage (%G) and germination speed index (GSI) were used as indicators of germination success and seed vigor. Under non-stress conditions, no significant differences among treatments were observed. In contrast, under saline and osmotic stress, clear strain-dependent responses emerged. ZnO supplementation consistently enhanced microbial effects under severe stress, resulting in significantly higher %G and GSI compared with stressed controls. *Microbacterium hydrothermale* (PSR 33) showed the greatest improvement under salinity, whereas *Rhodotorula mucilaginosa* (PSR 34) and *Arthrobacter koreensis* (PSR 37) performed best under osmotic stress. Radiation pre-treatment acted as a secondary modulator of microbial performance and did not override strain- or ZnO-dependent effects. Overall, the results indicate that extremophilic microorganisms from photovoltaic panels, particularly when combined with ZnO crystals, can improve seed germination and vigor under contrasting abiotic stress conditions. This approach represents a promising seed-priming strategy for enhancing early plant establishment in stress-prone environments.

Keywords: extremophilic microorganisms; zinc oxide (ZnO); seed priming; abiotic stress; salinity; osmotic stress.

3.1 INTRODUCTION

Salinity and water deficit are among the most limiting abiotic stresses affecting crop establishment worldwide, particularly during seed germination and early seedling development (Jovović et al. 2018; Uçarlı 2020; Bayindir and Coşkun 2022). These stressors reduce water availability, impair metabolic activation during imbibition, and delay or inhibit radicle protrusion, ultimately compromising plant establishment and yield (Maucieri et al. 2018; Silva et al. 2019). Although salinity and drought are often grouped as water-related constraints, they impose distinct physiological challenges on seeds: salinity combines osmotic limitation with ionic toxicity, whereas osmotic stress primarily restricts water uptake without direct ionic effects (Miranda et al. 2014; Sena et al. 2023; Sghayar et al. 2023).

Seed priming has emerged as an effective strategy to enhance germination performance under adverse environmental conditions. By partially activating metabolic processes prior to germination, priming treatments can improve germination rate, uniformity, and stress tolerance (Mondal et al. 2021; Louis et al. 2023; Janah et al. 2025; Rhaman 2025). Among priming approaches, the use of plant growth-promoting microorganisms (PGPMs) has gained increasing attention due to their ability to influence early plant responses through phytohormone production, osmotic adjustment, extracellular polymeric substances, and stress-related metabolites (Koza et al. 2022; Ahmad et al. 2022a; Teiba et al. 2024; Sherzad et al. 2025; Rhaman 2025).

The effectiveness of microbial priming is strongly influenced by strain identity and ecological origin. Microorganisms adapted to extreme environments often possess enhanced tolerance to desiccation, radiation, and oxidative stress, traits that may confer advantages when applied to seeds exposed to salinity or water deficit (Lastochkina et al. 2020; Zenteno-Alegría et al. 2024; Sibanda et al. 2024; Marzban and Tesei 2025). In this context, extremophilic microorganisms isolated from photovoltaic panels represent a novel and largely unexplored biological resource. These artificial surfaces are characterized by intense solar radiation, temperature fluctuations, and prolonged desiccation, selecting for microbial communities with robust stress-resistance mechanisms (Tanner et al. 2018; Porcar et al. 2018).

In addition to biological priming agents, inorganic supplements such as zinc oxide (ZnO) have been reported to improve seed germination and early growth under abiotic stress. Zinc plays a central role in antioxidant defense, membrane stability, and enzyme function, processes that are

particularly sensitive during early germination (Mazhar et al. 2022; Singh et al. 2022; Ramzan et al. 2024; El-Shazoly et al. 2025). When applied as particulate materials in seed treatments, ZnO can act as a localized source of zinc during imbibition, potentially enhancing stress tolerance without requiring internal nanoparticle uptake.

Despite growing interest in both microbial and ZnO-based priming strategies, studies evaluating their combined effects during seed germination under contrasting abiotic stresses remain limited. Moreover, few investigations have explicitly compared microbial performance under saline versus osmotic stress, even though these stressors differ markedly in their physiological impacts (Mazhar et al. 2022; Donia and Carbone 2023a; Singh et al. 2024).

Therefore, the objective of this study was to evaluate whether extremophilic microorganisms isolated from photovoltaic panels, after irradiation pretreatments, can improve the germination performance and vigor of *Eruca sativa* seeds under saline and osmotic stress, applied alone or in combination with ZnO crystals.

3.2 MATERIALS AND METHODS

Microorganisms and Preparation of Suspensions

Four extremophilic microorganisms previously isolated from photovoltaic panels in southeastern Brazil were used: PSR 33 (*Microbacterium hydrothermale*), PSR 34 (*Rhodotorula mucilaginosa*), PSR 37 (*Arthrobacter koreensis*), and PSR 51 (*Kocuria sp.).* These strains were selected based on their documented tolerance to ultraviolet radiation, desiccation, and environmental stress.

Prior to seed inoculation, microbial cultures were subjected to different radiation pre-treatments in order to evaluate their influence on subsequent germination performance (Pulschen et al. 2015). Three conditions were applied: (i) no radiation (non-irradiated control), (ii) exposure to ambient environmental UV radiation, and (iii) exposure to UVC radiation. These treatments were applied to actively growing cultures before seed priming and were not intended to impose stress on the seeds themselves, but rather to pre-condition the microorganisms.

Bacterial strains (PSR 33, PSR 37, and PSR 51) were cultivated on Tryptic Soy Agar at 35 ± 0.5 °C for 48 h, while the yeast strain PSR 34 was cultivated on Sabouraud Agar at 25 ± 0.5 °C

for 5 days. Cultures were then transferred to liquid media (Brain Heart Infusion for bacteria and Yeast Extract Peptone Dextrose for yeast) and incubated under agitation (150 rpm) until reaching an optical density of approximately OD_{600} = 0.7 abs, corresponding to ~7×10^7 CFU mL^{-1}.

Synthesis and characterization of crystalline ZnO

Zinc oxide (ZnO) crystals were synthesized in duplicate using the modified Pechini method adapted from literature (Rodrigues et al. 2019). Zinc acetate (99.57%, Neon Reagentes Analíticos) was used as a zinc precursor, citric acid (99.5%, Labsynth) served as the chelating agent, and ethylene glycol (99.0%, Quimisul SC) was used as the polyalcohol for polyesterification.

The zinc precursor and citric acid were mixed in a crucible at a molar ratio of 1:3 (Zn:citric acid) in deionized water and heated to 50 °C for 5 min under stirring to promote chelation. Ethylene glycol was then added in excess at a molar ratio of 1:4 (citric acid:ethylene glycol), and the mixture was heated to 90 °C, still under stirring, to evaporate excess water and form a polymeric gel. The resulting gel was dried in an oven at 90 °C for 12 h and subsequently calcined at 500 °C for 2 h.

The crystalline structure of the ZnO powders was analyzed using a Shimadzu XRD-6100 diffractometer (XRD) with Cu Kα radiation (40 kV, 30 mA, λ = 1.5418 Å), using a glass sample holder for the powders, continuous scans from 20° to 70° (2θ) at a scan speed of 2°/min and step size of 0.02°. A fixed divergence slit and anti-scatter slit, both with 1.0° beam divergence, were used. Phase identification was performed by comparison with JCPDS reference patterns, and crystallite size was estimated using 6 diffraction peaks from each sample using the Scherrer equation:

$$\tau = \frac{k \cdot \lambda}{\cos(\theta) \cdot (FWHM)}$$

Where τ is the Scherrer crystallite size in nanometers, k is the shape factor (0.9), λ is the wavelength of the X-rays in nanometers, θ is the peak position in radians and FWHM is the full width half max of the diffraction peak, also in radians, obtained using Gaussian fitting for each diffraction peak of the ZnO samples. Peak widening inherent from the diffractometer was determined using a Si standard (99%, 325 mesh, Shimadzu Corporation) and used as a correction factor for more precise crystallite size calculation.

Raman spectra were obtained using a Renishaw inVia Reflex micro-Raman spectrometer. The powders were pressed on top of a glass sample holder and characterized using a 532 nm 50 mW diode pumped solid state laser, with 3.00 s exposure time, 50% power setting and 10 accumulations, in the range of 0 to 1262 cm-1.

The Fourier-transform infrared spectra (FTIR) were collected using a PerkinElmer Frontier spectrometer with an attenuated total reflectance apparatus (ATR). Transmittance analyses were done for the powders in the range of 4000 cm-1 to 400 cm-1 with a spectral resolution of 4 cm-1 and 16 accumulations. The spectra were treated with the smooth and baseline functions of the PerkinElmer Spectrum software, associated with the equipment.

Scanning electron microscopy (SEM) and Energy dispersive X-ray spectroscopy (EDS) were performed using a Hitachi TM3000 microscope. The powders were set on conductive carbon tape on top of an aluminum stub sample holder. Micrographs and EDS spectra were obtained at 1000x and 2000x magnifications under an accelerating voltage of 15 kV with no previous sample treatment.

Seed material and surface disinfection

Seeds of Eruca sativa (arugula) were obtained from Agristar do Brasil LTDA (TSV Seeds line). Prior to treatment, seeds were surface-disinfected by immersion in 70% (v/v) ethanol for 5 min, followed by three rinses with sterile deionized water (Barampuram et al. 2014). Seeds were then dried on sterile Whatman filter paper (150 mm) under laminar airflow

Seed inoculation and ZnO treatment

Disinfected seeds were immersed for 2 h in one of the following solutions: (i) microbial suspension, (ii) microbial suspension supplemented with ZnO crystals (50 mM), (iii) sterile deionized water (control), or (iv) sterile deionized water supplemented with ZnO (50 mM). This step was performed to allow microbial adhesion and/or ZnO surface association during seed priming (O'Callaghan 2016; Singh et al. 2023).

After inoculation, seeds were rinsed three times with a 0.85% (w/v) NaCl isotonic solution. This rinsing step was applied uniformly to all inoculated treatments and was intended solely to remove loosely attached cells while preserving microbial adhesion to the seed surface. Importantly,

this procedure was not designed to impose saline stress and was performed prior to the application of abiotic stress treatments. Seeds were subsequently dried under laminar airflow before exposure to stress conditions.

Abiotic stress treatments

Salinity stress

Seeds were immersed in NaCl solutions at concentrations of 0, 50, or 150 mM.

Osmotic stress

Osmotic stress was imposed using polyethylene glycol (PEG 6000; 99.0%, Química Contemporânea LTDA) solutions adjusted to water potentials of 0, −0.5, or −1.5 MPa, following established protocols.

For treatments involving prolonged exposure to salinity or osmotic stress, seeds were not rinsed after stress application, ensuring continuous stress during the germination period.

Germination conditions

Following stress treatment, seeds were placed in sterile Petri dishes containing sterile Whatman filter paper moistened with sterile deionized water. Dishes were incubated in a B.O.D. growth chamber under a 12 h light/12 h dark photoperiod with alternating temperatures of 25 °C (day) and 15 °C (night). Germination was monitored daily until stabilization.

Germination Percentage evaluation

The germination percentage (G%) of arugula seeds was evaluated by conducting daily counts of germinated seeds (BRASIL, 2009; ISTA 1993). Seeds were considered germinated when they exhibited visible radicle protrusion. The germination percentage was calculated using the formula:

$$G\% = \frac{NG \times 100}{NT}$$

where "NG" represents the number of germinated seeds, and "NT" is the total number of seeds set for germination. This calculation allowed for the assessment of the effectiveness of each treatment in promoting seed germination under the various stress conditions tested.

Germination Speed Index (GSI)

The Germination Speed Index (GSI) was calculated to evaluate the rate of seed germination under each treatment (BRASIL, 2009; ISTA 1993). GSI provides a measure of how quickly seeds respond to the various treatments, specifically assessing the effectiveness of microorganism-only treatments and microorganism + ZnO treatments under different stress conditions, including radiation exposure, salinity, and osmotic stress. The GSI was calculated using the formula:

$$GSI = \frac{G1}{N1} + \frac{G2}{N2} + \frac{G3}{N3} + \cdots + \frac{GN}{NN}$$

where "G" represents the number of seeds germinated on each respective day, and "N" corresponds to the day of each evaluation (from the first day, second day, up to the final assessment day). This index reflects the response rate of seeds to each experimental condition, allowing a comparative analysis of the resilience induced by the microorganism treatments and the ZnO supplementation in overcoming abiotic stresses.

Experimental design and statistical analysis

The experiment followed a completely randomized design. Microbial strain and ZnO presence were considered primary experimental factors, while radiation pre-treatment and abiotic stress levels were treated as conditional modulators of microbial performance rather than independent drivers.

Data were analyzed using Python (v. 3.14) with the pandas, scipy, statsmodels, and scikit-posthocs libraries. Germination percentage data were arcsine square-root transformed prior to analysis to meet ANOVA assumptions. Residual normality and variance homogeneity were verified using Shapiro–Wilk and Levene tests, respectively.

Multi-way ANOVA was conducted, and Dunnett's test ($p < 0.05$) was used to compare treatment combinations directly against their respective abiotic stress controls. Detailed ANOVA outputs and Dunnett's post hoc test results are provided in the Supplementary Material.

3.3 RESULTS

Evaluation of the Synthesis of crystalline ZnO

Figure 1 shows the X-ray diffractograms for all synthesized samples. The use of zinc acetate as a precursor for both samples allowed for pure zinc oxide to be synthesized via the modified Pechini route. Both diffractograms showed that the ZnO crystallized with the hexagonal wurtzite structure (JCPDS 36-1451), as can be seen by the comparison with the reference sheet peaks shown at the bottom of the figure (Fig. 1). These results were expected after the calcination step at 500 °C for 2 hours and agree with those obtained in previous studies (Rodrigues et al. 2019; Zahra et al. 2022).

Figure 1 – X-ray diffraction (XRD) patterns of ZnO crystals synthesized by the modified Pechini method. Zinc acetate as a precursor allowed for the formation of phase-pure ZnO with a hexagonal wurtzite structure.

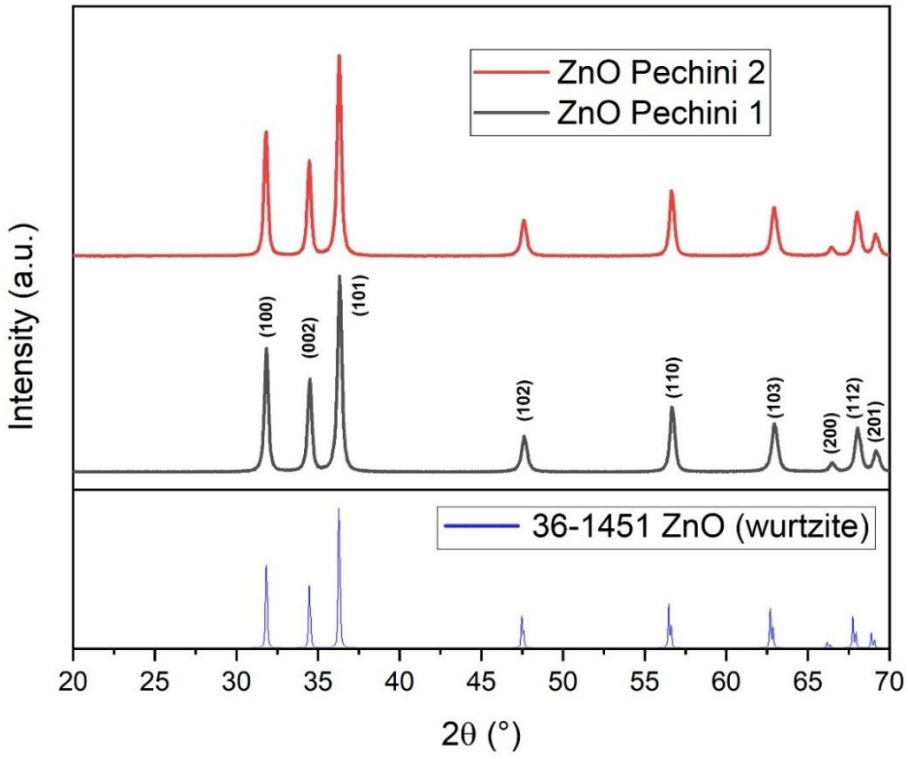

The Scherrer crystallite sizes calculated using the Scherrer equation are shown in Table 1, where it can be noted that all samples formed slightly larger average Scherrer crystallite sizes within the nanometric scale when compared to previous literature (Rodrigues et al. 2019; Zahra et al. 2022; Ramos et al. 2025). This may be a result of different factors, such as the calcination time or the large amount of ZnO generated per synthesis in this study, upwards of 3 grams, demanding a higher amount of citric acid and ethylene glycol. During the calcination step, the polyester reacts with the open atmosphere and the combustion of organic components leads to the formation of mostly water and carbon dioxide, among other subproducts, leading to a very high-energy environment inside the crucible and causing crystal growth and particle agglomeration (Ianculescu et al. 2015; Zahra et al. 2022; Sharma et al. 2023).

When specific peaks are considered instead of the average, some anisotropic crystalline growth is observed, favoring the (100), (002) and (101) planes, which showed larger Scherrer crystallite sizes for both synthesized powders. This is an indication of non-spherical nanocrystals, which have also been reported in previous studies (Saravanan et al. 2018; Zahra et al. 2022).

Table 1 – Scherrer crystallite sizes for all ZnO samples

Sample	θ (rad)	FWHM (rad)	τ (nm)	Average τ (nm)
ZnO Pechini 1	0.278	0.00278	126 ± 3	92 ± 2
	0.301	0.00295	111 ± 2	
	0.317	0.00314	97 ± 2	
	0.416	0.00385	69 ± 2	
	0.495	0.00342	89 ± 2	
	0.550	0.00421	63 ± 1	
ZnO Pechini 2	0.278	0.00270	136 ± 3	100 ± 2
	0.301	0.00282	123 ± 3	
	0.317	0.00300	107 ± 2	
	0.415	0.00368	74 ± 2	
	0.495	0.00334	93 ± 2	
	0.549	0.00409	66 ± 1	

Figure 2 shows the Raman and FTIR spectra for both ZnO powders. The crystalline hexagonal wurtzite structure of zinc oxide that was observed in the diffractograms were confirmed via Raman, showing bands at 101, 339, 388 and 437 cm^{-1}, like those in previous research (Pereira et al. 2017). The first order non-polar optical phonon modes, E_{2L} and E_{2H}, can be seen in the form of the 101 cm^{-1} and 437 cm^{-1} peaks, which are characteristic of the hexagonal wurtzite zinc oxide (Ahmad et al. 2022b). The broad band around 1000 cm^{-1} corresponds to second order Raman modes (Pereira et al. 2017).

FTIR spectra are also seen in Figure 2. The stretching of Zn-O bonds tends to form different peaks in the fingerprint region depending on particle size and were here seen around 415 to 490 cm^{-1} (Mahamuni et al. 2019; Jayachandran et al. 2021; Zahra et al. 2022) The FTIR spectra also showed that the powders had minimal bands pertaining to -OH group stretching in the region of 3200 cm^{-1} to 3600 cm^{-1}, indicating that the calcination step not only led to the crystallization of the zinc oxide, but samples kept dry after being stored for weeks. The absence of relevant peaks in the 3000 cm^{-1} to 800 cm^{-1} interval is compatible with a metal oxide synthesized using the modified Pechini process, which tends to be free of any organic contaminants after calcination (Pereira et al. 2017; Ramos et al. 2025). A small band can be noted around 2350 cm^{-1}, produced by atmospheric carbon dioxide during the analysis.

Figure 2 – Raman and FTIR spectra of ZnO crystals synthesized by the modified Pechini method. Raman spectra showed a crystalline hexagonal wurtzite structure for both samples, while FTIR spectra highlighted the Zn-O bonds in samples, with minimal -OH stretching due to a dry product after calcination.

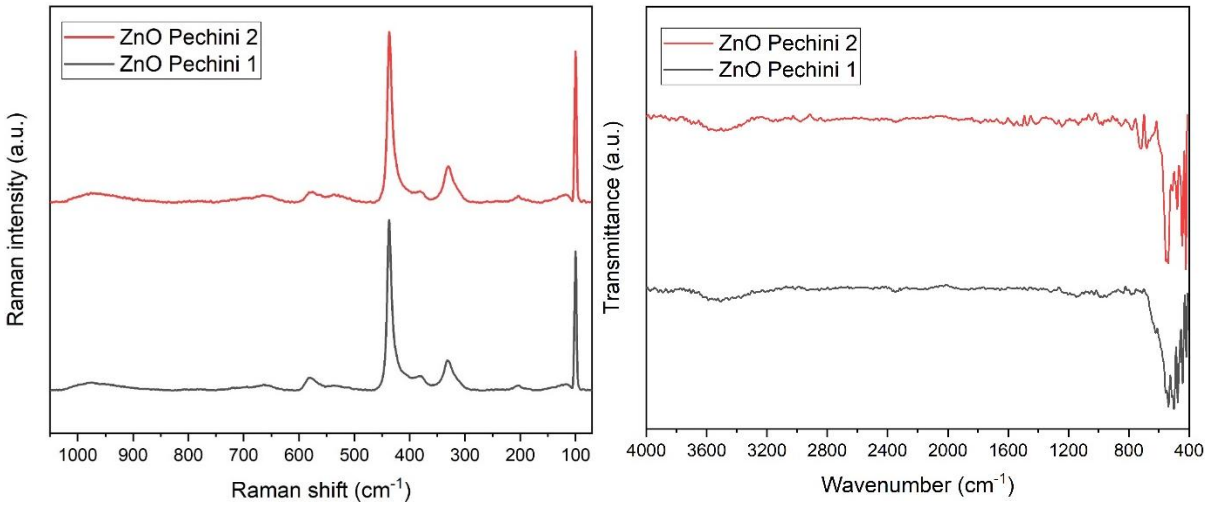

Figure 3 shows the SEM and EDS micrographs for both ZnO samples. The micrometer scale highlights the agglomeration phenomenon present in the zinc oxide powders, which is commonly observed in metal oxide materials synthesized via the modified Pechini route, especially due to the high temperatures and calcination times (Chrunik et al. 2017; Zahra et al. 2022). As seen in Scherrer equation calculations (Table 1), the ZnO samples formed non-spherical nanocrystals, but these tended to agglomerate to form particles in the micrometer scale, as seen in the SEM micrographs. The irregular surface of ZnO particles can also be noted under both 1000x and 2000x magnifications, formed in the context of the high energy environment during the calcination step (Raza et al. 2022; Balasubramaniyam et al. 2025).

Figure 3 – SEM and EDS micrographs of ZnO crystals synthesized by the modified Pechini method. ZnO Pechini 1 is shown to the left and ZnO Pechini 2 to the right. Zinc is in red and oxygen in green. Agglomeration can be seen, while EDS showed good Zn and O distribution.

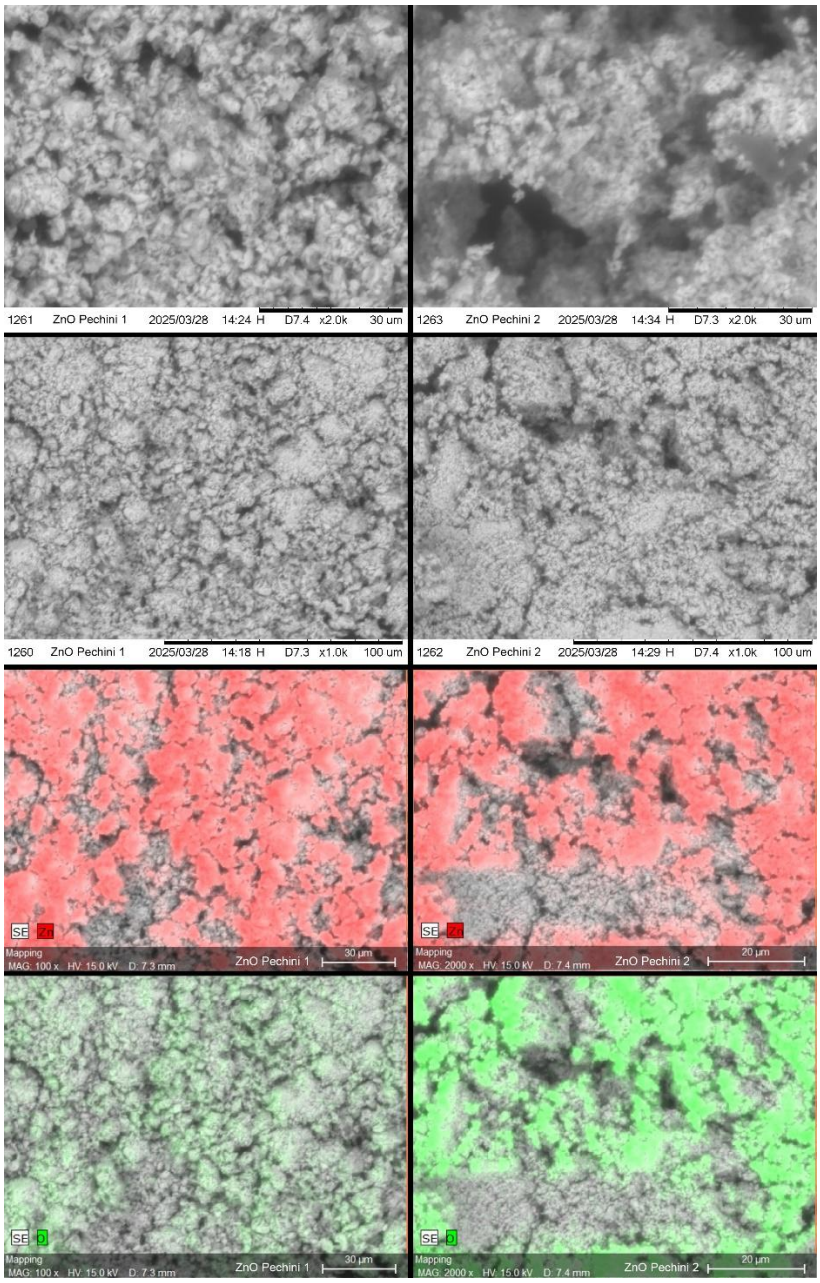

The EDS micrographs showed a uniform distribution of zinc and oxygen atoms across both samples, confirming the formation of very pure zinc oxide, with very similar atom percentages for zinc and oxygen (Table 2). This was further highlighted in Figure 4, which presents the EDS spectra for both powders, where the higher counts peaks for Zn and O were noted. The formation of pure products is expected for modified Pechini synthesis of metal oxides (Fang et al. 2013).

The only other chemical elements that had relevant signals in the EDS spectra were carbon and aluminum, which were attributed to the conductive carbon tape and aluminum stub sample

holder that were used in the SEM characterization step. Quantification of these chemical elements, performed for ZnO Pechini 1 and ZnO Pechini 2 using Quantax70 along with the electron microscope, can be seen in Table 2:

Table 2 – Elemental composition for ZnO samples measured by EDS and quantified using Quantax70.

Sample	Chemical Element	Mass (wt.%)	Atom fraction (at. %)
ZnO Pechini 1	Zn	71.5	36.3
	O	17.5	36.3
	C	9.1	25.1
	Al	1.9	2.3
ZnO Pechini 2	Zn	72.1	37.1
	O	17.0	35.8
	C	8.8	24.5
	Al	2.1	2.6

Figure 4 – EDS spectra of ZnO crystals synthesized by the modified Pechini method. ZnO Pechini 1 is shown above and ZnO Pechini 2 below. Zn and O peaks were observed. C and Al peaks can be attributed to the carbon tape and aluminum sample stub holder for SEM.

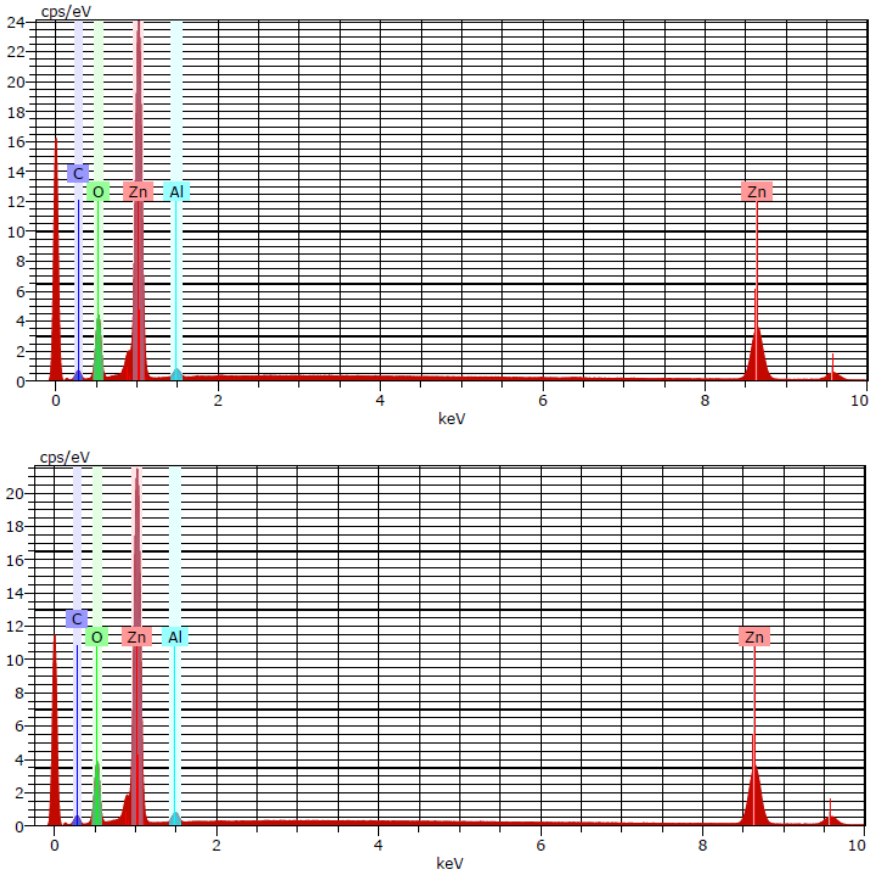

Overview of statistical responses

Statistical analysis revealed a high level of complexity in the experimental system. For both Germination Percentage (%G) and Germination Speed Index (GSI), the four-way interaction between Strain × ZnO × Radiation × Stress was statistically significant (for %G under saline stress; for GSI under both stresses), indicating a high level of system complexity (Supplementary Tables S1-S4). This indicates that the effect of microbial inoculation is not independent but varies significantly according to the presence of zinc oxide nanoparticles (ZnO), the radiation pre-treatment, and the osmotic or saline stress levels applied.

Germination percentage (%G) under saline and osmotic stress

Under non-stress conditions, all treatments exhibited high germination rates, with no statistically significant differences relative to the water control ($p > 0.05$). In contrast, under saline and osmotic stress, clear and reproducible performance patterns emerged (Figures 5 and 6). Detailed pairwise comparisons against the stressed controls are provided in Supplementary Tables S5 and S6.

Figure 5. Effects of microbial inoculation and ZnO supplementation on the germination percentage (%G) of *Eruca sativa* seeds under saline stress (0, 50, and 150 mM NaCl). Data represents adjusted means of arcsine-transformed values ± 95% confidence intervals. Comparisons emphasize treatment performance relative to stressed water control, highlighting the modulatory role of ZnO under increasing salinity.

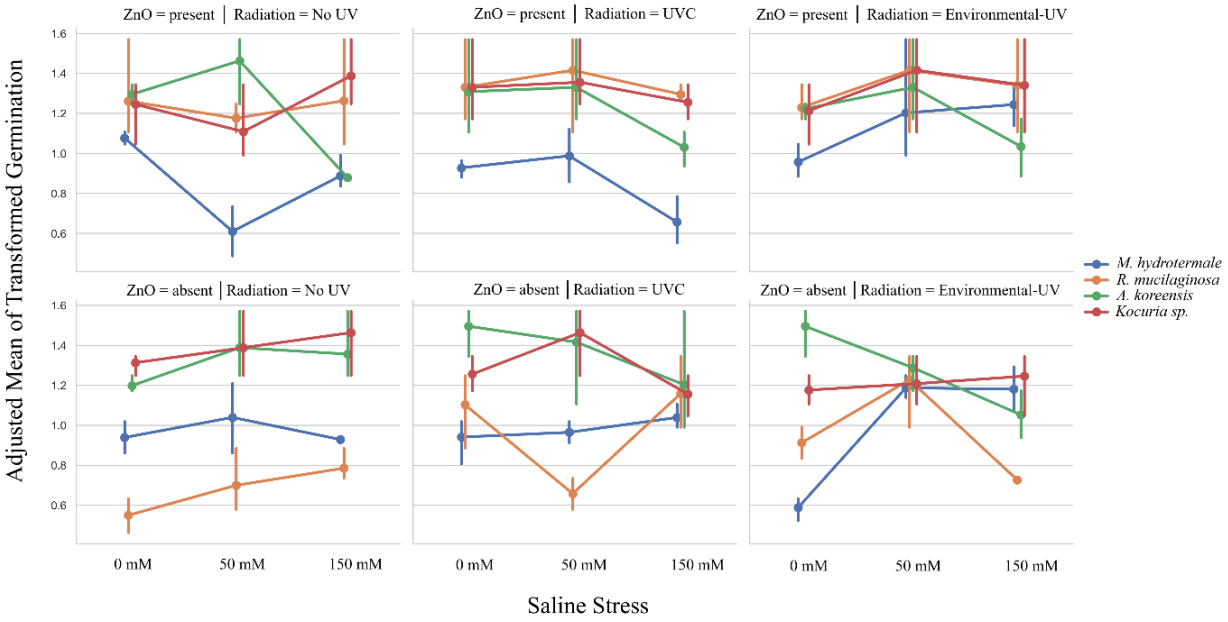

Figure 6. Germination percentage (%G) of *Eruca sativa* seeds subjected to osmotic stress (0, −0.5, and −1.5 MPa PEG 6000) following microbial inoculation with or without ZnO supplementation. Data represent adjusted means ± 95% confidence intervals. Enhanced germination under severe osmotic stress is observed primarily in ZnO-supplemented treatments, particularly for strains PSR 34 and PSR 37.

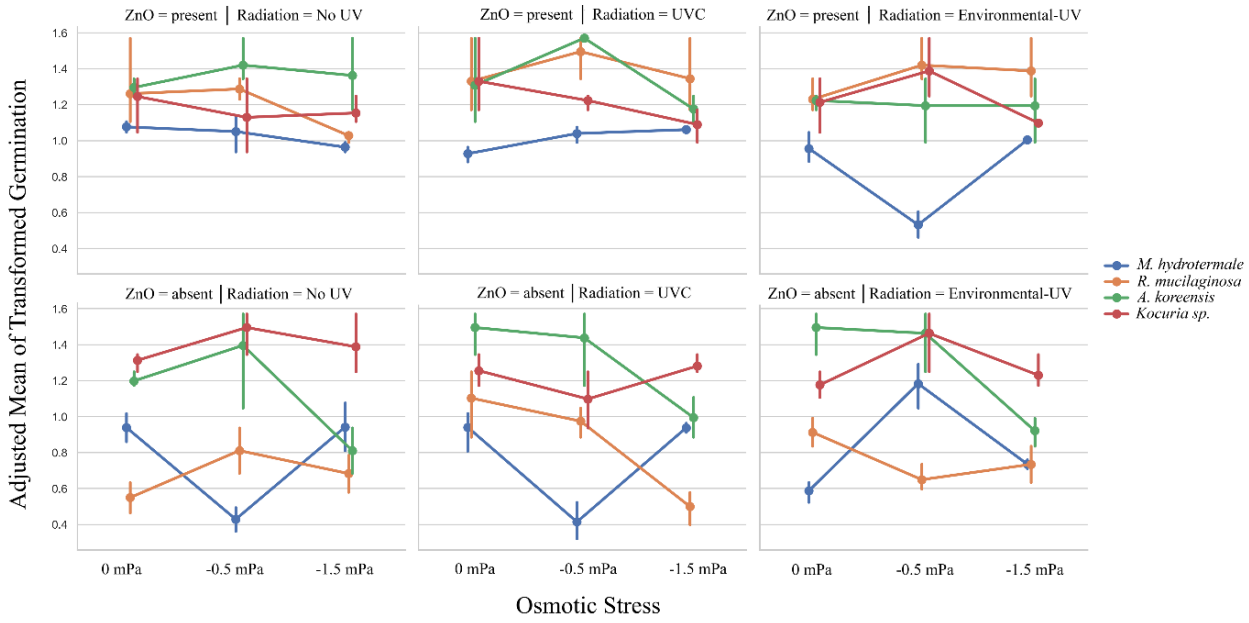

Across both stress types, ZnO presence consistently enhanced germination performance, particularly under severe stress conditions (150 mM NaCl and −1.5 MPa PEG). In the absence of ZnO, several microbial treatments exhibited germination rates comparable to or lower than the stressed control. This effect was most evident for strain PSR 34, which showed limited efficacy when applied alone under high stress.

The addition of ZnO significantly altered this response. For example, under 150 mM NaCl, the combination of PSR 34 with ZnO resulted in germination percentages significantly higher than the control ($p < 0.001$), particularly when coupled with radiation pre-treatment.

Radiation acted as a context-dependent modulator rather than a primary determinant. Under severe osmotic stress, UVC pre-treatment enhanced the performance of PSR 34 and PSR 37 in the presence of ZnO, maintaining germination rates above 90% ($p < 0.01$), whereas radiation effects were less pronounced under moderate stress.

Strain-specific differences were evident. PSR 37 and PSR 51 displayed greater stability across stress levels, but statistically significant superiority over the control was consistently observed only when ZnO was present ($p < 0.05$).

Germination Speed Index (GSI) as an indicator of seed vigor

Patterns observed for GSI closely paralleled those of germination percentage but provided additional resolution regarding seed vigor (Figures 7 and 8). In treatments lacking ZnO, microbial inoculation frequently resulted in GSI values equivalent to or lower than stressed control, particularly under moderate salinity (50 mM NaCl). Complete Dunnet's post hoc test results supporting these comparisons are available in Supplementary Tables S7 and S8.

Figure 7. Germination Speed Index (GSI) of *Eruca sativa* seeds under saline stress. Panels illustrate strain-specific responses across salinity levels, modulated by ZnO presence and radiation pre-treatment. ZnO-supplemented treatments exhibit consistently higher germination speed under severe salinity, with PSR 33 displaying a pronounced rapid-germination ("sprinter") phenotype.

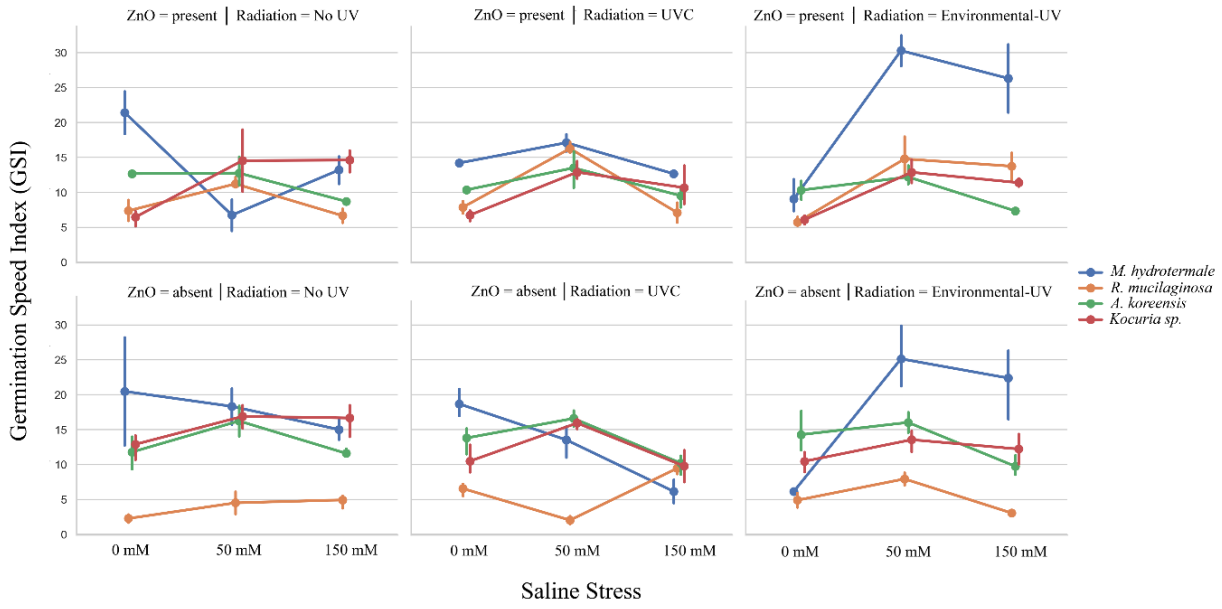

Figure 8. Germination Speed Index (GSI) of *Eruca sativa* seeds subjected to osmotic stress (PEG 6000). Distinct performance peaks are observed for strains PSR 34 and PSR 37 under severe stress (−1.5 MPa) when combined with ZnO and UVC pre-treatment, indicating stress-specific enhancement of seed vigor.

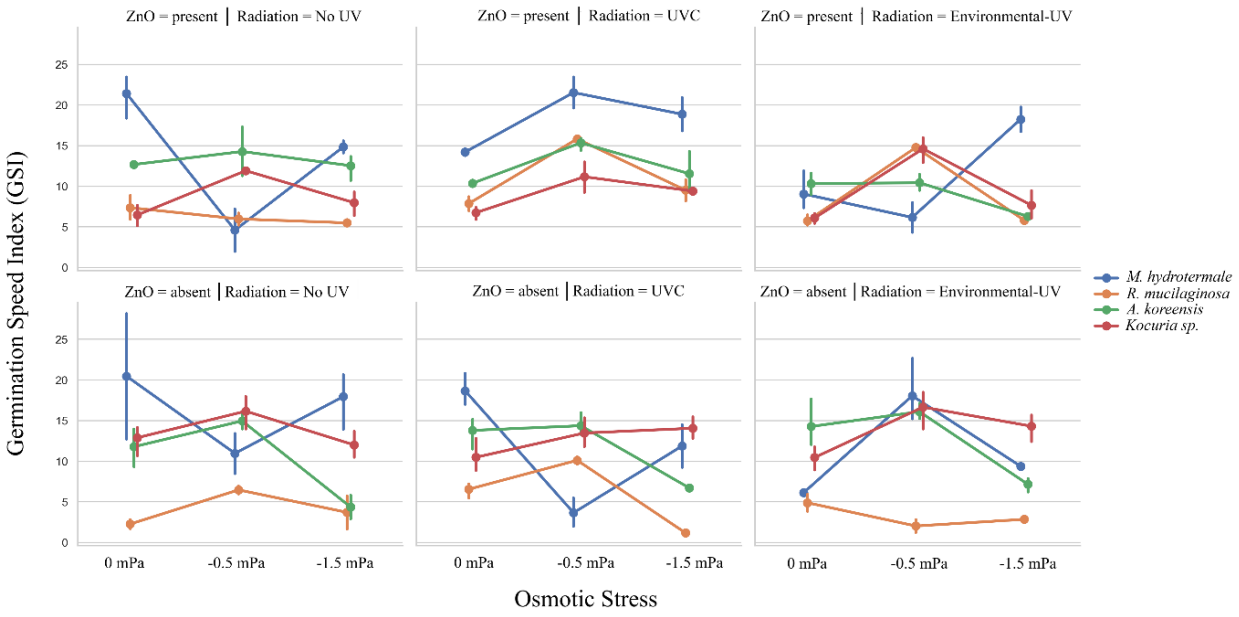

In contrast, ZnO-supplemented treatments displayed marked improvements in germination speed, especially under severe stress. A pronounced strain-specific response was observed for PSR 33 under saline stress. The combination of PSR 33 + ZnO + Environmental-UV yielded a GSI of 26.33 under 150 mM NaCl, representing an increase of more than 100% relative to the water control (12.88; $p < 0.001$), characterizing a rapid-germination or "sprinter" phenotype.

Stress specificity was also evident. While PSR 33 was the most effective strain for enhancing vigor under saline stress, PSR 34 and PSR 37 exhibited the highest GSI values under severe osmotic stress (−1.5 MPa) when combined with ZnO and UVC radiation, significantly surpassing the control ($p < 0.001$).

3.4 DISCUSSION

Extremophilic origin as a determinant of stress-mitigating capacity

All microbial strains evaluated enhanced germination under at least one abiotic stress condition, corroborating extensive evidence that plant growth-promoting microorganisms (PGPMs) contribute to early stress tolerance through phytohormone production, osmotic adjustment, and extracellular polymeric substance (EPS) synthesis (Meza et al. 2022; Fiodor et al. 2023). However, the magnitude and consistency of the responses observed here exceeded those

typically reported for soil-derived PGPMs under comparable stress intensities (Abdul Rahman et al. 2021; Lopes et al. 2021; Masmoudi et al. 2023)

This enhanced performance is plausibly linked to the extremophilic origin of the strains, which were isolated from photovoltaic panel surfaces – environments characterized by intense solar radiation, desiccation, and thermal fluctuations (Dorado-Morales et al. 2016; Tanner et al. 2018; Porcar et al. 2018; Moura et al. 2021). Such habitats select for microorganisms with robust oxidative stress defenses, DNA repair systems, and protective pigmentation traits directly relevant to seed protection during imbibition and early germination (Karentz 2015; Mutungi et al. 2022).

Strain-specific patterns further reinforce this interpretation. PSR 33 (*Microbacterium hydrothermale*) showed superior performance under saline stress, consistent with known osmoadaptive strategies and ion homeostasis mechanisms in actinobacteria (Zhang et al. 2014; Okabe et al. 2024). In contrast, PSR 34 (*Rhodotorula mucilaginosa*) and PSR 37 (*Arthrobacter koreensis*) performed best under osmotic stress, aligning with reports describing carotenoid-rich yeasts and desiccation-tolerant actinobacteria as effective mitigators of water deficit (Selim et al. 2019; Soni et al. 2023)

Crystalline ZnO as a functional amplifier of microbial effects

ZnO supplementation consistently enhanced germination percentage and germination speed under severe stress, revealing a synergistic interaction between microbial inoculation and inorganic cofactors. Similar improvements in plant performance under salinity and drought following ZnO application have been widely reported (Akhtar et al. 2022; Safaeipour et al. 2023; Singh et al. 2024)

Although the ZnO crystals synthesized in this study exhibited relatively large crystallite sizes, this characteristic does not limit their biological relevance in seed priming systems. In such applications, ZnO is not intended to penetrate plant tissues as ultra-small nanoparticles but rather to act as a surface-associated source of zinc ions and redox modulation during early imbibition (Rawashdeh et al. 2020; Caser et al. 2024; El-Shazoly et al. 2025). Zinc plays a central role in antioxidant enzyme activity, membrane stabilization, and ion homeostasis—processes particularly vulnerable under saline and osmotic stress (Ahmed et al. 2023; Mushtaq et al. 2023; Das et al. 2025).

The observation that certain strains—especially PSR 34—showed limited efficacy when applied alone but responded strongly when combined with ZnO highlights the complementary nature of biological and physicochemical mechanisms. While microorganisms contribute to phytohormones, EPS, and stress-responsive metabolites, ZnO likely reduces oxidative damage and stabilizes cellular environments, enabling microbial benefits to be fully expressed (Moradtalab et al. 2020; Akhtar et al. 2022; Mazhar et al. 2022; Ahmed et al. 2023; Muhae-Ud-Din et al. 2025)

Radiation pre-conditioning as a contextual modulator

Radiation pre-treatment did not act as a primary determinant of germination outcomes but functioned as a context-dependent modulator of microbial performance. Under severe osmotic stress, UVC pre-treatment enhanced the efficacy of PSR 34 and PSR 37 in the presence of ZnO. Extremophilic microorganisms are known to possess robust photoprotective mechanisms, including DNA repair enzymes, antioxidant systems, and pigment production (Oren and Gunde-Cimerman 2007; Albarracín et al. 2012; Jones and Baxter 2017; Núñez et al. 2025)

Previous studies have shown that UV exposure can stimulate biofilm formation and protective metabolite synthesis in microorganisms, suggesting that controlled UV pre-conditioning may prime extremophilic inoculants for improved performance under subsequent abiotic stress. However, given its context-specific effects, radiation should be interpreted as an auxiliary optimization strategy rather than a universal requirement (Pezzoni et al. 2018; González-García et al. 2023)

Germination speed and stress specificity

In addition to germination percentage, germination speed index (GSI) provided valuable insight into seed vigor and stress resilience. Rapid germination under stress is a critical determinant of successful seedling establishment, particularly in saline or drought-prone environments (Eesha et al. 2023; Tao et al. 2024)

A pronounced strain-specific response was observed. PSR 33 displayed a rapid-germination or “sprinter” phenotype under severe salinity, while PSR 34 and PSR 37 exhibited the highest vigor under osmotic stress when combined with ZnO and UVC. Such differentiation reflects ecological specialization shaped by native habitats and reinforces the importance of selecting microbial

inoculants according to dominant environmental stressors rather than pursuing universally effective strains (Valliere et al. 2020; Fouad et al. 2025; Dagher et al. 2025).

The present study focused on early germination parameters under controlled conditions, which are widely recognized as sensitive indicators of stress tolerance and seedling establishment. Nevertheless, future studies should incorporate morphophysiological analyses to elucidate the mechanisms underlying the observed microbial–ZnO synergy and validate these effects at later developmental stages and under field conditions.

3.5 CONCLUSIONS

This study demonstrates that extremophilic microorganisms isolated from photovoltaic panels constitute an effective biological resource for enhancing seed germination under abiotic stress conditions. When applied to *Eruca sativa* seeds, these microorganisms improved germination performance and seed vigor under both salinity and osmotic stress, with outcomes strongly dependent on strain identity.

The incorporation of ZnO crystals markedly amplified microbial efficacy, particularly under severe stress, revealing a robust synergistic interaction between biological inoculants and inorganic cofactors. Rather than acting as an independent stimulant, ZnO functioned as a performance enhancer, enabling microbial-derived benefits to be fully expressed during early germination. This effect was especially evident for strains that showed limited activity when applied alone, highlighting the importance of combined formulations.

Strain-specific and stress-dependent responses were observed, with *Microbacterium hydrothermale* (PSR 33) exhibiting superior performance under saline stress, while *Rhodotorula mucilaginosa* (PSR 34) and *Arthrobacter koreensis* (PSR 37) were most effective under osmotic stress. These findings underscore the relevance of ecological specialization in selecting microbial inoculants for targeted agricultural applications.

Overall, the results support the integration of extremophilic microorganisms and ZnO crystals as a promising, sustainable seed-priming strategy to improve germination and early seedling establishment in environments affected by salinity and water deficit. Future studies should

expand this approach to later developmental stages and field conditions to validate its agronomic potential.

Supplementary Material to

Extremophilic Microorganisms from Photovoltaic Panels Enhance Seed Germination under Salinity and Osmotic Stress in the Presence of Zinc Oxide Crystals

Table S1. ANOVA summary for germination percentage (%G) of *Eruca sativa* under saline stress

	Sum_sq	***Df***	***F***	***PR(>F)***
Intercept	3,4796	1	136,9088	1,20E-22
Strain	0,0859	3	1,1264	3,41E-01
ZnO	0,0285	1	1,1224	2,91E-01
Radiation	0,0374	2	0,7365	4,81E-01
Stress	0,3309	2	6,5095	1,97E-03
Strain:ZnO	0,5197	3	6,8160	2,50E-04
Strain:Radiation	0,0528	6	0,3462	9,11E-01
ZnO:Radiation	0,1112	2	2,1873	1,16E-01
Strain:Stress	0,8836	6	5,7942	1,98E-05
ZnO:Stress	0,2522	2	4,9615	8,25E-03
Radiation:Stress	0,6439	4	6,3341	1,01E-04
Strain:ZnO:Radiation	0,3252	6	2,1324	5,31E-02
Strain:ZnO:Stress	0,4097	6	2,6866	1,68E-02
Strain:Radiation:Stress	0,5422	12	1,7777	5,70E-02
ZnO:Radiation:Stress	0,2612	4	2,5691	4,05E-02
Strain:ZnO:Radiation:Stress	0,7947	12	2,6057	3,61E-03
Residual	3,6599	144		

Table S2. ANOVA summary for germination percentage (%G) of *Eruca sativa* under osmotic stress

	Sum_sq	***Df***	***F***	***PR(>F)***
Intercept	3,3149	1	198,4282	7,10E-29
Strain	0,2441	3	4,8702	2,95E-03
ZnO	0,5805	1	34,7503	2,55E-08
Radiation	0,5271	2	15,7751	6,39E-07
Stress	0,0209	2	0,6250	5,37E-01
Strain:ZnO	0,9078	3	18,1133	4,99E-10
Strain:Radiation	0,6732	6	6,7159	2,74E-06
ZnO:Radiation	1,6254	2	48,6475	7,22E-17
Strain:Stress	0,1187	6	1,1843	3,18E-01

ZnO:Stress	0,3034	2	9,0822	1,93E-04
Radiation:Stress	0,3627	4	5,4276	4,24E-04
Strain:ZnO:Radiation	1,5089	6	15,0539	2,50E-13
Strain:ZnO:Stress	0,7122	6	7,1058	1,20E-06
Strain:Radiation:Stress	0,6055	12	3,0205	8,31E-04
ZnO:Radiation:Stress	1,5837	4	23,6997	4,52E-15
Strain:ZnO:Radiation:Stress	1,7080	12	8,5202	4,51E-12
Residual	2,4056	144		

Table S3. ANOVA summary for germination speed index (GSI) of *Eruca sativa* under saline stress

	Sum_sq	***Df***	***F***	***PR(>F)***
Intercept	1377,3061	1	295,4693	1,04E-36
Strain	424,1031	3	30,3272	2,95E-15
ZnO	1,3538	1	0,2904	5,91E-01
Radiation	231,8878	2	24,8731	5,26E-10
Stress	324,6615	2	34,8243	4,61E-13
Strain:ZnO	103,3353	3	7,3894	1,22E-04
Strain:Radiation	145,8144	6	5,2135	6,96E-05
ZnO:Radiation	43,7053	2	4,6880	1,07E-02
Strain:Stress	516,2547	6	18,4584	7,68E-16
ZnO:Stress	130,0081	2	13,9451	2,91E-06
Radiation:Stress	1071,0413	4	57,4418	6,77E-29
Strain:ZnO:Radiation	65,1742	6	2,3303	3,54E-02
Strain:ZnO:Stress	160,7790	6	5,7486	2,18E-05
Strain:Radiation:Stress	789,0557	12	14,1061	4,79E-19
ZnO:Radiation:Stress	193,7516	4	10,3912	2,01E-07
Strain:ZnO:Radiation:Stress	298,3883	12	5,3344	2,02E-07
Residual	671,2442	144		

Table S4. ANOVA summary for germination speed index (GSI) of *Eruca sativa* under osmotic stress

	Sum_sq	***Df***	***F***	***PR(>F)***
Intercept	63,4800	1	18,0617	3,82E-05
Strain	194,0431	3	18,4034	3,66E-10
ZnO	60,9928	1	17,3540	5,32E-05
Radiation	525,3267	2	74,7343	5,47E-23
Stress	431,4518	2	61,3795	5,27E-20
Strain:ZnO	36,8131	3	3,4914	1,74E-02
Strain:Radiation	475,6487	6	22,5557	1,25E-18
ZnO:Radiation	751,5625	2	106,9193	3,44E-29
Strain:Stress	442,2993	6	20,9742	1,39E-17
ZnO:Stress	40,4174	2	5,7499	3,96E-03

Radiation:Stress	555,0573	4	39,4820	2,73E-22
Strain:ZnO:Radiation	669,4140	6	31,7442	3,98E-24
Strain:ZnO:Stress	89,9230	6	4,2642	5,51E-04
Strain:Radiation:Stress	460,7767	12	10,9252	3,01E-15
ZnO:Radiation:Stress	698,2454	4	49,6671	3,33E-26
Strain:ZnO:Radiation:Stress	681,9683	12	16,1698	2,69E-21
Residual	506,1063	144		

Table S5. Dunnett's post hoc test comparing germination percentage (%G) under saline stress

Treatment	***Mean***	***Difference vs. control***	***p-value***
PSR_33_Absent_ZnO_Environmental_UV_0 mM	0,5878	-0,5528	0,0005
PSR_33_Present_ZnO_Environmental_UV_0 mM	0,9570	-0,1835	0,2321
PSR_33_Absent_ZnO_UVC_0 mM	0,9409	-0,1996	0,1948
PSR_33_Present_ZnO_UVC_0 mM	0,9280	-0,2125	0,1667
PSR_33_Absent_ZnO_Absent_UV_0 mM	0,9391	-0,2015	0,1900
PSR_33_Present_ZnO_Absent_UV_0 mM	1,0770	-0,0635	0,6774
PSR_33_Absent_ZnO_Environmental_UV_50 mM	1,1833	0,0428	0,7798
PSR_33_Present_ZnO_Environmental_UV_50 mM	0,5324	-0,6081	0,0002
PSR_33_Absent_ZnO_UVC_50 mM	0,4143	-0,7262	0,0000
PSR_33_Present_ZnO_UVC_50 mM	1,0402	-0,1003	0,5119
PSR_33_Absent_ZnO_Absent_UV_50 mM	0,4291	-0,7115	0,0000
PSR_33_Present_ZnO_Absent_UV_50 mM	1,0512	-0,0893	0,5596
PSR_33_Absent_ZnO_Environmental_UV_150 mM	0,7353	-0,4052	0,0095
PSR_33_Present_ZnO_Environmental_UV_150 mM	1,0049	-0,1356	0,3757
PSR_33_Absent_ZnO_UVC_150 mM	0,9379	-0,2026	0,1870
PSR_33_Present_ZnO_UVC_150 mM	1,0618	-0,0787	0,6065
PSR_33_Absent_ZnO_Absent_UV_150 mM	0,9416	-0,1989	0,1966
PSR_33_Present_ZnO_Absent_UV_150 mM	0,9644	-0,1762	0,2506
PSR_34_Absent_ZnO_Environmental_UV_0 mM	0,9128	-0,2277	0,1391
PSR_34_Present_ZnO_Environmental_UV_0 mM	1,2305	0,0900	0,5568
PSR_34_Absent_ZnO_UVC_0 mM	1,1027	-0,0378	0,8060
PSR_34_Present_ZnO_UVC_0 mM	1,3310	0,1905	0,2186
PSR_34_Absent_ZnO_Absent_UV_0 mM	0,5496	-0,5909	0,0002
PSR_34_Present_ZnO_Absent_UV_0 mM	1,2617	0,1212	0,4349
PSR_34_Absent_ZnO_Environmental_UV_50 mM	0,6493	-0,4912	0,0019
PSR_34_Present_ZnO_Environmental_UV_50 mM	1,4205	0,2799	0,0707
PSR_34_Absent_ZnO_UVC_50 mM	0,9748	-0,1657	0,2802
PSR_34_Present_ZnO_UVC_50 mM	1,4956	0,3551	0,0228
PSR_34_Absent_ZnO_Absent_UV_50 mM	0,8110	-0,3296	0,0341
PSR_34_Present_ZnO_Absent_UV_50 mM	1,2879	0,1474	0,3368
PSR_34_Absent_ZnO_Environmental_UV_150 mM	0,7346	-0,4059	0,0095
PSR_34_Present_ZnO_Environmental_UV_150 mM	1,3884	0,2479	0,1094
PSR_34_Absent_ZnO_UVC_150 mM	0,5003	-0,6402	0,0001
PSR_34_Present_ZnO_UVC_150 mM	1,3458	0,2052	0,1850

PSR_34_Absent_ZnO_Absent_UV_150 mM	0,6833	-0,4573	0,0037
PSR_34_Present_ZnO_Absent_UV_150 mM	1,0285	-0,1120	0,4639
PSR_37_Absent_ZnO_Environmental_UV_0 mM	1,4956	0,3551	0,0228
PSR_37_Present_ZnO_Environmental_UV_0 mM	1,2237	0,0832	0,5861
PSR_37_Absent_ZnO_UVC_0 mM	1,4956	0,3551	0,0228
PSR_37_Present_ZnO_UVC_0 mM	1,3090	0,1685	0,2771
PSR_37_Absent_ZnO_Absent_UV_0 mM	1,1984	0,0579	0,7047
PSR_37_Present_ZnO_Absent_UV_0 mM	1,2959	0,1554	0,3106
PSR_37_Absent_ZnO_Environmental_UV_50 mM	1,4635	0,3230	0,0384
PSR_37_Present_ZnO_Environmental_UV_50 mM	1,1952	0,0546	0,7223
PSR_37_Absent_ZnO_UVC_50 mM	1,4382	0,2977	0,0567
PSR_37_Present_ZnO_UVC_50 mM	1,5708	0,4303	0,0060
PSR_37_Absent_ZnO_Absent_UV_50 mM	1,3963	0,2557	0,1031
PSR_37_Present_ZnO_Absent_UV_50 mM	1,4205	0,2799	0,0707
PSR_37_Absent_ZnO_Environmental_UV_150 mM	0,9215	-0,2191	0,1546
PSR_37_Present_ZnO_Environmental_UV_150 mM	1,1952	0,0546	0,7223
PSR_37_Absent_ZnO_UVC_150 mM	0,9948	-0,1457	0,3424
PSR_37_Present_ZnO_UVC_150 mM	1,1764	0,0359	0,8142
PSR_37_Absent_ZnO_Absent_UV_150 mM	0,8110	-0,3296	0,0341
PSR_37_Present_ZnO_Absent_UV_150 mM	1,3631	0,2225	0,1510
PSR_51_Absent_ZnO_Environmental_UV_0 mM	1,1764	0,0359	0,8142
PSR_51_Present_ZnO_Environmental_UV_0 mM	1,2138	0,0733	0,6328
PSR_51_Absent_ZnO_UVC_0 mM	1,2558	0,1153	0,4516
PSR_51_Present_ZnO_UVC_0 mM	1,3310	0,1905	0,2186
PSR_51_Absent_ZnO_Absent_UV_0 mM	1,3132	0,1727	0,2602
PSR_51_Present_ZnO_Absent_UV_0 mM	1,2459	0,1054	0,4931
PSR_51_Absent_ZnO_Environmental_UV_50 mM	1,4635	0,3230	0,0384
PSR_51_Present_ZnO_Environmental_UV_50 mM	1,3884	0,2479	0,1094
PSR_51_Absent_ZnO_UVC_50 mM	1,0980	-0,0425	0,7816
PSR_51_Present_ZnO_UVC_50 mM	1,2237	0,0832	0,5861
PSR_51_Absent_ZnO_Absent_UV_50 mM	1,4956	0,3551	0,0228
PSR_51_Present_ZnO_Absent_UV_50 mM	1,1301	-0,0105	0,9458
PSR_51_Absent_ZnO_Environmental_UV_150 mM	1,2305	0,0900	0,5568
PSR_51_Present_ZnO_Environmental_UV_150 mM	1,0990	-0,0416	0,7855
PSR_51_Absent_ZnO_UVC_150 mM	1,2811	0,1406	0,3586
PSR_51_Present_ZnO_UVC_150 mM	1,0905	-0,0501	0,7435
PSR_51_Absent_ZnO_Absent_UV_150 mM	1,3884	0,2479	0,1094
PSR_51_Present_ZnO_Absent_UV_150 mM	1,1544	0,0139	0,9274

Table S6. Dunnett's post hoc test comparing germination percentage (%G) under osmotic stress

Treatment	*Mean*	*Difference vs. control*	*p-value*
PSR_33_Absent_ZnO_Environmental_UV_0 mPa	0,5878	-0,5528	0,0000
PSR_33_Present_ZnO_Environmental_UV_0 mPa	0,9570	-0,1835	0,0314
PSR_33_Absent_ZnO_UVC_0 mPa	0,9409	-0,1996	0,0754
PSR_33_Present_ZnO_UVC_0 mPa	0,9280	-0,2125	0,0001
PSR_33_Absent_ZnO_Absent_UV_0 mPa	0,9391	-0,2015	0,0197
PSR_33_Present_ZnO_Absent_UV_0 mPa	1,0770	-0,0635	0,0835
PSR_33_Absent_ZnO_Environmental_UV_-0.5 mPa	1,1871	0,0466	0,3325
PSR_33_Present_ZnO_Environmental_UV_-0.5 mPa	1,2031	0,0625	0,7685
PSR_33_Absent_ZnO_UVC_-0.5 mPa	0,9649	-0,1756	0,0041
PSR_33_Present_ZnO_UVC_-0.5 mPa	0,9880	-0,1525	0,1711
PSR_33_Absent_ZnO_Absent_UV_-0.5 mPa	1,0394	-0,1011	0,4229
PSR_33_Present_ZnO_Absent_UV_-0.5 mPa	0,6100	-0,5305	0,0079
PSR_33_Absent_ZnO_Environmental_UV_-1.5 mPa	1,1810	0,0405	0,6019
PSR_33_Present_ZnO_Environmental_UV_-1.5 mPa	1,2445	0,1040	0,2128
PSR_33_Absent_ZnO_UVC_-1.5 mPa	1,0390	-0,1015	0,0709
PSR_33_Present_ZnO_UVC_-1.5 mPa	0,6568	-0,4837	0,0085
PSR_33_Absent_ZnO_Absent_UV_-1.5 mPa	0,9291	-0,2114	0,0000
PSR_33_Present_ZnO_Absent_UV_-1.5 mPa	0,8874	-0,2531	0,0167
PSR_34_Absent_ZnO_Environmental_UV_0 mPa	0,9128	-0,2277	0,0120
PSR_34_Present_ZnO_Environmental_UV_0 mPa	1,2305	0,0900	0,2531
PSR_34_Absent_ZnO_UVC_0 mPa	1,1027	-0,0378	0,7693
PSR_34_Present_ZnO_UVC_0 mPa	1,3310	0,1905	0,2549
PSR_34_Absent_ZnO_Absent_UV_0 mPa	0,5496	-0,5909	0,0006
PSR_34_Present_ZnO_Absent_UV_0 mPa	1,2617	0,1212	0,5170
PSR_34_Absent_ZnO_Environmental_UV_-0.5 mPa	1,2272	0,0867	0,5429
PSR_34_Present_ZnO_Environmental_UV_-0.5 mPa	1,4162	0,2757	0,2128
PSR_34_Absent_ZnO_UVC_-0.5 mPa	0,6580	-0,4825	0,0006
PSR_34_Present_ZnO_UVC_-0.5 mPa	1,4162	0,2757	0,2128
PSR_34_Absent_ZnO_Absent_UV_-0.5 mPa	0,6996	-0,4409	0,0322
PSR_34_Present_ZnO_Absent_UV_-0.5 mPa	1,1764	0,0359	0,5160
PSR_34_Absent_ZnO_Environmental_UV_-1.5 mPa	0,7269	-0,4136	0,0000
PSR_34_Present_ZnO_Environmental_UV_-1.5 mPa	1,3411	0,2006	0,2700
PSR_34_Absent_ZnO_UVC_-1.5 mPa	1,1585	0,0180	0,8797
PSR_34_Present_ZnO_UVC_-1.5 mPa	1,2959	0,1554	0,0042
PSR_34_Absent_ZnO_Absent_UV_-1.5 mPa	0,7856	-0,3550	0,0046
PSR_34_Present_ZnO_Absent_UV_-1.5 mPa	1,2637	0,1232	0,5186
PSR_37_Absent_ZnO_Environmental_UV_0 mPa	1,4956	0,3551	0,0269
PSR_37_Present_ZnO_Environmental_UV_0 mPa	1,2237	0,0832	0,0598
PSR_37_Absent_ZnO_UVC_0 mPa	1,4956	0,3551	0,0269
PSR_37_Present_ZnO_UVC_0 mPa	1,3090	0,1685	0,3436
PSR_37_Absent_ZnO_Absent_UV_0 mPa	1,1984	0,0579	0,1733

PSR_37_Present_ZnO_Absent_UV_0 mPa	1,2959	0,1554	0,0042
PSR_37_Absent_ZnO_Environmental_UV_-0.5 mPa	1,2879	0,1474	0,1003
PSR_37_Present_ZnO_Environmental_UV_-0.5 mPa	1,3310	0,1905	0,2549
PSR_37_Absent_ZnO_UVC_-0.5 mPa	1,4162	0,2757	0,2128
PSR_37_Present_ZnO_UVC_-0.5 mPa	1,3310	0,1905	0,2549
PSR_37_Absent_ZnO_Absent_UV_-0.5 mPa	1,3884	0,2479	0,1093
PSR_37_Present_ZnO_Absent_UV_-0.5 mPa	1,4635	0,3230	0,0843
PSR_37_Absent_ZnO_Environmental_UV_-1.5 mPa	1,0527	-0,0878	0,3268
PSR_37_Present_ZnO_Environmental_UV_-1.5 mPa	1,0355	-0,1051	0,3331
PSR_37_Absent_ZnO_UVC_-1.5 mPa	1,2031	0,0625	0,7685
PSR_37_Present_ZnO_UVC_-1.5 mPa	1,0307	-0,1098	0,1364
PSR_37_Absent_ZnO_Absent_UV_-1.5 mPa	1,3563	0,2158	0,1738
PSR_37_Present_ZnO_Absent_UV_-1.5 mPa	0,8793	-0,2612	0,0000
PSR_51_Absent_ZnO_Environmental_UV_0 mPa	1,1764	0,0359	0,5160
PSR_51_Present_ZnO_Environmental_UV_0 mPa	1,2138	0,0733	0,4982
PSR_51_Absent_ZnO_UVC_0 mPa	1,2558	0,1153	0,1240
PSR_51_Present_ZnO_UVC_0 mPa	1,3310	0,1905	0,2549
PSR_51_Absent_ZnO_Absent_UV_0 mPa	1,3132	0,1727	0,0057
PSR_51_Present_ZnO_Absent_UV_0 mPa	1,2459	0,1054	0,4019
PSR_51_Absent_ZnO_Environmental_UV_-0.5 mPa	1,2085	0,0680	0,4480
PSR_51_Present_ZnO_Environmental_UV_-0.5 mPa	1,4162	0,2757	0,2128
PSR_51_Absent_ZnO_UVC_-0.5 mPa	1,4635	0,3230	0,0843
PSR_51_Present_ZnO_UVC_-0.5 mPa	1,3563	0,2158	0,1738
PSR_51_Absent_ZnO_Absent_UV_-0.5 mPa	1,3884	0,2479	0,1093
PSR_51_Present_ZnO_Absent_UV_-0.5 mPa	1,1092	-0,0313	0,8187
PSR_51_Absent_ZnO_Environmental_UV_-1.5 mPa	1,2459	0,1054	0,4019
PSR_51_Present_ZnO_Environmental_UV_-1.5 mPa	1,3411	0,2006	0,2700
PSR_51_Absent_ZnO_UVC_-1.5 mPa	1,1564	0,0159	0,8249
PSR_51_Present_ZnO_UVC_-1.5 mPa	1,2558	0,1153	0,1240
PSR_51_Absent_ZnO_Absent_UV_-1.5 mPa	1,4635	0,3230	0,0843
PSR_51_Present_ZnO_Absent_UV_-1.5 mPa	1,3884	0,2479	0,1093

Table S7. Dunnett's post hoc test comparing germination speed index (GSI) under saline stress

Treatment	*Mean*	*Difference vs. control*	*p-value*
PSR_33_Absent_ZnO_Environmental_UV_0 mM	6,1500	-4,3126	0,1578
PSR_33_Present_ZnO_Environmental_UV_0 mM	9,0500	-1,4126	0,6426
PSR_33_Absent_ZnO_UVC_0 mM	18,6767	8,2140	0,0083
PSR_33_Present_ZnO_UVC_0 mM	14,2100	3,7474	0,2189
PSR_33_Absent_ZnO_Absent_UV_0 mM	20,4767	10,0140	0,0019
PSR_33_Present_ZnO_Absent_UV_0 mM	21,4267	10,9640	0,0006
PSR_33_Absent_ZnO_Environmental_UV_50 mM	25,1333	14,6707	0,0000
PSR_33_Present_ZnO_Environmental_UV_50 mM	30,3000	19,8374	0,0000
PSR_33_Absent_ZnO_UVC_50 mM	13,5267	3,0640	0,3152
PSR_33_Present_ZnO_UVC_50 mM	17,1133	6,6507	0,0310
PSR_33_Absent_ZnO_Absent_UV_50 mM	18,3267	7,8640	0,0115
PSR_33_Present_ZnO_Absent_UV_50 mM	6,7500	-3,7126	0,2243
PSR_33_Absent_ZnO_Environmental_UV_150 mM	22,3867	11,9240	0,0002
PSR_33_Present_ZnO_Environmental_UV_150 mM	26,3267	15,8640	0,0000
PSR_33_Absent_ZnO_UVC_150 mM	6,1600	-4,3026	0,1593
PSR_33_Present_ZnO_UVC_150 mM	12,6667	2,2040	0,4681
PSR_33_Absent_ZnO_Absent_UV_150 mM	15,0100	4,5474	0,1371
PSR_33_Present_ZnO_Absent_UV_150 mM	13,2067	2,7440	0,3678
PSR_34_Absent_ZnO_Environmental_UV_0 mM	4,9000	-5,5626	0,0699
PSR_34_Present_ZnO_Environmental_UV_0 mM	5,7433	-4,7193	0,1227
PSR_34_Absent_ZnO_UVC_0 mM	6,5600	-3,9026	0,2008
PSR_34_Present_ZnO_UVC_0 mM	7,8700	-2,5926	0,3939
PSR_34_Absent_ZnO_Absent_UV_0 mM	2,2767	-8,1860	0,0084
PSR_34_Present_ZnO_Absent_UV_0 mM	7,3667	-3,0960	0,3095
PSR_34_Absent_ZnO_Environmental_UV_50 mM	7,9400	-2,5226	0,4067
PSR_34_Present_ZnO_Environmental_UV_50 mM	14,7900	4,3274	0,1581
PSR_34_Absent_ZnO_UVC_50 mM	2,0367	-8,4260	0,0068
PSR_34_Present_ZnO_UVC_50 mM	16,2767	5,8140	0,0583
PSR_34_Absent_ZnO_Absent_UV_50 mM	4,5167	-5,9460	0,0532
PSR_34_Present_ZnO_Absent_UV_50 mM	11,2200	0,7574	0,8029
PSR_34_Absent_ZnO_Environmental_UV_150 mM	3,0567	-7,4060	0,0166
PSR_34_Present_ZnO_Environmental_UV_150 mM	13,7500	3,2874	0,2811
PSR_34_Absent_ZnO_UVC_150 mM	9,4567	-1,0060	0,7402
PSR_34_Present_ZnO_UVC_150 mM	7,1100	-3,3526	0,2713
PSR_34_Absent_ZnO_Absent_UV_150 mM	4,9300	-5,5326	0,0713
PSR_34_Present_ZnO_Absent_UV_150 mM	6,6600	-3,8026	0,2125
PSR_37_Absent_ZnO_Environmental_UV_0 mM	14,2800	3,8174	0,2126
PSR_37_Present_ZnO_Environmental_UV_0 mM	10,3167	-0,1460	0,9616
PSR_37_Absent_ZnO_UVC_0 mM	13,8000	3,3374	0,2740
PSR_37_Present_ZnO_UVC_0 mM	10,3600	-0,1026	0,9730
PSR_37_Absent_ZnO_Absent_UV_0 mM	11,7833	1,3207	0,6642

PSR_37_Present_ZnO_Absent_UV_0 mM	12,6767	2,2140	0,4661
PSR_37_Absent_ZnO_Environmental_UV_50 mM	16,0267	5,5640	0,0699
PSR_37_Present_ZnO_Environmental_UV_50 mM	12,2100	1,7474	0,5653
PSR_37_Absent_ZnO_UVC_50 mM	16,6000	6,1374	0,0460
PSR_37_Present_ZnO_UVC_50 mM	13,5033	3,0407	0,3193
PSR_37_Absent_ZnO_Absent_UV_50 mM	16,2367	5,7740	0,0606
PSR_37_Present_ZnO_Absent_UV_50 mM	12,7600	2,2974	0,4510
PSR_37_Absent_ZnO_Environmental_UV_150 mM	9,7500	-0,7126	0,8144
PSR_37_Present_ZnO_Environmental_UV_150 mM	7,3467	-3,1160	0,3059
PSR_37_Absent_ZnO_UVC_150 mM	10,2067	-0,2560	0,9328
PSR_37_Present_ZnO_UVC_150 mM	9,5233	-0,9393	0,7571
PSR_37_Absent_ZnO_Absent_UV_150 mM	11,6000	1,1374	0,7078
PSR_37_Present_ZnO_Absent_UV_150 mM	8,7067	-1,7560	0,5629
PSR_51_Absent_ZnO_Environmental_UV_0 mM	10,4667	0,0040	0,9989
PSR_51_Present_ZnO_Environmental_UV_0 mM	6,0967	-4,3660	0,1528
PSR_51_Absent_ZnO_UVC_0 mM	10,4933	0,0307	0,9919
PSR_51_Present_ZnO_UVC_0 mM	6,7533	-3,7093	0,2237
PSR_51_Absent_ZnO_Absent_UV_0 mM	12,9000	2,4374	0,4234
PSR_51_Present_ZnO_Absent_UV_0 mM	6,4700	-3,9926	0,1909
PSR_51_Absent_ZnO_Environmental_UV_50 mM	13,5533	3,0907	0,3104
PSR_51_Present_ZnO_Environmental_UV_50 mM	12,8733	2,4107	0,4282
PSR_51_Absent_ZnO_UVC_50 mM	15,9400	5,4774	0,0741
PSR_51_Present_ZnO_UVC_50 mM	12,8900	2,4274	0,4249
PSR_51_Absent_ZnO_Absent_UV_50 mM	16,8900	6,4274	0,0371
PSR_51_Present_ZnO_Absent_UV_50 mM	14,5600	4,0974	0,1837
PSR_51_Absent_ZnO_Environmental_UV_150 mM	12,2200	1,7574	0,5636
PSR_51_Present_ZnO_Environmental_UV_150 mM	11,3867	0,9240	0,7607
PSR_51_Absent_ZnO_UVC_150 mM	9,7733	-0,6893	0,8207
PSR_51_Present_ZnO_UVC_150 mM	10,6700	0,2074	0,9457
PSR_51_Absent_ZnO_Absent_UV_150 mM	16,6667	6,2040	0,0442
PSR_51_Present_ZnO_Absent_UV_150 mM	14,6133	4,1507	0,1743

Table S8. Dunnett's post hoc test comparing germination speed index (GSI) under osmotic stress

Treatment	*Mean*	*Difference vs. control*	*p-value*
PSR_33_Absent_ZnO_Environmental_UV_0 mPa	6,1500	-4,3126	0,1578
PSR_33_Present_ZnO_Environmental_UV_0 mPa	9,0500	-1,4126	0,6426
PSR_33_Absent_ZnO_UVC_0 mPa	18,6767	8,2140	0,0083
PSR_33_Present_ZnO_UVC_0 mPa	14,2100	3,7474	0,2189
PSR_33_Absent_ZnO_Absent_UV_0 mPa	20,4767	10,0140	0,0019
PSR_33_Present_ZnO_Absent_UV_0 mPa	21,4267	10,9640	0,0006
PSR_33_Absent_ZnO_Environmental_UV_-0.5 mPa	18,0500	7,5874	0,0151
PSR_33_Present_ZnO_Environmental_UV_-0.5 mPa	6,1667	-4,2960	0,1601
PSR_33_Absent_ZnO_UVC_-0.5 mPa	3,6667	-6,7960	0,0278
PSR_33_Present_ZnO_UVC_-0.5 mPa	21,5333	11,0707	0,0005
PSR_33_Absent_ZnO_Absent_UV_-0.5 mPa	10,9767	0,5140	0,8658
PSR_33_Present_ZnO_Absent_UV_-0.5 mPa	4,6000	-5,8626	0,0571
PSR_33_Absent_ZnO_Environmental_UV_-1.5 mPa	9,3900	-1,0726	0,7236
PSR_33_Present_ZnO_Environmental_UV_-1.5 mPa	18,2500	7,7874	0,0121
PSR_33_Absent_ZnO_UVC_-1.5 mPa	11,8767	1,4140	0,6424
PSR_33_Present_ZnO_UVC_-1.5 mPa	18,8700	8,4074	0,0070
PSR_33_Absent_ZnO_Absent_UV_-1.5 mPa	17,9600	7,4974	0,0162
PSR_33_Present_ZnO_Absent_UV_-1.5 mPa	14,8500	4,3874	0,1509
PSR_34_Absent_ZnO_Environmental_UV_0 mPa	4,9000	-5,5626	0,0699
PSR_34_Present_ZnO_Environmental_UV_0 mPa	5,7433	-4,7193	0,1227
PSR_34_Absent_ZnO_UVC_0 mPa	6,5600	-3,9026	0,2008
PSR_34_Present_ZnO_UVC_0 mPa	7,8700	-2,5926	0,3939
PSR_34_Absent_ZnO_Absent_UV_0 mPa	2,2767	-8,1860	0,0084
PSR_34_Present_ZnO_Absent_UV_0 mPa	7,3667	-3,0960	0,3095
PSR_34_Absent_ZnO_Environmental_UV_-0.5 mPa	2,0367	-8,4260	0,0068
PSR_34_Present_ZnO_Environmental_UV_-0.5 mPa	14,7700	4,3074	0,1583
PSR_34_Absent_ZnO_UVC_-0.5 mPa	10,1200	-0,3426	0,9100
PSR_34_Present_ZnO_UVC_-0.5 mPa	15,8267	5,3640	0,0800
PSR_34_Absent_ZnO_Absent_UV_-0.5 mPa	6,4800	-3,9826	0,1917
PSR_34_Present_ZnO_Absent_UV_-0.5 mPa	5,9800	-4,4826	0,1424
PSR_34_Absent_ZnO_Environmental_UV_-1.5 mPa	2,8567	-7,6060	0,0140
PSR_34_Present_ZnO_Environmental_UV_-1.5 mPa	5,8167	-4,6460	0,1285
PSR_34_Absent_ZnO_UVC_-1.5 mPa	1,1800	-9,2826	0,0030
PSR_34_Present_ZnO_UVC_-1.5 mPa	9,5167	-0,9460	0,7553
PSR_34_Absent_ZnO_Absent_UV_-1.5 mPa	3,7167	-6,7460	0,0290
PSR_34_Present_ZnO_Absent_UV_-1.5 mPa	5,4967	-4,9660	0,1046
PSR_37_Absent_ZnO_Environmental_UV_0 mPa	14,2800	3,8174	0,2126
PSR_37_Present_ZnO_Environmental_UV_0 mPa	10,3167	-0,1460	0,9616
PSR_37_Absent_ZnO_UVC_0 mPa	13,8000	3,3374	0,2740
PSR_37_Present_ZnO_UVC_0 mPa	10,3600	-0,1026	0,9730
PSR_37_Absent_ZnO_Absent_UV_0 mPa	11,7833	1,3207	0,6642

PSR_37_Present_ZnO_Absent_UV_0 mPa	12,6767	2,2140	0,4661
PSR_37_Absent_ZnO_Environmental_UV_-0.5 mPa	16,1033	5,6407	0,0661
PSR_37_Present_ZnO_Environmental_UV_-0.5 mPa	10,4333	-0,0293	0,9923
PSR_37_Absent_ZnO_UVC_-0.5 mPa	14,3767	3,9140	0,1998
PSR_37_Present_ZnO_UVC_-0.5 mPa	15,3433	4,8807	0,1107
PSR_37_Absent_ZnO_Absent_UV_-0.5 mPa	14,9667	4,5040	0,1406
PSR_37_Present_ZnO_Absent_UV_-0.5 mPa	14,2767	3,8140	0,2130
PSR_37_Absent_ZnO_Environmental_UV_-1.5 mPa	7,1733	-3,2893	0,2801
PSR_37_Present_ZnO_Environmental_UV_-1.5 mPa	6,3000	-4,1626	0,1726
PSR_37_Absent_ZnO_UVC_-1.5 mPa	6,7267	-3,7360	0,2203
PSR_37_Present_ZnO_UVC_-1.5 mPa	11,5500	1,0874	0,7209
PSR_37_Absent_ZnO_Absent_UV_-1.5 mPa	4,3700	-6,0926	0,0477
PSR_37_Present_ZnO_Absent_UV_-1.5 mPa	12,5333	2,0707	0,4959
PSR_51_Absent_ZnO_Environmental_UV_0 mPa	10,4667	0,0040	0,9989
PSR_51_Present_ZnO_Environmental_UV_0 mPa	6,0967	-4,3660	0,1528
PSR_51_Absent_ZnO_UVC_0 mPa	10,4933	0,0307	0,9919
PSR_51_Present_ZnO_UVC_0 mPa	6,7533	-3,7093	0,2237
PSR_51_Absent_ZnO_Absent_UV_0 mPa	12,9000	2,4374	0,4234
PSR_51_Present_ZnO_Absent_UV_0 mPa	6,4700	-3,9926	0,1909
PSR_51_Absent_ZnO_Environmental_UV_-0.5 mPa	16,6667	6,2040	0,0442
PSR_51_Present_ZnO_Environmental_UV_-0.5 mPa	14,6133	4,1507	0,1743
PSR_51_Absent_ZnO_UVC_-0.5 mPa	13,4800	3,0174	0,3221
PSR_51_Present_ZnO_UVC_-0.5 mPa	11,1667	0,7040	0,8167
PSR_51_Absent_ZnO_Absent_UV_-0.5 mPa	16,1667	5,7040	0,0636
PSR_51_Present_ZnO_Absent_UV_-0.5 mPa	11,9167	1,4540	0,6318
PSR_51_Absent_ZnO_Environmental_UV_-1.5 mPa	14,3167	3,8540	0,2069
PSR_51_Present_ZnO_Environmental_UV_-1.5 mPa	7,6633	-2,7993	0,3580
PSR_51_Absent_ZnO_UVC_-1.5 mPa	14,0667	3,6040	0,2373
PSR_51_Present_ZnO_UVC_-1.5 mPa	9,4100	-1,0526	0,7286
PSR_51_Absent_ZnO_Absent_UV_-1.5 mPa	12,0100	1,5474	0,6106
PSR_51_Present_ZnO_Absent_UV_-1.5 mPa	7,9767	-2,4860	0,4139

4 ARTIGO 3

Extremophilic *Arthrobacter koreensis* and ZnO crystals modulate early seedling growth and biomass allocation of Eruca sativa under salinity and osmotic stress

ABSTRACT

Microbial biostimulants capable of enhancing early plant establishment under abiotic stress are of increasing interest for sustainable agriculture. Extremophilic microorganisms isolated from photovoltaic panels exhibit exceptional tolerance to radiation and desiccation-associated stresses, traits that may confer functional advantages when applied to plants under adverse conditions. In this study, we evaluated the effects of the extremophilic bacterium *Arthrobacter koreensis* on early seedling growth and biomass allocation of *Eruca sativa* cultivated in soil under saline and osmotic stress, in the presence or absence of zinc oxide (ZnO) crystals and under different radiation regimes. Seedlings were grown for 30 days, and growth parameters including leaf area, shoot and root length, and fresh and dry biomass were assessed. Multifactorial ANOVA revealed significant interactions among microbial inoculation, ZnO supplementation, radiation exposure, and stress intensity, indicating strongly context-dependent effects on plant performance. In general, *A. koreensis* promoted shoot development and biomass accumulation under moderate stress conditions, whereas severe stress constrained plant growth regardless of treatment. ZnO crystals further modulated these responses, depending on stress type and radiation regime. Biomass allocation patterns indicated increased root investment under osmotic stress, partially mitigated by microbial inoculation. Together, these findings demonstrate that extremophilic microorganisms can function as conditional biostimulants during early seedling establishment and highlight the importance of environmental context when evaluating microbe–nanomaterial–plant interactions in soil systems.

Keywords: plant growth-promoting microorganisms, abiotic stress, extremophilic bacteria, zinc oxide, biomass allocation

3.1 INTRODUCTION

Abiotic stresses are among the main limiting factors for crop establishment and productivity worldwide, particularly in regions affected by salinity and water deficit. These stresses impair plant growth at multiple developmental stages, from seed germination to early seedling establishment,

ultimately compromising biomass accumulation and yield (Lei et al. 2021; Nowicki et al. 2025).While seed germination represents a critical initial checkpoint for plant survival, successful crop establishment depends on the capacity of seedlings to sustain growth, maintain biomass allocation, and adapt morphophysiologically under adverse environmental conditions (Wang et al. 2019; Suneja et al. 2019; Bao et al. 2025).

Salinity stress exerts a dual constraint on plant development, combining osmotic stress with ion toxicity. Excessive Na^+ and Cl^- accumulation disrupts cellular homeostasis, impairs nutrient uptake, and reduces photosynthetic efficiency, leading to growth inhibition and premature senescence (Hanin et al. 2016; Mahmood et al. 2024; Tripathi et al. 2025). In contrast, osmotic stress induced by water deficit primarily affects plant water relations, cell expansion, and turgor maintenance, triggering adaptive responses such as altered root architecture, reduced leaf expansion, and reprogramming of biomass allocation. Although both stresses reduce plant growth, their physiological bases differ substantially, and strategies effective against one stress are not necessarily transferable to the other (Barcia et al. 2014; Álvarez and Sánchez-Blanco 2015).

In recent years, plant growth-promoting microorganisms (PGPMs) have emerged as promising tools to enhance plant tolerance to abiotic stress. These microorganisms can improve plant performance through multiple mechanisms, including phytohormone production, modulation of antioxidant systems, synthesis of osmoprotective compounds, and improvement of nutrient and water acquisition (Khan et al. 2020; Dagher et al. 2025). However, the efficacy of PGPMs is often strain-specific and highly dependent on environmental context, highlighting the importance of selecting microorganisms with intrinsic stress tolerance and adaptive capabilities.

Extremophilic microorganisms constitute a particularly attractive but still underexplored resource for agricultural applications. These organisms thrive in environments characterized by intense radiation, desiccation, and temperature fluctuations, such as deserts, polar regions, and artificial extreme habitats. Microbial communities colonizing photovoltaic panel surfaces represent a striking example of such environments, combining high ultraviolet (UV) radiation, thermal stress, and chronic water limitation (Dorado-Morales et al. 2016b; Porcar et al. 2018; Tanner et al. 2019). The selective pressures imposed by these conditions favor microorganisms with robust DNA repair systems, efficient antioxidant defenses, and protective metabolic strategies, traits that are directly

relevant for mitigating abiotic stress in plants (Cimini et al. 2019; Zannier et al. 2022; Straková et al. 2025).

Among these extremophiles, *Arthrobacter koreensis* has been reported as a desiccation-tolerant and plant growth-promoting bacterium, capable of surviving prolonged water deficit and contributing to plant stress resilience (Manzanera et al. 2015). Nevertheless, the potential of extremophilic *Arthrobacter* strains isolated from photovoltaic panels to modulate seedling growth and biomass allocation under abiotic stress remains largely unexplored, particularly under realistic growth conditions such as soil cultivation (Hernández-Fernández et al. 2022)

In parallel, nanomaterials have gained increasing attention as auxiliary tools to enhance plant stress tolerance. Zinc oxide (ZnO) particles are of particular interest due to the essential role of zinc in plant metabolism, including antioxidant enzyme activity, membrane stabilization, and regulation of growth-related processes (Akhtar et al. 2022; Muhae-Ud-Din et al. 2025; El-Shazoly et al. 2025). ZnO has been shown to improve germination, growth, and stress tolerance in several crop species under salinity and drought conditions, either alone or in combination with biological inputs (Abdelkhalik et al. 2025; Ochoa-Chaparro et al. 2025; Das et al. 2025). Rather than acting as a conventional fertilizer, ZnO can function as a physiological modulator, enhancing redox balance and cellular stability during early developmental stages (Rizk et al. 2025; Kumar et al. 2025).

Recent studies suggest that combining plant growth-promoting microorganisms with inorganic materials such as ZnO nanoparticles can produce synergistic effects, amplifying microbial-mediated growth promotion through enhanced physicochemical stress mitigation (Hosseinpour et al. 2020; Akhtar et al. 2022; Shafiq et al. 2022). However, most investigations have focused on seed germination or early seedling assays conducted under highly controlled laboratory conditions. Far fewer studies have evaluated whether such synergistic interactions persist during prolonged growth periods and under more realistic cultivation scenarios, such as soil-grown seedlings exposed to sustained abiotic stress (Alharbi et al. 2023; Verma et al. 2024; Strekalovskaya et al. 2024).

Extremophilic microorganisms isolated from photovoltaic panels have recently attracted attention due to their remarkable tolerance to radiation, desiccation, and nutrient limitation. These

environments host highly diverse microbial communities adapted to intense solar irradiation and prolonged water scarcity, selecting traits associated with oxidative stress management, extracellular polymer production, and metabolic flexibility (Porcar et al. 2018; Tanner et al. 2020; Moura et al. 2021). Such functional attributes may confer advantages when extremophilic microorganisms are applied in plant–soil systems exposed to abiotic stress. Previous studies have demonstrated that extremophilic bacteria and yeasts can enhance seed germination and early vigor under saline and osmotic stress, particularly when combined with zinc oxide (ZnO) nanoparticles or crystals (Mishra et al. 2023; Trzcińska-Wencel et al. 2023; Raklami et al. 2024). However, most available evidence remains restricted to short-term germination assays or simplified growth systems, leaving uncertainty regarding whether these beneficial effects persist during subsequent stages of seedling establishment in soil (Donia and Carbone 2023; Strekalovskaya et al. 2024)

In this context, the present study aimed to evaluate whether the extremophilic *Arthrobacter koreensis* can modulate early seedling growth and biomass allocation of *Eruca sativa* cultivated in soil under saline and osmotic stress, and whether these effects are further influenced by ZnO crystals and radiation exposure. *Arthrobacter* species are known for their desiccation tolerance and plant growth-promoting potential, including stress-related functional traits (Manzanera et al. 2015; Hernández-Fernández et al. 2022). We hypothesized that microbial inoculation would exert context-dependent effects, promoting shoot development and biomass accumulation under moderate stress conditions, whereas severe stress would constrain plant growth regardless of treatment, consistent with established models of plant stress physiology. By extending previous germination-based observations to a soil-grown seedling system, this work seeks to provide a more ecologically relevant assessment of extremophilic microorganisms as conditional biostimulants in stressed agroecosystems.

3.2 MATERIALS AND METHODS

Experimental design

The experiment followed a factorial design comprising 40 treatments resulting from the combination of microbial inoculation (*Arthrobacter koreensis* or non-inoculated control – deionized water), ZnO supplementation (with or without ZnO), radiation pre-treatment (no UV,

enrivonmental-UV, or UV-C), and abiotic stress conditions (saline and osmotic stresses). A detailed description of all treatment combinations is provided in Supplementary Table S1.

Salinity stress was imposed using sodium chloride (NaCl) at concentrations of 50 mM and 150 mM. Osmotic stress was induced using polyethylene glycol (PEG 6000) at osmotic potentials of −0.5 MPa and −1.5 MPa. Non-stressed treatments were included as controls for both stress types. Each treatment consisted of ten biological replicates (n = 10).

Microorganism, ZnO and seed treatment

The extremophilic *A. koreensis* was isolated from photovoltaic panel surfaces and previously characterized for its stress tolerance and germination traits. Details regarding microbial isolation, identification, culture conditions, inoculum preparation, ZnO synthesis and characterization, as well as seed treatment procedures were performed as described in our previous seed germination study.

Briefly, seeds were subjected to microbial inoculation (presence or absence of *A. koreensis*), ZnO supplementation (with or without ZnO), and radiation pre-treatment (no UV, Environmental-UV, or UV-C) prior to sowing. These treatments were selected based on their previously demonstrated effects on seed germination and early stress responses.

Greenhouse conditions and plant cultivation

The experiment was conducted in a greenhouse specifically constructed for this study, measuring 8 m in length, 3 m in width, and 3 m in height. The lateral sides were covered with a white anti-aphid screen (50 mesh), ensuring ventilation while preventing insect infestation. The roof was covered with a translucent polyethylene film (150 μm thickness), allowing natural light penetration while protecting plants from excessive rainfall.

Seeds were sown in black plastic plant bags filled with the characterized agricultural soil and arranged on raised benches inside the greenhouse. After emergence, seedlings were maintained under greenhouse conditions for a growth period of 30 days, corresponding to the fully developed vegetative stage of *Eruca sativa* prior to flowering (Lee et al. 2024). During this period, salinity and osmotic stress treatments were maintained according to the experimental design.

Soil characterization

Seedlings were cultivated in agricultural soil collected from a local cropping area (-23.336103, -47.584014) and chemically characterized prior to use. Soil analysis indicated a pH ($CaCl_2$) of 7.5, high base saturation (96%), and absence of aluminum toxicity (Al^{3+} = 0 mmolc dm^{-3}). The soil presented adequate macronutrient availability, with elevated calcium and potassium levels, as well as sufficient micronutrient contents, supporting plant growth under greenhouse conditions.

Growth and biomass measurements

After 30 days of growth, seedlings were harvested and evaluated for morphophysiological parameters. Shoot length and root length were measured using a digital caliper and expressed in centimeters (cm). Fresh shoot and root biomass were determined immediately after harvest using a semi-analytical balance with a precision of 0.01 g.

For dry biomass determination, shoot and root tissues were oven-dried at 60 °C for 48 h until constant weight and subsequently weighed using the same balance. Leaf area was estimated by selecting one representative leaf per plant and calculating leaf area using the formula:

$$Leaf\ area\ (cm^2) = leaf\ lenght \times leaf\ width \times 0.75$$

where 0.75 corresponds to a correction factor commonly applied for *E. sativa* leaf morphology (Guijarro-Real et al. 2020).

Statistical analysis

Plant growth data were analyzed using multifactorial analysis of variance (ANOVA) to evaluate the effects of microbial inoculation, ZnO crystal supplementation, radiation regime, and stress intensity, as well as their interactions, on all measured variables. When significant main effects or interactions were detected ($p < 0.05$), post hoc comparisons against the respective non-inoculated controls were performed using Dunnett's test. This approach was selected to specifically assess the biostimulant potential of microbial inoculation and ZnO supplementation relative to control treatments, rather than to exhaustively compare all treatment combinations. Statistical analyses were conducted using Python-based statistical libraries, and full ANOVA tables and Dunnett's post hoc test results for all growth parameters are provided in the Supplementary Material.

3.3 RESULTS

A. koreensis and ZnO modulate seedling growth under salinity stress

Plant growth of *Eruca sativa* was significantly affected by the interaction between microbial inoculation (*A. koreensis*), ZnO crystal supplementation, radiation regime, and salinity level (0, 50, and 150 mM NaCl). Multifactorial ANOVA revealed significant main effects and interactions for all evaluated growth parameters ($p < 0.05$), indicating a strong context dependence of plant responses under saline conditions (Supplementary Tables S1–S7).

Leaf area responded consistently to microbial inoculation across salinity levels (Fig. 1). In most treatments, *A. koreensis*-inoculated plants exhibited greater leaf expansion than non-inoculated controls, particularly in the presence of ZnO under no-UV and environmental-UV radiation. Under moderate salinity (50 mM NaCl), inoculated plants maintained higher leaf area even when control plants showed clear reductions. Under UVC exposure, although leaf area was reduced overall, *A. koreensis*-treated plants retained higher values relative to controls, suggesting increased tolerance to the combined effects of salinity and radiation stress.

Figure 1. Leaf area (cm^2) of *Eruca sativa* plants subjected to saline stress (0, 50, and 150 mM NaCl) under different radiation regimes (no UV, UVC, and environmental UV), in the presence or absence of ZnO crystals and inoculated or not with *Arthrobacter koreensis*. Data represent mean ± standard deviation (n = 10). Statistical differences relative to the non-inoculated control were assessed by ANOVA followed by Dunnett's test ($p < 0.05$).

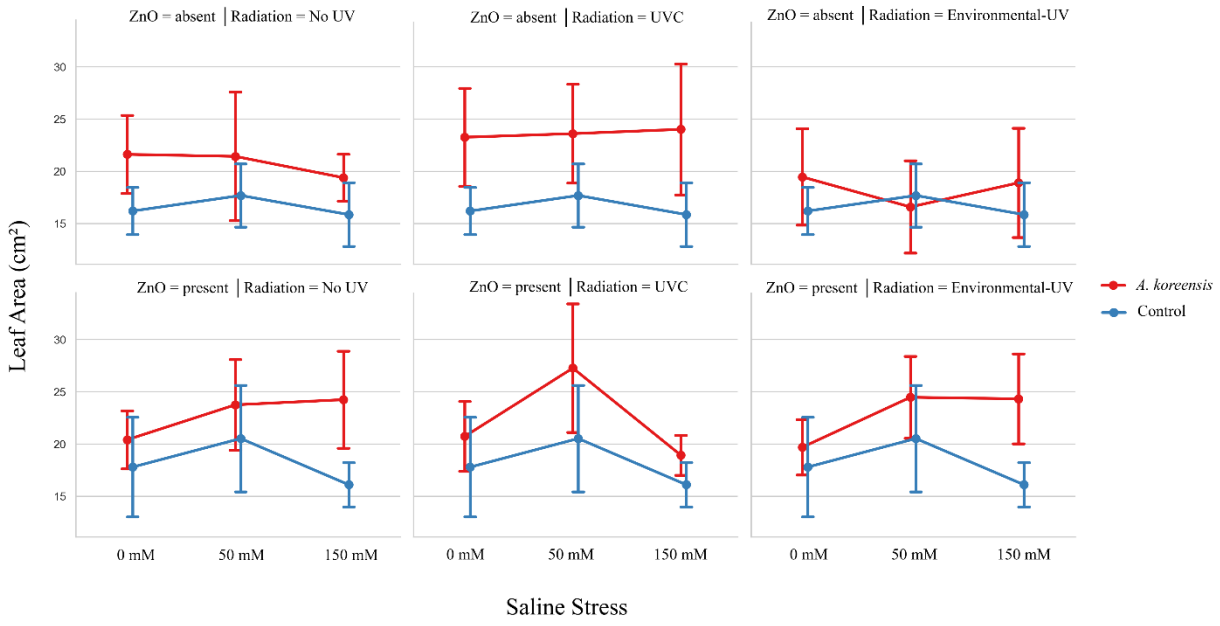

Fresh shoot biomass followed a similar trend (Fig. 2). In the absence of ZnO, *A. koreensis* inoculation promoted higher shoot biomass across salinity levels and radiation regimes. ZnO supplementation further enhanced this response, particularly under no-UV and environmental-UV conditions, where inoculated plants showed a clear biomass advantage at both moderate and high salinity. Under UVC exposure, shoot biomass declined in all treatments; however, *A. koreensis*-treated plants still outperformed non-inoculated controls at moderate salinity.

Figure 2. Fresh shoot biomass (g) of *E. sativa* under saline stress (0, 50, and 150 mM NaCl) as affected by *A. koreensis* inoculation, ZnO supplementation, and radiation regime. Values are mean ± standard deviation (n = 10). Statistical analysis was performed using ANOVA and Dunnett's test ($p < 0.05$).

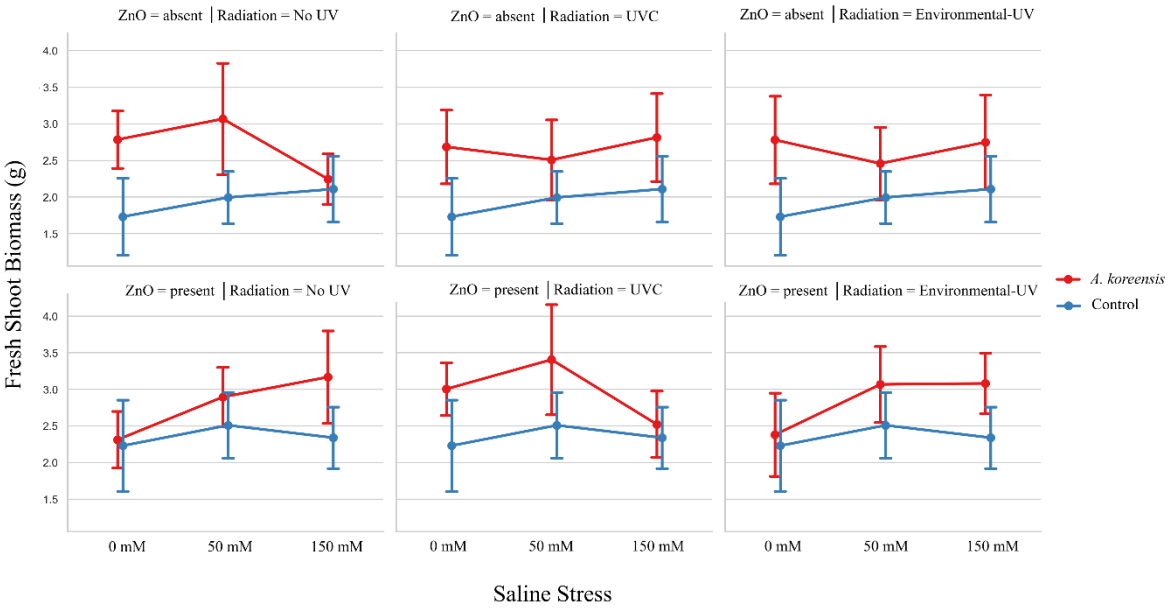

In contrast, fresh root biomass displayed a more variable response to salinity and radiation interactions (Fig. 3). Under higher salinity levels, control plants frequently exhibited greater root biomass, especially in the presence of ZnO. Nevertheless, *A. koreensis* inoculation mitigated abrupt declines in root biomass under UVC exposure at moderate salinity, indicating a stabilizing effect rather than a consistent enhancement of root growth.

Figure 3. Fresh root biomass (g) of *E. sativa* grown under saline stress (0, 50, and 150 mM NaCl) under different radiation regimes, with or without ZnO and *A. koreensis* inoculation. Values are mean ± standard deviation (n = 10).

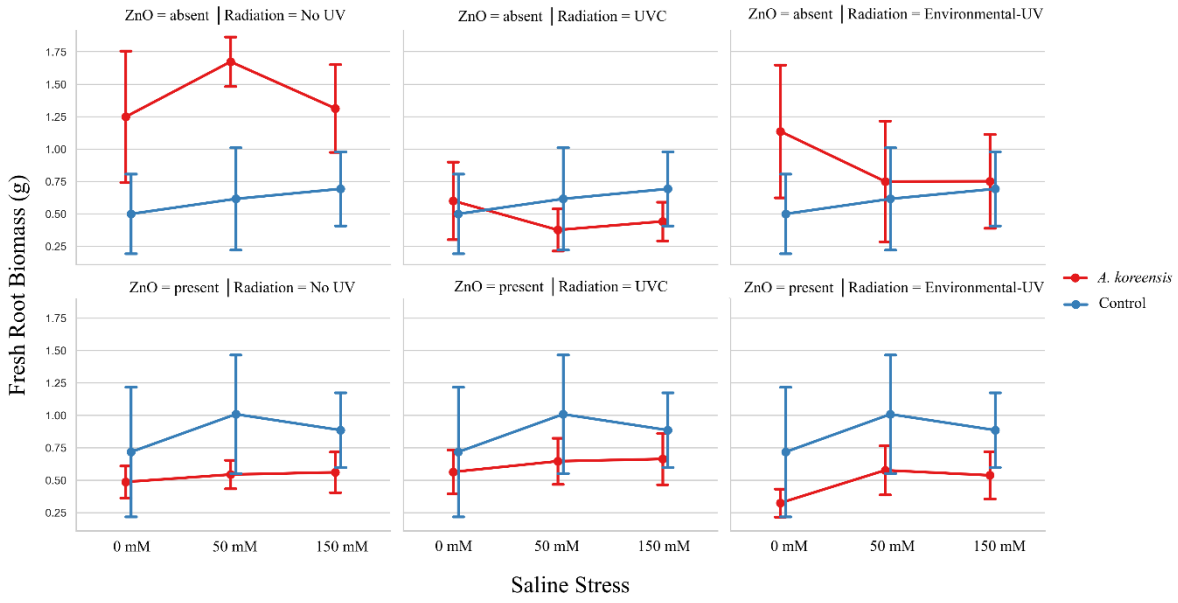

Dry biomass measurements generally corroborated patterns observed for fresh biomass (Figs. 4 and 5). Dry shoot biomass was increased in *A. koreensis*-treated plants under ZnO supplementation, particularly under environmental-UV radiation and moderate salinity. Dry root biomass responses were more heterogeneous, with no systematic superiority of inoculated plants across treatments; however, inoculated seedlings often exhibited reduced variability compared to controls, suggesting improved physiological stability under saline stress.

Figure 4. Dry shoot biomass (g) of *E. sativa* after 30 days of growth under saline stress (0, 50, and 150 mM NaCl), evaluating the effects of *A. koreensis* inoculation, ZnO presence, and radiation regime. Data are shown as mean ± standard deviation (n = 10).

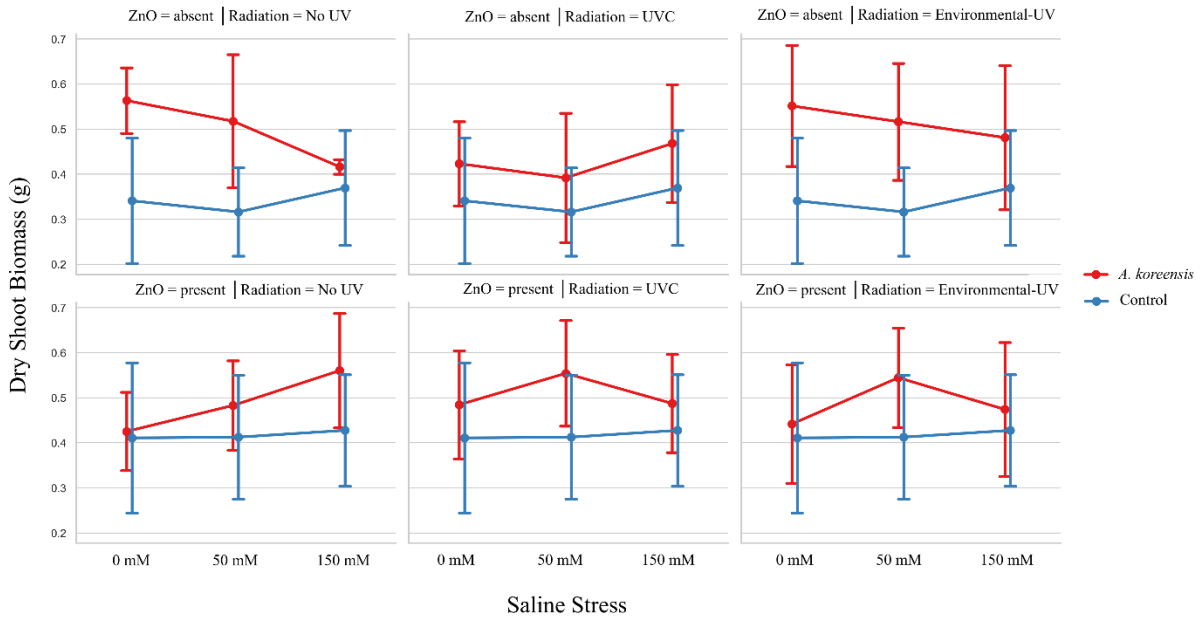

Figure 5. Dry root biomass (g) of *E. sativa* under saline stress conditions (0, 50, and 150 mM NaCl) as influenced by microbial inoculation, ZnO, and radiation exposure. Values represent mean ± standard deviation (n = 10).

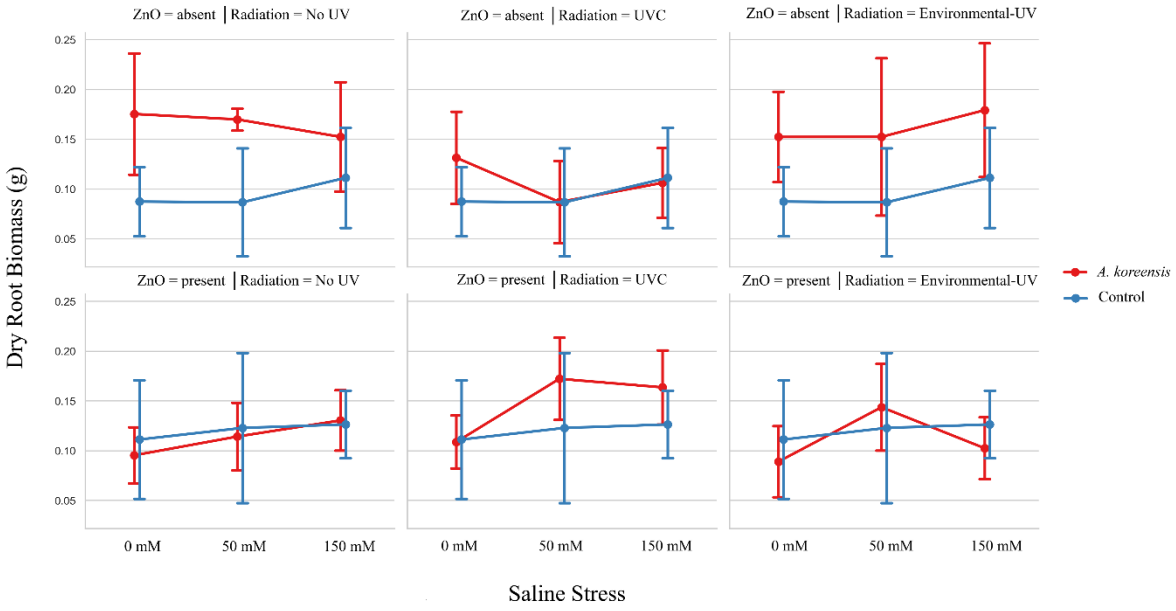

Shoot length was significantly influenced by microbial inoculation and radiation regime (Fig. 6). Under no-UV and environmental-UV conditions, *A. koreensis*-treated plants generally exhibited greater shoot elongation than controls, especially when combined with ZnO. Under UVC

exposure, shoot length was reduced across all treatments, yet inoculated plants maintained relatively greater elongation at moderate salinity.

Figure 6. Shoot length (cm) of *E. sativa* plants subjected to saline stress (0, 50, and 150 mM NaCl), comparing inoculated (*A. koreensis*) and non-inoculated plants under different radiation regimes and ZnO conditions. Data are mean ± standard deviation (n = 10).

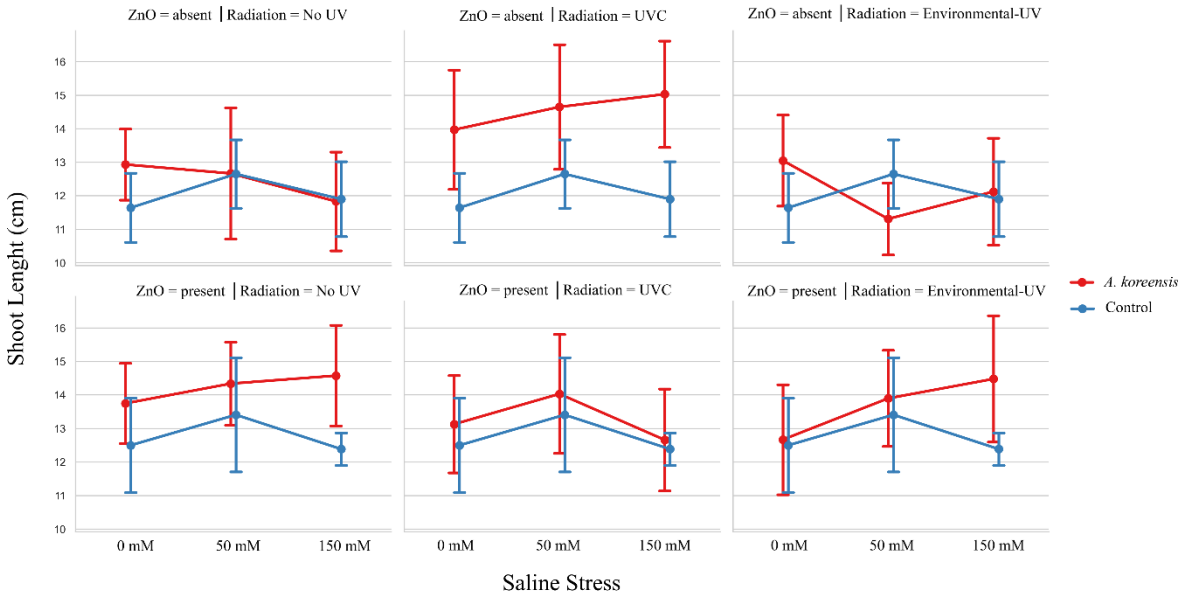

Root length responses were primarily driven by salinity intensity (Fig. 7). Control plants frequently showed increased root elongation under higher salinity, whereas *A. koreensis*-treated plants displayed more conservative root growth, particularly under ZnO supplementation and UVC exposure. This pattern suggests a shift in biomass allocation and growth strategy rather than simple stimulation of root elongation.

Figure 7. Root length (cm) of *E. sativa* under saline stress (0, 50, and 150 mM NaCl), evaluating the combined effects of *A. koreensis* inoculation, ZnO, and radiation regime. Data represent mean ± standard deviation (n = 10). Statistical comparisons are shown in Supplementary Table S3.

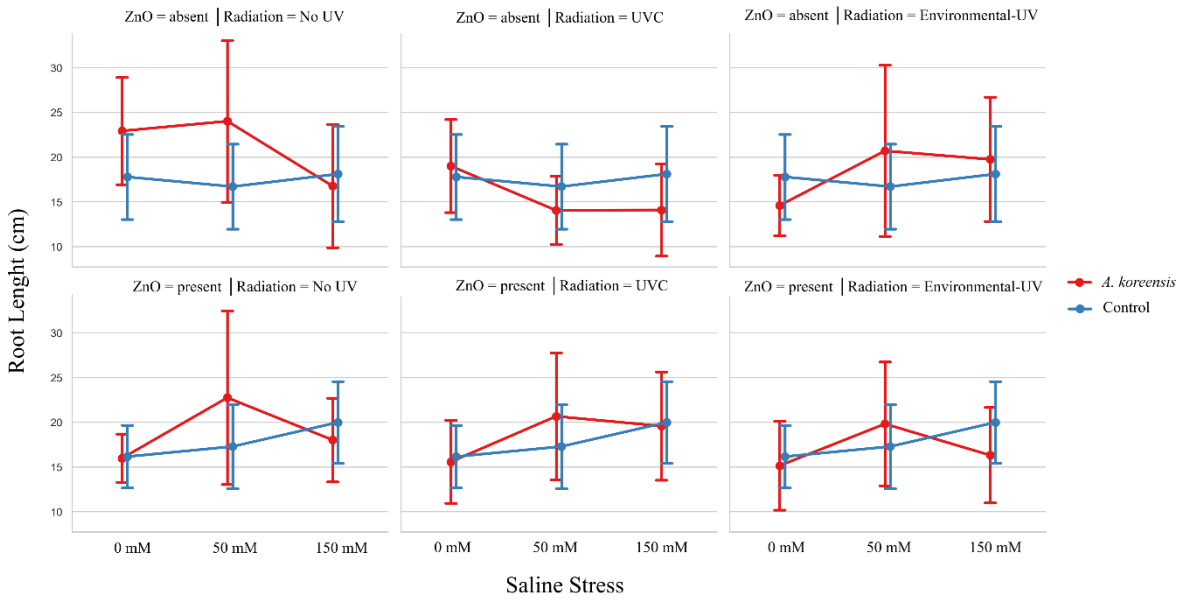

Overall, statistical analysis confirmed significant main effects and interactions among microbial inoculation, ZnO supplementation, radiation regime, and salinity for most growth parameters (ANOVA, $p < 0.05$). Dunnett's post hoc comparisons against the non-inoculated controls identified *A. koreensis*-mediated growth advantages primarily under moderate salinity and non-UVC radiation conditions, whereas severe salinity constrained plant growth regardless of treatment (Supplementary Tables S15–S20).

Effects of *A. koreensis* and ZnO on seedling growth under osmotic stress

Under osmotic stress imposed by PEG-induced water potentials (0, −0.5, and −1.5 MPa), seedling growth of *Eruca sativa* exhibited response patterns distinct from those observed under salinity, indicating stress-specific interactions among microbial inoculation, ZnO crystal supplementation, radiation regime, and stress intensity. Multifactorial ANOVA revealed significant main effects and interactions for all evaluated growth parameters ($p < 0.05$), highlighting the strong context dependence of plant responses under osmotic stress (Supplementary Tables S8–S14).

Leaf area was strongly influenced by *A. koreensis* inoculation in combination with ZnO supplementation (Fig. 8). Under no-UV and environmental-UV conditions, inoculated plants exhibited greater leaf expansion than non-inoculated controls at moderate osmotic stress (−0.5 MPa), particularly in the presence of ZnO. Under UVC exposure, leaf area was reduced across all

treatments; however, *A. koreensis*-treated plants maintained values comparable to or slightly higher than those of control plants.

Figure 8. Leaf area (cm²) of *E. sativa* plants subjected to osmotic stress (0, −0.5, and −1.5 MPa) under different radiation regimes, with or without ZnO and *A. koreensis* inoculation. Data are mean ± standard deviation (n = 10).

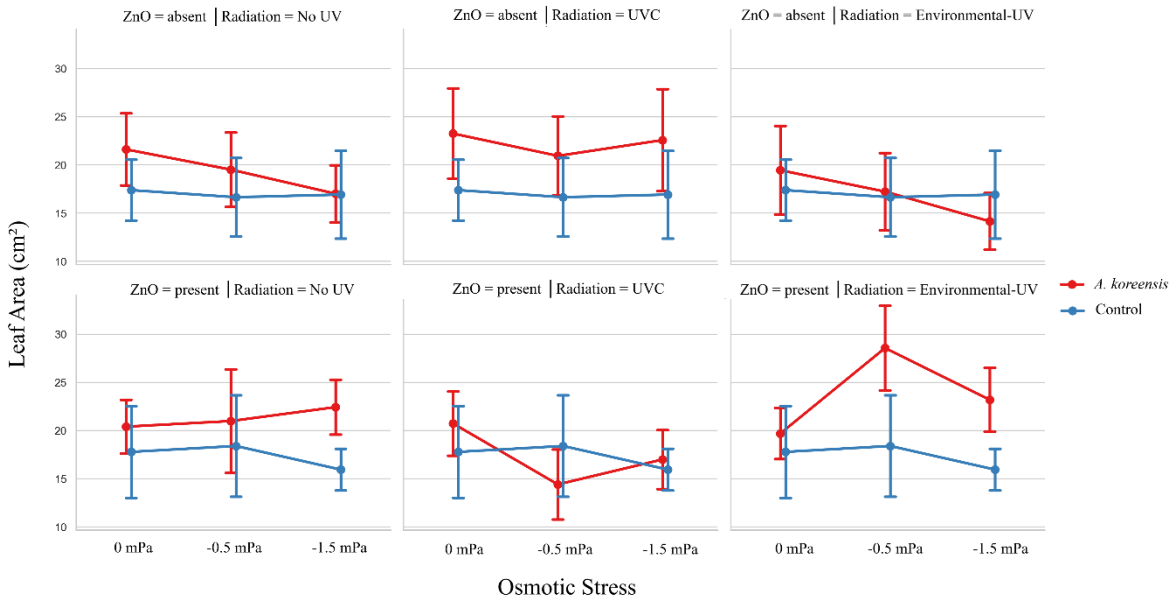

Fresh shoot biomass followed a similar trend (Fig. 9). *A. koreensis* inoculation consistently promoted shoot biomass accumulation under moderate osmotic stress, especially when combined with ZnO and environmental-UV radiation. At severe osmotic stress (−1.5 MPa), biomass reductions were evident in all treatments, although inoculated plants frequently retained higher shoot biomass relative to non-inoculated controls.

Figure 9. Fresh shoot biomass (g) of *E. sativa* grown under osmotic stress (0, −0.5, and −1.5 MPa), evaluating the effects of microbial inoculation, ZnO, and radiation exposure. Values are mean ± standard deviation (n = 10).

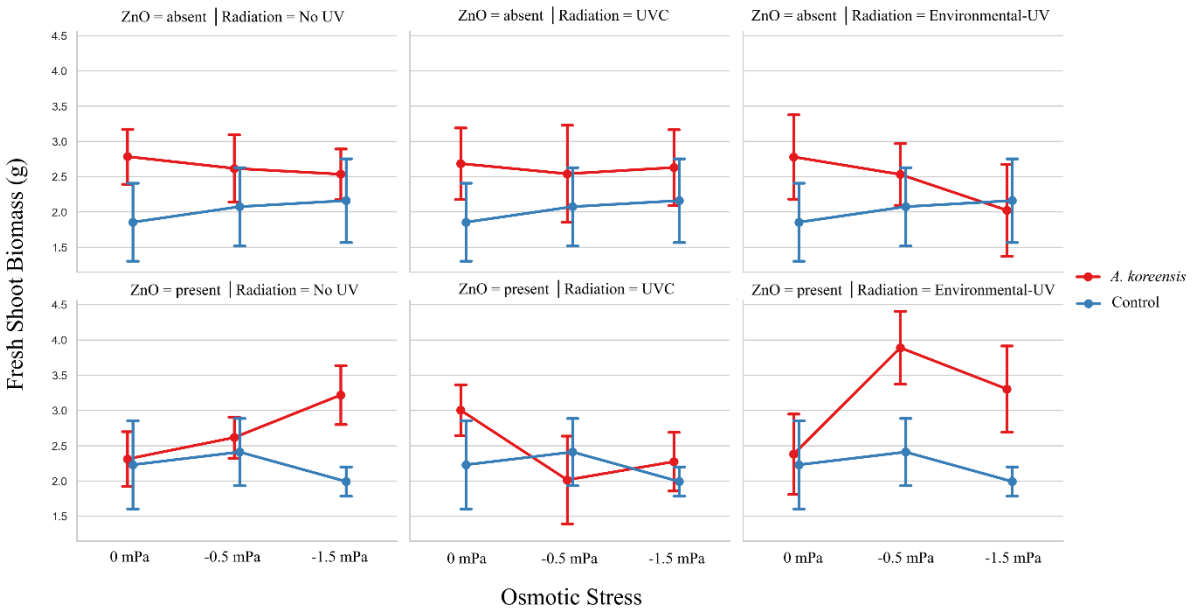

In contrast, fresh root biomass displayed divergent allocation patterns under osmotic stress (Fig. 10). Control plants often exhibited increased root biomass with increasing osmotic stress, whereas *A. koreensis*-treated plants maintained relatively stable but lower root biomass values, particularly in the presence of ZnO. This response suggests differential biomass allocation strategies under water deficit conditions rather than uniform stimulation of root growth.

Figure 10. Fresh root biomass (g) of *E. sativa* plants subjected to osmotic stress (0, −0.5, and −1.5 MPa), under different radiation regimes, ZnO conditions, and *A. koreensis* inoculation. Data are mean ± standard deviation (n = 10).

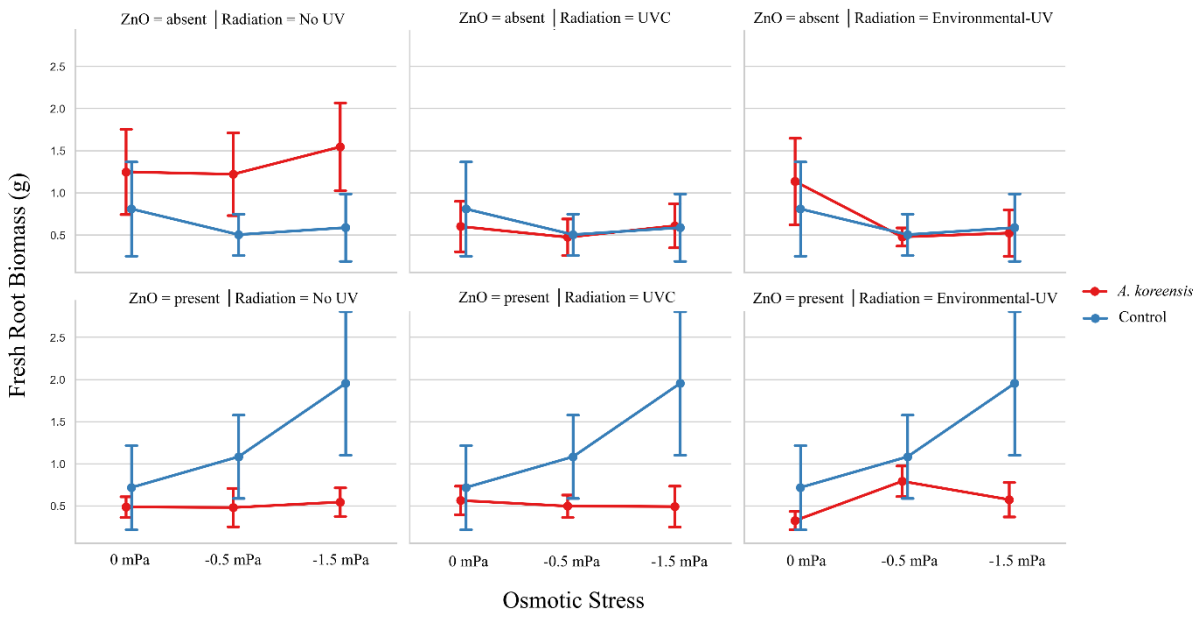

Dry biomass measurements generally corroborated trends observed for fresh biomass (Figs. 11 and 12). Dry shoot biomass was enhanced in *A. koreensis*-treated plants under ZnO supplementation and environmental-UV radiation at moderate osmotic stress. Dry root biomass responses were more variable and did not show consistent enhancement associated with microbial inoculation; however, inoculated plants often exhibited reduced variability compared to controls, indicating improved physiological stability under osmotic stress.

Figure 11. Dry shoot biomass (g) of *E. sativa* after 30 days of growth under osmotic stress (0, −0.5, and −1.5 MPa), comparing inoculated and non-inoculated plants under different radiation and ZnO conditions. Data are mean ± standard deviation (n = 10).

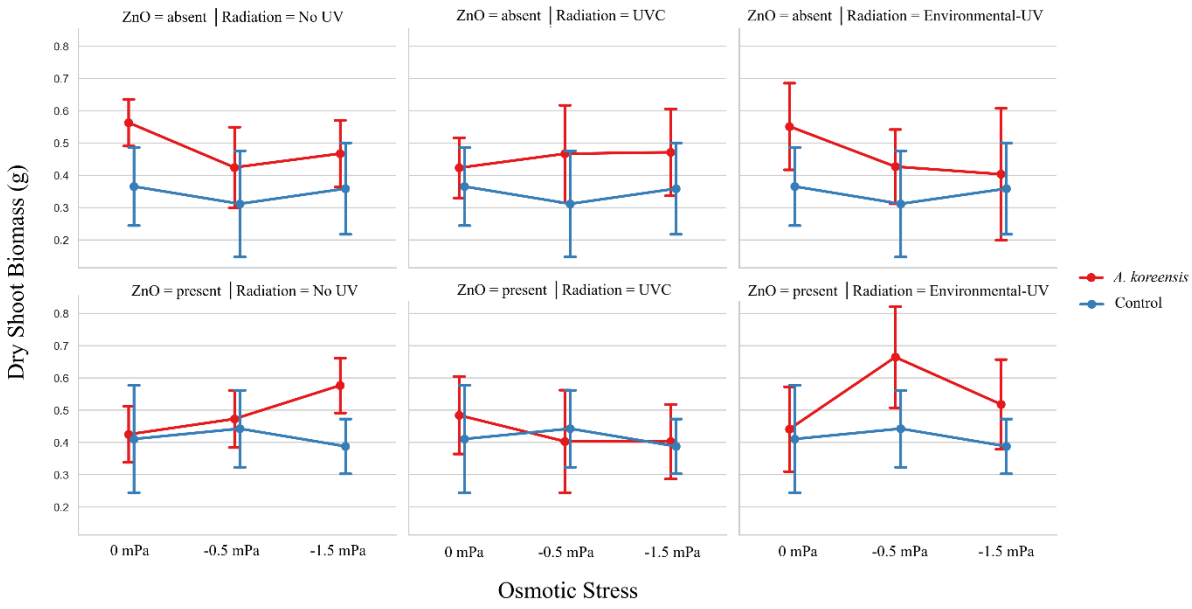

Figure 12. Dry root biomass (g) of *E. sativa* under osmotic stress conditions (0, −0.5, and −1.5 MPa), as affected by *A. koreensis* inoculation, ZnO presence, and radiation regime. Data represent mean ± standard deviation (n = 10). Statistical results are provided in Supplementary Table S5.

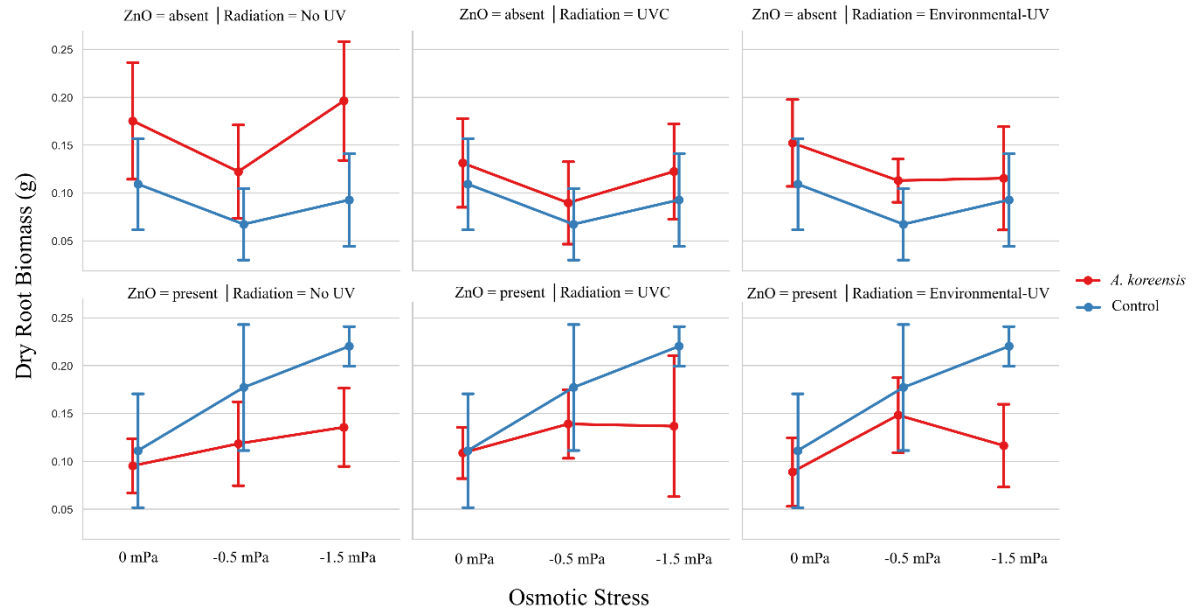

Shoot length was moderately affected by osmotic stress intensity and radiation regime (Fig. 13). Under no-UV and environmental-UV conditions, *A. koreensis*-treated plants displayed slightly greater shoot elongation than controls, particularly at −0.5 MPa. Under UVC exposure, shoot

length was reduced across all treatments, with minimal differences between inoculated and non-inoculated plants.

Figure 13. Shoot length (cm) of *E. sativa* plants subjected to osmotic stress (0, −0.5, and −1.5 MPa), comparing microbial inoculation, ZnO supplementation, and radiation regimes. Data are mean ± standard deviation (n = 10).

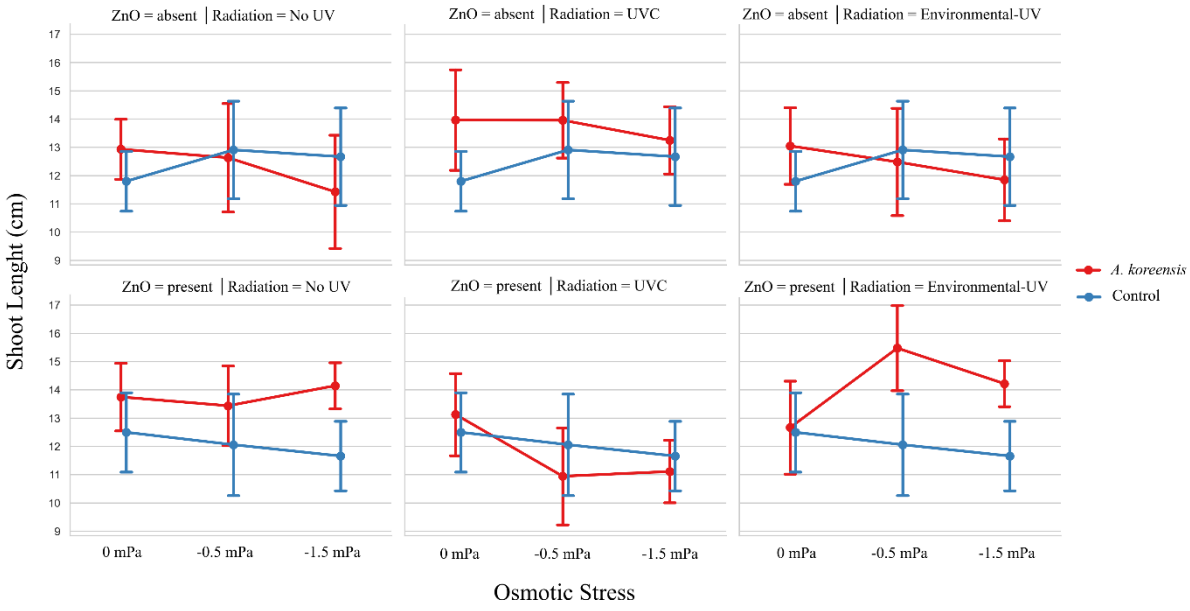

Root length increased with increasing osmotic stress in both inoculated and control plants (Fig. 14). However, under severe osmotic stress (−1.5 MPa), *A. koreensis*-treated plants often exhibited reduced root elongation relative to controls, suggesting a shift in growth strategy toward shoot maintenance rather than extensive root extension.

Figure 14. Root length (cm) of *E. sativa* under osmotic stress (0, −0.5, and −1.5 MPa), evaluating plant responses to *A. koreensis* inoculation, ZnO presence, and radiation exposure. Data are mean ± standard deviation (n = 10).

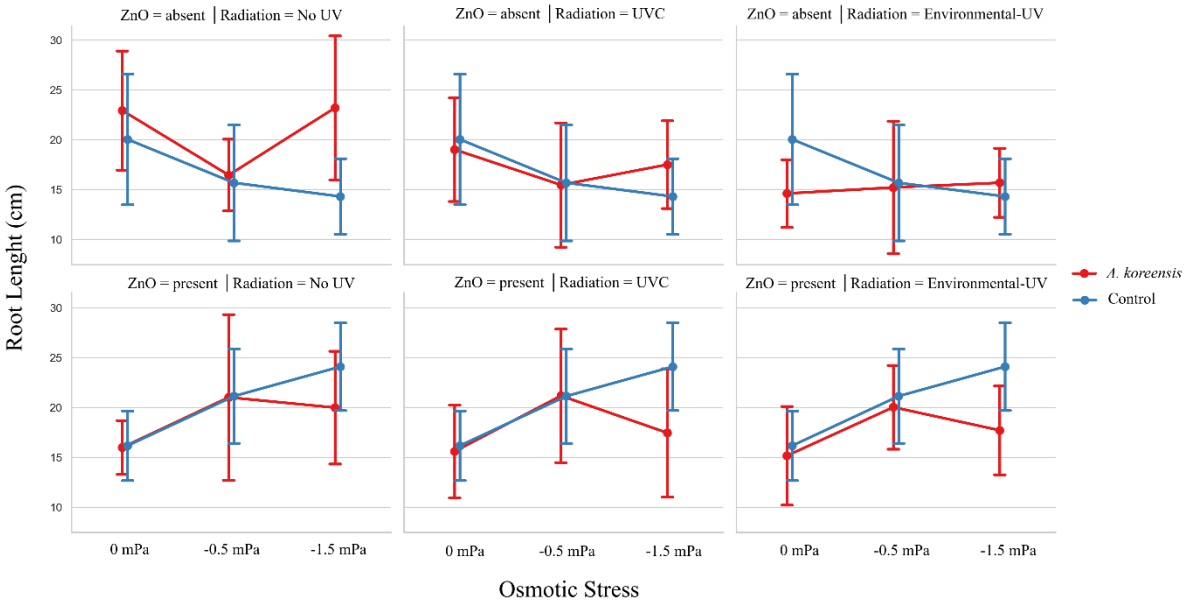

Overall, statistical analysis confirmed significant main effects and interactions among osmotic potential, microbial inoculation, ZnO supplementation, and radiation regime for most growth parameters (ANOVA, $p < 0.05$). Dunnett's post hoc comparisons against the non-inoculated controls identified A. koreensis-associated growth advantages primarily under moderate osmotic stress and non-UVC radiation conditions, whereas severe osmotic stress constrained plant growth regardless of treatment (Supplementary Tables S21–S26).

3.4 DISCUSSION

Early seedling establishment represents a critical bottleneck for plant performance under abiotic stress, as growth responses during this stage can strongly influence subsequent biomass accumulation, stress tolerance, and survival in soil systems (Lei et al. 2021; Cardarelli et al. 2022). In the present study, we demonstrate that the extremophilic *Arthrobacter koreensis* modulates early seedling growth and biomass allocation of *Eruca sativa* under saline and osmotic stress in a strongly context-dependent manner. Rather than promoting uniform growth enhancement across all experimental conditions, microbial inoculation exerted its most pronounced effects under moderate stress intensity, whereas severe salinity and osmotic stress constrained plant growth regardless of treatment. This response pattern was consistently observed across multiple growth parameters and reinforces the concept that the efficacy of microbial biostimulants depends on the

balance between stress severity and plant physiological plasticity (Lopes et al. 2021; Hasanuzzaman et al. 2021; Win et al. 2025).

A clear differentiation between saline and osmotic stress responses emerged from this study, highlighting that these stressors, although often grouped as water-related constraints, impose distinct physiological challenges on plants. Salinity stress combines osmotic limitation with ionic toxicity, directly disrupting ion homeostasis and cellular metabolism, while osmotic stress primarily limits water availability and cell expansion (Álvarez et al. 2012; Tokarz et al. 2020; Chourasia et al. 2021). Accordingly, under salinity, *A. koreensis* inoculation primarily supported shoot development and biomass accumulation under moderate NaCl concentrations, while root growth responses were more variable and frequently reflected stabilization rather than enhancement. In contrast, PEG-induced osmotic stress resulted in pronounced shifts in biomass allocation, with inoculated plants often exhibiting reduced root elongation and resource reallocation toward shoot maintenance under severe stress—highlighting the importance of distinguishing osmotic from saline stress in evaluating plant–microbe interactions (Hernández-Fernández et al. 2022; Kalleku et al. 2024).

The context-dependent growth modulation observed here is consistent with an expanding body of literature describing plant growth-promoting microorganisms as conditional rather than universal enhancers of plant performance under abiotic stress. Numerous studies report that microbial inoculation enhances growth, nutrient acquisition, or stress tolerance primarily under moderate stress, while benefits decline as stress severity increases .(Pereira 2016; Silva et al. 2019; Lopes et al. 2021; Liu et al. 2023) Within this framework, *A. koreensis* appears to function as a stabilizing agent, reducing variability in growth and biomass accumulation rather than maximizing absolute growth under all conditions. Such stabilization may be particularly relevant during early seedling establishment in heterogeneous soil environments, where resilience and consistency of growth can be as critical as peak biomass production (Manzanera et al. 2015; Vílchez et al. 2016; Fernández-González et al. 2017; Rebelo Romão et al. 2022).

The observed responses are also consistent with known functional traits of *Arthrobacter* species, which include tolerance to desiccation, radiation, and nutrient limitation, as well as metabolic flexibility and stress-associated regulatory mechanisms (Mongodin et al. 2006; Dsouza et al. 2015; Hernández-Fernández et al. 2022). Microbial traits may indirectly support plant

performance by modulating rhizosphere dynamics, influencing stress signaling, or mitigating oxidative damage, even in the absence of direct growth promotion. However, since physiological and molecular responses were not directly assessed, these mechanisms should be viewed as hypothesis-driven interpretations consistent with current frameworks of microbe-mediated stress modulation (Muhammad et al. 2024; Wankhade et al. 2025; Chen et al. 2025).

ZnO crystals further modulated plant responses to both saline and osmotic stress, reinforcing their role as functional modifiers of plant–microbe interactions rather than as conventional zinc fertilizers (Alharbi et al. 2023; Shoukat et al. 2025; Ghaffari Yaichi et al. 2025). At the concentrations applied, ZnO did not uniformly enhance growth but instead modified the direction and strength of microbial or plant responses depending on stress type and environmental conditions. Similar context-dependent effects of ZnO nanoparticles have been reported in various plant systems, where ZnO modulated stress tolerance through antioxidant, hormonal, membrane, and signaling pathways rather than direct nutritional supplementation (Zhai et al. 2025; Anwar et al. 2025; Das et al. 2025). The interaction between ZnO and *A. koreensis* observed here supports the view that nanomaterials may act as amplifiers or attenuators of microbial biostimulant effects depending on environmental context.

Biomass allocation patterns revealed adaptive plant strategies under stress: under both salinity and osmotic stress, non-inoculated control plants often showed increased root investment or elongation, consistent with classical stress-avoidance mechanisms that enhance water and ion uptake (Zhang et al. 2020; Hammami et al. 2022; Li et al. 2023). In contrast, *A. koreensis*-treated plants often displayed more conservative root growth while maintaining shoot biomass under moderate stress, suggesting improved resource-use efficiency or altered stress perception. Similar microbe-induced shifts in root–shoot allocation have been reported in plants inoculated with stress-tolerant bacteria and fungi and are increasingly recognized as part of adaptive stress responses rather than simple growth stimulation (Adhikari et al. 2020; Kalleku et al. 2024; Bao et al. 2025).

Radiation exposure further shaped plant–microbe–ZnO interactions, with non-UVC conditions allowing more pronounced microbial and nanomaterial effects. Although UVC does not simulate typical agricultural environments, its use here acted as a stress-amplification mechanism to test system resilience under compounded abiotic pressures. Under UVC, growth reductions were observed across treatments, yet inoculated plants often maintained relatively higher growth metrics

under moderate stress compared to controls, indicating that microbial-mediated stabilization effects may persist even under extreme stress combinations, albeit within physiological limits. Similar experimental approaches employing intensified stress conditions have been used to dissect resilience mechanisms in extremophilic microorganisms and plant–microbe systems (Pérez et al. 2017; Zenteno-Alegría et al. 2024; Srinivasan 2024; Ellington et al. 2025).

Taken together, these findings demonstrate that extremophilic microorganisms isolated from harsh environments can function as conditional biostimulants during early seedling establishment in soil. The beneficial effects of *A. koreensis* were not universal but depended on stress intensity, stress type, and interactions with ZnO and radiation factors. This nuanced response highlights the need to move beyond binary assessments of biostimulant efficacy and to explicitly consider environmental context and interaction complexity when evaluating plant–microbe–nanomaterial systems. From an applied perspective, such context-dependent modulation may offer opportunities to enhance crop establishment under moderate stress conditions, while also emphasizing the limitations of biostimulant strategies under extreme abiotic constraints.

3.5 CONCLUSION

This study demonstrates that the extremophilic bacterium *Arthrobacter koreensis* modulates early seedling growth and biomass allocation of *Eruca sativa* under saline and osmotic stress in a strongly context-dependent manner. Microbial inoculation did not result in uniform growth enhancement across all stress conditions; instead, its beneficial effects were most evident under moderate stress intensity, whereas severe salinity and osmotic stress constrained plant growth regardless of treatment. These findings highlight the importance of stress severity as a key determinant of biostimulant efficacy during early seedling establishment in soil.

The interaction between *A. koreensis* and ZnO crystals further influenced plant responses to abiotic stress, reinforcing the role of nanomaterials as modulators rather than simple nutrient sources. ZnO supplementation altered the magnitude and direction of microbial effects depending on stress type and radiation regime, underscoring the complexity of plant–microbe–nanomaterial interactions under environmental constraints. Such context-specific modulation emphasizes the need to evaluate combined biostimulant strategies within realistic soil-based systems.

Differences observed between saline and osmotic stress responses further demonstrate that these stressors impose distinct physiological challenges, resulting in divergent growth and biomass allocation strategies. While salinity primarily affected shoot development and biomass accumulation, osmotic stress induced stronger shifts in resource allocation, particularly under severe water deficit. Microbial inoculation partially mitigated these effects under moderate stress, contributing to more balanced growth patterns.

Overall, the present findings indicate that extremophilic microorganisms isolated from harsh environments can function as conditional biostimulants during early seedling establishment, enhancing growth stability rather than maximizing biomass under all conditions. This nuanced understanding supports a move away from binary evaluations of biostimulant performance and toward context-aware applications in sustainable agriculture. Future studies integrating physiological, molecular, and field-based approaches will be essential to further elucidate the mechanisms underlying these interactions and to assess their agronomic relevance under diverse environmental scenarios.

Supplementary Material to

Extremophilic *Arthrobacter koreensis* and ZnO crystals modulate early seedling growth and biomass allocation of Eruca sativa under salinity and osmotic stress

Table S1. ANOVA summary for leaf area (cm²) of *Eruca sativa* under saline stress

	Sum_sq	***Df***	***F***	***PR(>F)***
Intercept	5291,1076	1	273,1420	2,44E-35
C(ZnO)	84,9140	1	4,3835	3,80E-02
C(Radiação)	162,2136	2	4,1870	1,70E-02
C(Estresse)	85,1131	2	2,1969	1,15E-01
C(ZnO):C(Radiação)	302,6839	2	7,8127	5,96E-04
C(ZnO):C(Estresse)	77,5876	2	2,0026	1,39E-01
C(Radiação):C(Estresse)	230,3145	4	2,9724	2,14E-02
C(ZnO):C(Radiação):C(Estresse)	166,2269	4	2,1453	7,81E-02
Residual	2847,5767	147		

Table S2. ANOVA summary for Shoot Length (cm) of *Eruca sativa* under saline stress

	Sum_sq	***Df***	***F***	***PR(>F)***
Intercept	1912,6044	1	813,1352	8,90E-62

C(ZnO)	27,1151	1	11,5279	8,82E-04
C(Radiação)	19,6015	2	4,1668	1,74E-02
C(Estresse)	3,5023	2	0,7445	4,77E-01
C(ZnO):C(Radiação)	68,9470	2	14,6563	1,57E-06
C(ZnO):C(Estresse)	7,6031	2	1,6162	2,02E-01
C(Radiação):C(Estresse)	15,0515	4	1,5998	1,77E-01
C(ZnO):C(Radiação):C(Estresse)	28,0353	4	2,9798	2,11E-02
Residual	345,7640	147		

Table S3. ANOVA summary for Root Length (cm) of *Eruca sativa* under saline stress

	Sum_sq	***Df***	***F***	***PR(>F)***
Intercept	2926,8100	1	75,9309	5,67E-15
C(ZnO)	5,6250	1	0,1459	7,03E-01
C(Radiação)	47,8604	2	0,6208	5,39E-01
C(Estresse)	240,3373	2	3,1176	4,72E-02
C(ZnO):C(Radiação)	177,3435	2	2,3004	1,04E-01
C(ZnO):C(Estresse)	149,5118	2	1,9394	1,47E-01
C(Radiação):C(Estresse)	40,8982	4	0,2653	9,00E-01
C(ZnO):C(Radiação):C(Estresse)	292,4367	4	1,8967	1,14E-01
Residual	5666,2149	147		

Table S4. ANOVA summary for Fresh Shoot Biomass (g) of *Eruca sativa* under saline stress

	Sum_sq	***Df***	***F***	***PR(>F)***
Intercept	90,3767	1	321,6781	7,70E-39
C(ZnO)	3,0618	1	10,8978	1,21E-03
C(Radiação)	2,0584	2	3,6633	2,80E-02
C(Estresse)	3,6766	2	6,5430	1,90E-03
C(ZnO):C(Radiação)	2,9472	2	5,2449	6,31E-03
C(ZnO):C(Estresse)	4,2152	2	7,5017	7,90E-04
C(Radiação):C(Estresse)	5,4603	4	4,8587	1,04E-03
C(ZnO):C(Radiação):C(Estresse)	6,8844	4	6,1259	1,38E-04
Residual	41,3002	147		

Table S5. ANOVA summary for Fresh Root Biomass (g) of *Eruca sativa* under saline stress

	Sum_sq	***Df***	***F***	***PR(>F)***
Intercept	2,8336	1	37,1051	9,33E-09
C(ZnO)	2,0370	1	26,6740	7,71E-07
C(Radiação)	0,0767	2	0,5024	6,06E-01
C(Estresse)	0,0292	2	0,1909	8,26E-01
C(ZnO):C(Radiação)	1,8868	2	12,3533	1,10E-05
C(ZnO):C(Estresse)	0,3574	2	2,3400	9,99E-02
C(Radiação):C(Estresse)	0,1175	4	0,3848	8,19E-01

C(ZnO):C(Radiação):C(Estresse)	1,2254	4	4,0115	4,06E-03
Residual	11,2260	147		

Table S6. ANOVA summary for Dry Shoot Biomass (g) of *Eruca sativa* under saline stress

	Sum_sq	***Df***	***F***	***PR(>F)***
Intercept	2,8250	1	194,8052	1,01E-28
C(ZnO)	0,0744	1	5,1314	2,50E-02
C(Radiação)	0,0394	2	1,3569	2,61E-01
C(Estresse)	0,0865	2	2,9826	5,37E-02
C(ZnO):C(Radiação)	0,0501	2	1,7272	1,81E-01
C(ZnO):C(Estresse)	0,1634	2	5,6326	4,40E-03
C(Radiação):C(Estresse)	0,0768	4	1,3248	2,63E-01
C(ZnO):C(Radiação):C(Estresse)	0,1462	4	2,5200	4,37E-02
Residual	2,1317	147		

Table S7. ANOVA summary for Dry Root Biomass (g) of *Eruca sativa* under saline stress

	Sum_sq	***Df***	***F***	***PR(>F)***
Intercept	0,1532	1	77,8835	2,96E-15
C(ZnO)	0,0017	1	0,8829	3,49E-01
C(Radiação)	0,0166	2	4,2241	1,65E-02
C(Estresse)	0,0059	2	1,4874	2,29E-01
C(ZnO):C(Radiação)	0,0404	2	10,2655	6,71E-05
C(ZnO):C(Estresse)	0,0069	2	1,7522	1,77E-01
C(Radiação):C(Estresse)	0,0118	4	1,5043	2,04E-01
C(ZnO):C(Radiação):C(Estresse)	0,0198	4	2,5127	4,42E-02
Residual	0,2891	147		

Table S8. ANOVA summary for leaf area (cm²) of *Eruca sativa* under osmotic stress

	Sum_sq	***Df***	***F***	***PR(>F)***
Intercept	4404,9614	1	292,1114	9,40E-37
C(ZnO)	10,1848	1	0,6754	4,13E-01
C(Radiação)	953,9960	2	31,6317	3,76E-12
C(Estresse)	21,7820	2	0,7222	4,87E-01
C(ZnO):C(Radiação)	667,6792	2	22,1383	3,94E-09
C(ZnO):C(Estresse)	101,4724	2	3,3645	3,73E-02
C(Radiação):C(Estresse)	593,4731	4	9,8389	4,42E-07
C(ZnO):C(Radiação):C(Estresse)	328,4139	4	5,4446	4,08E-04
Residual	2216,7208	147		

Table S9. ANOVA summary for Shoot Length (cm) of *Eruca sativa* under osmotic stress

	Sum_sq	***Df***	***F***	***PR(>F)***

Intercept	1806,3360	1	864,2691	1,96E-63
C(ZnO)	3,0823	1	1,4748	2,27E-01
C(Radiação)	97,5198	2	23,3299	1,59E-09
C(Estresse)	2,5340	2	0,6062	5,47E-01
C(ZnO):C(Radiação)	79,7868	2	19,0876	4,27E-08
C(ZnO):C(Estresse)	11,0751	2	2,6495	7,41E-02
C(Radiação):C(Estresse)	69,8993	4	8,3611	4,18E-06
C(ZnO):C(Radiação):C(Estresse)	42,8529	4	5,1259	6,79E-04
Residual	307,2323	147		

Table S10. ANOVA summary for Root Length (cm) of *Eruca sativa* under osmotic stress

	Sum_sq	***Df***	***F***	***PR(>F)***
Intercept	4418,4040	1	151,4317	2,28E-24
C(ZnO)	98,6881	1	3,3823	6,79E-02
C(Radiação)	7,5454	2	0,1293	8,79E-01
C(Estresse)	141,2060	2	2,4198	9,25E-02
C(ZnO):C(Radiação)	3,3759	2	0,0579	9,44E-01
C(ZnO):C(Estresse)	326,6894	2	5,5983	4,54E-03
C(Radiação):C(Estresse)	19,3700	4	0,1660	9,55E-01
C(ZnO):C(Radiação):C(Estresse)	62,8639	4	0,5386	7,08E-01
Residual	4289,0974	147		

Table S11. ANOVA summary for Fresh Shoot Biomass (g) of *Eruca sativa* under osmotic stress

	Sum_sq	***Df***	***F***	***PR(>F)***
Intercept	68,4869	1	270,4727	3,91E-35
C(ZnO)	0,0000	1	0,0001	9,93E-01
C(Radiação)	17,5977	2	34,7489	4,39E-13
C(Estresse)	4,2622	2	8,4164	3,46E-04
C(ZnO):C(Radiação)	7,7020	2	15,2086	9,92E-07
C(ZnO):C(Estresse)	3,0906	2	6,1028	2,84E-03
C(Radiação):C(Estresse)	18,4334	4	18,1996	3,65E-12
C(ZnO):C(Radiação):C(Estresse)	10,4731	4	10,3402	2,09E-07
Residual	37,2221	147		

Table S12. ANOVA summary for Fresh Root Biomass (g) of *Eruca sativa* under osmotic stress

	Sum_sq	***Df***	***F***	***PR(>F)***
Intercept	2,3040	1	26,1517	9,69E-07
C(ZnO)	2,6017	1	29,5306	2,23E-07
C(Radiação)	0,6072	2	3,4461	3,45E-02
C(Estresse)	0,0255	2	0,1445	8,66E-01
C(ZnO):C(Radiação)	2,6059	2	14,7892	1,41E-06
C(ZnO):C(Estresse)	0,1897	2	1,0767	3,43E-01

C(Radiação):C(Estresse)	0,8801	4	2,4974	4,52E-02
C(ZnO):C(Radiação):C(Estresse)	2,2974	4	6,5192	7,40E-05
Residual	12,9509	147		

Table S13. ANOVA summary for Dry Shoot Biomass (g) of *Eruca sativa* under osmotic stress

	Sum_sq	***Df***	***F***	***PR(>F)***
Intercept	2,2385	1	142,7670	2,02E-23
C(ZnO)	0,0112	1	0,7128	4,00E-01
C(Radiação)	0,3531	2	11,2597	2,82E-05
C(Estresse)	0,1205	2	3,8417	2,36E-02
C(ZnO):C(Radiação)	0,1909	2	6,0871	2,89E-03
C(ZnO):C(Estresse)	0,1547	2	4,9328	8,44E-03
C(Radiação):C(Estresse)	0,3485	4	5,5567	3,41E-04
C(ZnO):C(Radiação):C(Estresse)	0,3447	4	5,4965	3,75E-04
Residual	2,3049	147		

Table S14. ANOVA summary for Dry Root Biomass (g) of *Eruca sativa* under osmotic stress

	Sum_sq	***Df***	***F***	***PR(>F)***
Intercept	0,1405	1	67,5790	9,74E-14
C(ZnO)	0,0001	1	0,0349	8,52E-01
C(Radiação)	0,0046	2	1,1169	3,30E-01
C(Estresse)	0,0082	2	1,9665	1,44E-01
C(ZnO):C(Radiação)	0,0071	2	1,7138	1,84E-01
C(ZnO):C(Estresse)	0,0148	2	3,5525	3,11E-02
C(Radiação):C(Estresse)	0,0068	4	0,8220	5,13E-01
C(ZnO):C(Radiação):C(Estresse)	0,0027	4	0,3202	8,64E-01
Residual	0,3056	147		

Table S15. Dunnett's post hoc test comparing leaf area (cm²) under saline stress

Treatment	***p-value vs. control***	***Significance***
A_KOREENSIS_Absent_ZnO_No_UV_Absent	0,0156	*
A_KOREENSIS_Present_ZnO_No_UV_Absent	0,0541	ns
Control_Present_ZnO_No_UV_Absent	0,4631	ns
A_KOREENSIS_Absent_ZnO_No_UV_Saline_50mM	0,1015	ns
A_KOREENSIS_Present_ZnO_No_UV_Saline_50mM	0,0024	*
Control_Present_ZnO_No_UV_Saline_50mM	0,1507	ns
A_KOREENSIS_Absent_ZnO_No_UV_Saline_150mM	0,1217	ns
A_KOREENSIS_Present_ZnO_No_UV_Saline_150mM	0,0001	*
Control_Present_ZnO_No_UV_Saline_150mM	0,9061	ns
A_KOREENSIS_Absent_ZnO_UVC_Absent	0,0014	*

A_KOREENSIS_Present_ZnO_UVC_Absent	0,0381	*
Control_Present_ZnO_UVC_Absent	0,4631	ns
A_KOREENSIS_Absent_ZnO_UVC_Saline_50mM	0,0031	*
A_KOREENSIS_Present_ZnO_UVC_Saline_50mM	0,0000	*
Control_Present_ZnO_UVC_Saline_50mM	0,1507	ns
A_KOREENSIS_Absent_ZnO_UVC_Saline_150mM	0,0001	*
A_KOREENSIS_Present_ZnO_UVC_Saline_150mM	0,1436	ns
Control_Present_ZnO_UVC_Saline_150mM	0,9061	ns
A_KOREENSIS_Absent_ZnO_Environmental_UV_Absent	0,1349	ns
A_KOREENSIS_Present_ZnO_Environmental_UV_Absent	0,1090	ns
Control_Present_ZnO_Environmental_UV_Absent	0,4631	ns
A_KOREENSIS_Absent_ZnO_Environmental_UV_Saline_50mM	0,5775	ns
A_KOREENSIS_Present_ZnO_Environmental_UV_Saline_50mM	0,0007	*
Control_Present_ZnO_Environmental_UV_Saline_50mM	0,1507	ns
A_KOREENSIS_Absent_ZnO_Environmental_UV_Saline_150mM	0,1472	ns
A_KOREENSIS_Present_ZnO_Environmental_UV_Saline_150mM	0,0000	*
Control_Present_ZnO_Environmental_UV_Saline_150mM	0,9061	ns

Table S16. Dunnett's post hoc test comparing shoot length (cm) under saline stress

Treatment	***p-value vs. control***	***Significance***
A_KOREENSIS_Absent_ZnO_No_UV_Absent	0,0971	ns
A_KOREENSIS_Present_ZnO_No_UV_Absent	0,0060	*
Control_Present_ZnO_No_UV_Absent	0,2586	ns
A_KOREENSIS_Absent_ZnO_No_UV_Saline_50mM	0,9832	ns
A_KOREENSIS_Present_ZnO_No_UV_Saline_50mM	0,0149	*
Control_Present_ZnO_No_UV_Saline_50mM	0,2696	ns
A_KOREENSIS_Absent_ZnO_No_UV_Saline_150mM	0,9330	ns
A_KOREENSIS_Present_ZnO_No_UV_Saline_150mM	0,0002	*
Control_Present_ZnO_No_UV_Saline_150mM	0,5038	ns
A_KOREENSIS_Absent_ZnO_UVC_Absent	0,0025	*
A_KOREENSIS_Present_ZnO_UVC_Absent	0,0510	ns
Control_Present_ZnO_UVC_Absent	0,2586	ns
A_KOREENSIS_Absent_ZnO_UVC_Saline_50mM	0,0041	*
A_KOREENSIS_Present_ZnO_UVC_Saline_50mM	0,0515	ns
Control_Present_ZnO_UVC_Saline_50mM	0,2696	ns
A_KOREENSIS_Absent_ZnO_UVC_Saline_150mM	0,0000	*
A_KOREENSIS_Present_ZnO_UVC_Saline_150mM	0,2963	ns
Control_Present_ZnO_UVC_Saline_150mM	0,5038	ns
A_KOREENSIS_Absent_ZnO_Environmental_UV_Absent	0,0646	ns
A_KOREENSIS_Present_ZnO_Environmental_UV_Absent	0,1762	ns
Control_Present_ZnO_Environmental_UV_Absent	0,2586	ns
A_KOREENSIS_Absent_ZnO_Environmental_UV_Saline_50mM	0,0526	ns
A_KOREENSIS_Present_ZnO_Environmental_UV_Saline_50mM	0,0704	ns

Control_Present_ZnO_Environmental_UV_Saline_50mM	0,2696	ns
A_KOREENSIS_Absent_ZnO_Environmental_UV_Saline_150mM	0,7575	ns
A_KOREENSIS_Present_ZnO_Environmental_UV_Saline_150mM	0,0002	*
Control_Present_ZnO_Environmental_UV_Saline_150mM	0,5038	ns

Table S17. Dunnett's post hoc test comparing root length (cm) under saline stress

Treatment	*p-value vs. control*	*Significance*
A_KOREENSIS_Absent_ZnO_No_UV_Absent	0,1023	ns
A_KOREENSIS_Present_ZnO_No_UV_Absent	0,5550	ns
Control_Present_ZnO_No_UV_Absent	0,5950	ns
A_KOREENSIS_Absent_ZnO_No_UV_Saline_50mM	0,0240	*
A_KOREENSIS_Present_ZnO_No_UV_Saline_50mM	0,0312	*
Control_Present_ZnO_No_UV_Saline_50mM	0,8348	ns
A_KOREENSIS_Absent_ZnO_No_UV_Saline_150mM	0,6751	ns
A_KOREENSIS_Present_ZnO_No_UV_Saline_150mM	0,9730	ns
Control_Present_ZnO_No_UV_Saline_150mM	0,5264	ns
A_KOREENSIS_Absent_ZnO_UVC_Absent	0,6907	ns
A_KOREENSIS_Present_ZnO_UVC_Absent	0,4712	ns
Control_Present_ZnO_UVC_Absent	0,5950	ns
A_KOREENSIS_Absent_ZnO_UVC_Saline_50mM	0,3396	ns
A_KOREENSIS_Present_ZnO_UVC_Saline_50mM	0,1674	ns
Control_Present_ZnO_UVC_Saline_50mM	0,8348	ns
A_KOREENSIS_Absent_ZnO_UVC_Saline_150mM	0,1488	ns
A_KOREENSIS_Present_ZnO_UVC_Saline_150mM	0,6214	ns
Control_Present_ZnO_UVC_Saline_150mM	0,5264	ns
A_KOREENSIS_Absent_ZnO_Environmental_UV_Absent	0,2988	ns
A_KOREENSIS_Present_ZnO_Environmental_UV_Absent	0,3896	ns
Control_Present_ZnO_Environmental_UV_Absent	0,5950	ns
A_KOREENSIS_Absent_ZnO_Environmental_UV_Saline_50mM	0,1518	ns
A_KOREENSIS_Present_ZnO_Environmental_UV_Saline_50mM	0,2645	ns
Control_Present_ZnO_Environmental_UV_Saline_50mM	0,8348	ns
A_KOREENSIS_Absent_ZnO_Environmental_UV_Saline_150mM	0,5802	ns
A_KOREENSIS_Present_ZnO_Environmental_UV_Saline_150mM	0,5155	ns
Control_Present_ZnO_Environmental_UV_Saline_150mM	0,5264	ns

Table S18. Dunnett's post hoc test comparing fresh shoot biomass (g) under saline stress

Treatment	*p-value vs. control*	*Significance*

A_KOREENSIS_Absent_ZnO_No_UV_Absent	0,0001	*
A_KOREENSIS_Present_ZnO_No_UV_Absent	0,0279	*
Control_Present_ZnO_No_UV_Absent	0,0585	ns
A_KOREENSIS_Absent_ZnO_No_UV_Saline_50mM	0,0001	*
A_KOREENSIS_Present_ZnO_No_UV_Saline_50mM	0,0002	*
Control_Present_ZnO_No_UV_Saline_50mM	0,0314	*
A_KOREENSIS_Absent_ZnO_No_UV_Saline_150mM	0,6183	ns
A_KOREENSIS_Present_ZnO_No_UV_Saline_150mM	0,0000	*
Control_Present_ZnO_No_UV_Saline_150mM	0,3618	ns
A_KOREENSIS_Absent_ZnO_UVC_Absent	0,0004	*
A_KOREENSIS_Present_ZnO_UVC_Absent	0,0000	*
Control_Present_ZnO_UVC_Absent	0,0585	ns
A_KOREENSIS_Absent_ZnO_UVC_Saline_50mM	0,0321	*
A_KOREENSIS_Present_ZnO_UVC_Saline_50mM	0,0000	*
Control_Present_ZnO_UVC_Saline_50mM	0,0314	*
A_KOREENSIS_Absent_ZnO_UVC_Saline_150mM	0,0034	*
A_KOREENSIS_Present_ZnO_UVC_Saline_150mM	0,1020	ns
Control_Present_ZnO_UVC_Saline_150mM	0,3618	ns
A_KOREENSIS_Absent_ZnO_Environmental_UV_Absent	0,0001	*
A_KOREENSIS_Present_ZnO_Environmental_UV_Absent	0,0142	*
Control_Present_ZnO_Environmental_UV_Absent	0,0585	ns
A_KOREENSIS_Absent_ZnO_Environmental_UV_Saline_50mM	0,0522	ns
A_KOREENSIS_Present_ZnO_Environmental_UV_Saline_50mM	0,0000	*
Control_Present_ZnO_Environmental_UV_Saline_50mM	0,0314	*
A_KOREENSIS_Absent_ZnO_Environmental_UV_Saline_150mM	0,0119	*
A_KOREENSIS_Present_ZnO_Environmental_UV_Saline_150mM	0,0001	*
Control_Present_ZnO_Environmental_UV_Saline_150mM	0,3618	ns

Table S19. Dunnett's post hoc test comparing fresh root biomass (g) under saline stress

Treatment	***p-value vs. control***	***Significance***
A_KOREENSIS_Absent_ZnO_No_UV_Absent	0,0000	*
A_KOREENSIS_Present_ZnO_No_UV_Absent	0,9241	ns
Control_Present_ZnO_No_UV_Absent	0,1116	ns
A_KOREENSIS_Absent_ZnO_No_UV_Saline_50mM	0,0000	*
A_KOREENSIS_Present_ZnO_No_UV_Saline_50mM	0,5611	ns
Control_Present_ZnO_No_UV_Saline_50mM	0,0018	*
A_KOREENSIS_Absent_ZnO_No_UV_Saline_150mM	0,0000	*
A_KOREENSIS_Present_ZnO_No_UV_Saline_150mM	0,3006	ns
Control_Present_ZnO_No_UV_Saline_150mM	0,1425	ns
A_KOREENSIS_Absent_ZnO_UVC_Absent	0,4595	ns
A_KOREENSIS_Present_ZnO_UVC_Absent	0,6391	ns
Control_Present_ZnO_UVC_Absent	0,1116	ns
A_KOREENSIS_Absent_ZnO_UVC_Saline_50mM	0,0541	ns

A_KOREENSIS_Present_ZnO_UVC_Saline_50mM	0,8095	ns
Control_Present_ZnO_UVC_Saline_50mM	0,0018	*
A_KOREENSIS_Absent_ZnO_UVC_Saline_150mM	0,0441	*
A_KOREENSIS_Present_ZnO_UVC_Saline_150mM	0,8237	ns
Control_Present_ZnO_UVC_Saline_150mM	0,1425	ns
A_KOREENSIS_Absent_ZnO_Environmental_UV_Absent	0,0000	*
A_KOREENSIS_Present_ZnO_Environmental_UV_Absent	0,2008	ns
Control_Present_ZnO_Environmental_UV_Absent	0,1116	ns
A_KOREENSIS_Absent_ZnO_Environmental_UV_Saline_50mM	0,2800	ns
A_KOREENSIS_Present_ZnO_Environmental_UV_Saline_50mM	0,7528	ns
Control_Present_ZnO_Environmental_UV_Saline_50mM	0,0018	*
A_KOREENSIS_Absent_ZnO_Environmental_UV_Saline_150mM	0,6574	ns
A_KOREENSIS_Present_ZnO_Environmental_UV_Saline_150mM	0,2118	ns
Control_Present_ZnO_Environmental_UV_Saline_150mM	0,1425	ns

Table S20. Dunnett's post hoc test comparing dry shoot biomass (g) under saline stress

Treatment	***p-value vs. control***	***Significance***
A_KOREENSIS_Absent_ZnO_No_UV_Absent	0,0003	*
A_KOREENSIS_Present_ZnO_No_UV_Absent	0,1578	ns
Control_Present_ZnO_No_UV_Absent	0,2407	ns
A_KOREENSIS_Absent_ZnO_No_UV_Saline_50mM	0,0015	*
A_KOREENSIS_Present_ZnO_No_UV_Saline_50mM	0,0023	*
Control_Present_ZnO_No_UV_Saline_50mM	0,0755	ns
A_KOREENSIS_Absent_ZnO_No_UV_Saline_150mM	0,4516	ns
A_KOREENSIS_Present_ZnO_No_UV_Saline_150mM	0,0007	*
Control_Present_ZnO_No_UV_Saline_150mM	0,3102	ns
A_KOREENSIS_Absent_ZnO_UVC_Absent	0,1676	ns
A_KOREENSIS_Present_ZnO_UVC_Absent	0,0168	*
Control_Present_ZnO_UVC_Absent	0,2407	ns
A_KOREENSIS_Absent_ZnO_UVC_Saline_50mM	0,1618	ns
A_KOREENSIS_Present_ZnO_UVC_Saline_50mM	0,0000	*
Control_Present_ZnO_UVC_Saline_50mM	0,0755	ns
A_KOREENSIS_Absent_ZnO_UVC_Saline_150mM	0,0690	ns
A_KOREENSIS_Present_ZnO_UVC_Saline_150mM	0,0409	*
Control_Present_ZnO_UVC_Saline_150mM	0,3102	ns
A_KOREENSIS_Absent_ZnO_Environmental_UV_Absent	0,0005	*
A_KOREENSIS_Present_ZnO_Environmental_UV_Absent	0,0916	ns
Control_Present_ZnO_Environmental_UV_Absent	0,2407	ns
A_KOREENSIS_Absent_ZnO_Environmental_UV_Saline_50mM	0,0003	*
A_KOREENSIS_Present_ZnO_Environmental_UV_Saline_50mM	0,0000	*
Control_Present_ZnO_Environmental_UV_Saline_50mM	0,0755	ns
A_KOREENSIS_Absent_ZnO_Environmental_UV_Saline_150mM	0,0525	ns
A_KOREENSIS_Present_ZnO_Environmental_UV_Saline_150mM	0,0539	ns

Control_Present_ZnO_Environmental_UV_Saline_150mM	0,3102	ns

Table S21. Dunnett's post hoc test comparing dry root biomass (g) under saline stress

Treatment	*p-value vs. control*	*Significance*
A_KOREENSIS_Absent_ZnO_No_UV_Absent	0,0001	*
A_KOREENSIS_Present_ZnO_No_UV_Absent	0,7140	ns
Control_Present_ZnO_No_UV_Absent	0,2758	ns
A_KOREENSIS_Absent_ZnO_No_UV_Saline_50mM	0,0004	*
A_KOREENSIS_Present_ZnO_No_UV_Saline_50mM	0,1675	ns
Control_Present_ZnO_No_UV_Saline_50mM	0,0701	ns
A_KOREENSIS_Absent_ZnO_No_UV_Saline_150mM	0,0744	ns
A_KOREENSIS_Present_ZnO_No_UV_Saline_150mM	0,3477	ns
Control_Present_ZnO_No_UV_Saline_150mM	0,4721	ns
A_KOREENSIS_Absent_ZnO_UVC_Absent	0,0456	*
A_KOREENSIS_Present_ZnO_UVC_Absent	0,3276	ns
Control_Present_ZnO_UVC_Absent	0,2758	ns
A_KOREENSIS_Absent_ZnO_UVC_Saline_50mM	0,9912	ns
A_KOREENSIS_Present_ZnO_UVC_Saline_50mM	0,0000	*
Control_Present_ZnO_UVC_Saline_50mM	0,0701	ns
A_KOREENSIS_Absent_ZnO_UVC_Saline_150mM	0,8001	ns
A_KOREENSIS_Present_ZnO_UVC_Saline_150mM	0,0138	*
Control_Present_ZnO_UVC_Saline_150mM	0,4721	ns
A_KOREENSIS_Absent_ZnO_Environmental_UV_Absent	0,0035	*
A_KOREENSIS_Present_ZnO_Environmental_UV_Absent	0,9398	ns
Control_Present_ZnO_Environmental_UV_Absent	0,2758	ns
A_KOREENSIS_Absent_ZnO_Environmental_UV_Saline_50mM	0,0012	*
A_KOREENSIS_Present_ZnO_Environmental_UV_Saline_50mM	0,0046	*
Control_Present_ZnO_Environmental_UV_Saline_50mM	0,0701	ns
A_KOREENSIS_Absent_ZnO_Environmental_UV_Saline_150mM	0,0015	*
A_KOREENSIS_Present_ZnO_Environmental_UV_Saline_150mM	0,6608	ns
Control_Present_ZnO_Environmental_UV_Saline_150mM	0,4721	ns

Table S22. Dunnett's post hoc test comparing leaf area (cm²) under osmotic stress

Treatment	*p-value vs. control*	*Significance*
A_KOREENSIS_Absent_ZnO_No_UV_Sem	0,0190	*
A_KOREENSIS_Present_ZnO_No_UV_Sem	0,0844	ns
Control_Present_ZnO_No_UV_Sem	0,8176	ns
A_KOREENSIS_Absent_ZnO_No_UV_Osmotic_0.5mPa	0,1104	ns
A_KOREENSIS_Present_ZnO_No_UV_Osmotic_0.5mPa	0,0137	*

Control_Present_ZnO_No_UV_Osmotic_0.5mPa	0,3162	ns
A_KOREENSIS_Absent_ZnO_No_UV_Osmotic_1.5mPa	0,9592	ns
A_KOREENSIS_Present_ZnO_No_UV_Osmotic_1.5mPa	0,0019	*
Control_Present_ZnO_No_UV_Osmotic_1.5mPa	0,6463	ns
A_KOREENSIS_Absent_ZnO_UVC_Sem	0,0009	*
A_KOREENSIS_Present_ZnO_UVC_Sem	0,0561	ns
Control_Present_ZnO_UVC_Sem	0,8176	ns
A_KOREENSIS_Absent_ZnO_UVC_Osmotic_0.5mPa	0,0146	*
A_KOREENSIS_Present_ZnO_UVC_Osmotic_0.5mPa	0,2108	ns
Control_Present_ZnO_UVC_Osmotic_0.5mPa	0,3162	ns
A_KOREENSIS_Absent_ZnO_UVC_Osmotic_1.5mPa	0,0014	*
A_KOREENSIS_Present_ZnO_UVC_Osmotic_1.5mPa	0,9664	ns
Control_Present_ZnO_UVC_Osmotic_1.5mPa	0,6463	ns
A_KOREENSIS_Absent_ZnO_Environmental_UV_Sem	0,2360	ns
A_KOREENSIS_Present_ZnO_Environmental_UV_Sem	0,1868	ns
Control_Present_ZnO_Environmental_UV_Sem	0,8176	ns
A_KOREENSIS_Absent_ZnO_Environmental_UV_Osmotic_0.5mPa	0,7713	ns
A_KOREENSIS_Present_ZnO_Environmental_UV_Osmotic_0.5mPa	0,0000	*
Control_Present_ZnO_Environmental_UV_Osmotic_0.5mPa	0,3162	ns
A_KOREENSIS_Absent_ZnO_Environmental_UV_Osmotic_1.5mPa	0,1681	ns
A_KOREENSIS_Present_ZnO_Environmental_UV_Osmotic_1.5mPa	0,0004	*
Control_Present_ZnO_Environmental_UV_Osmotic_1.5mPa	0,6463	ns

Table S23. Dunnett's post hoc test comparing shoot length (cm) under osmotic stress

Treatment	***p-value vs. control***	***Significance***
A_KOREENSIS_Absent_ZnO_No_UV_Sem	0,0901	ns
A_KOREENSIS_Present_ZnO_No_UV_Sem	0,0030	*
Control_Present_ZnO_No_UV_Sem	0,2807	ns
A_KOREENSIS_Absent_ZnO_No_UV_Osmotic_0.5mPa	0,6776	ns
A_KOREENSIS_Present_ZnO_No_UV_Osmotic_0.5mPa	0,4137	ns
Control_Present_ZnO_No_UV_Osmotic_0.5mPa	0,1907	ns
A_KOREENSIS_Absent_ZnO_No_UV_Osmotic_1.5mPa	0,0715	ns
A_KOREENSIS_Present_ZnO_No_UV_Osmotic_1.5mPa	0,0235	*
Control_Present_ZnO_No_UV_Osmotic_1.5mPa	0,2041	ns
A_KOREENSIS_Absent_ZnO_UVC_Sem	0,0010	*
A_KOREENSIS_Present_ZnO_UVC_Sem	0,0414	*
Control_Present_ZnO_UVC_Sem	0,2807	ns
A_KOREENSIS_Absent_ZnO_UVC_Osmotic_0.5mPa	0,1065	ns
A_KOREENSIS_Present_ZnO_UVC_Osmotic_0.5mPa	0,0036	*
Control_Present_ZnO_UVC_Osmotic_0.5mPa	0,1907	ns
A_KOREENSIS_Absent_ZnO_UVC_Osmotic_1.5mPa	0,3711	ns
A_KOREENSIS_Present_ZnO_UVC_Osmotic_1.5mPa	0,0246	*
Control_Present_ZnO_UVC_Osmotic_1.5mPa	0,2041	ns

A_KOREENSIS_Absent_ZnO_Environmental_UV_Sem	0,0551	ns
A_KOREENSIS_Present_ZnO_Environmental_UV_Sem	0,1805	ns
Control_Present_ZnO_Environmental_UV_Sem	0,2807	ns
A_KOREENSIS_Absent_ZnO_Environmental_UV_Osmotic_0.5mPa	0,5685	ns
A_KOREENSIS_Present_ZnO_Environmental_UV_Osmotic_0.5mPa	0,0001	*
Control_Present_ZnO_Environmental_UV_Osmotic_0.5mPa	0,1907	ns
A_KOREENSIS_Absent_ZnO_Environmental_UV_Osmotic_1.5mPa	0,2738	ns
A_KOREENSIS_Present_ZnO_Environmental_UV_Osmotic_1.5mPa	0,0178	*
Control_Present_ZnO_Environmental_UV_Osmotic_1.5mPa	0,2041	ns

Table S24. Dunnett's post hoc test comparing root length (cm) under osmotic stress

Treatment	***p-value vs. control***	***Significance***
A_KOREENSIS_Absent_ZnO_No_UV_Sem	0,2438	ns
A_KOREENSIS_Present_ZnO_No_UV_Sem	0,0958	ns
Control_Present_ZnO_No_UV_Sem	0,1113	ns
A_KOREENSIS_Absent_ZnO_No_UV_Osmotic_0.5mPa	0,7551	ns
A_KOREENSIS_Present_ZnO_No_UV_Osmotic_0.5mPa	0,0286	*
Control_Present_ZnO_No_UV_Osmotic_0.5mPa	0,0253	*
A_KOREENSIS_Absent_ZnO_No_UV_Osmotic_1.5mPa	0,0007	*
A_KOREENSIS_Present_ZnO_No_UV_Osmotic_1.5mPa	0,0200	*
Control_Present_ZnO_No_UV_Osmotic_1.5mPa	0,0012	*
A_KOREENSIS_Absent_ZnO_UVC_Sem	0,6735	ns
A_KOREENSIS_Present_ZnO_UVC_Sem	0,0675	ns
Control_Present_ZnO_UVC_Sem	0,1113	ns
A_KOREENSIS_Absent_ZnO_UVC_Osmotic_0.5mPa	0,9308	ns
A_KOREENSIS_Present_ZnO_UVC_Osmotic_0.5mPa	0,0283	*
Control_Present_ZnO_UVC_Osmotic_0.5mPa	0,0253	*
A_KOREENSIS_Absent_ZnO_UVC_Osmotic_1.5mPa	0,1873	ns
A_KOREENSIS_Present_ZnO_UVC_Osmotic_1.5mPa	0,2223	ns
Control_Present_ZnO_UVC_Osmotic_1.5mPa	0,0012	*
A_KOREENSIS_Absent_ZnO_Environmental_UV_Sem	0,0261	*
A_KOREENSIS_Present_ZnO_Environmental_UV_Sem	0,0452	*
Control_Present_ZnO_Environmental_UV_Sem	0,1113	ns
A_KOREENSIS_Absent_ZnO_Environmental_UV_Osmotic_0.5mPa	0,8683	ns
A_KOREENSIS_Present_ZnO_Environmental_UV_Osmotic_0.5mPa	0,0738	ns
Control_Present_ZnO_Environmental_UV_Osmotic_0.5mPa	0,0253	*
A_KOREENSIS_Absent_ZnO_Environmental_UV_Osmotic_1.5mPa	0,6232	ns
A_KOREENSIS_Present_ZnO_Environmental_UV_Osmotic_1.5mPa	0,1614	ns
Control_Present_ZnO_Environmental_UV_Osmotic_1.5mPa	0,0012	*

Table S25. Dunnett's post hoc test comparing fresh shoot biomass (g) under osmotic stress

Treatment	*p-value vs. control*	*Significance*
A_KOREENSIS_Absent_ZnO_No_UV_Sem	0,0001	*
A_KOREENSIS_Present_ZnO_No_UV_Sem	0,0441	*
Control_Present_ZnO_No_UV_Sem	0,0978	ns
A_KOREENSIS_Absent_ZnO_No_UV_Osmotic_0.5mPa	0,0202	*
A_KOREENSIS_Present_ZnO_No_UV_Osmotic_0.5mPa	0,0175	*
Control_Present_ZnO_No_UV_Osmotic_0.5mPa	0,1376	ns
A_KOREENSIS_Absent_ZnO_No_UV_Osmotic_1.5mPa	0,1190	ns
A_KOREENSIS_Present_ZnO_No_UV_Osmotic_1.5mPa	0,0000	*
Control_Present_ZnO_No_UV_Osmotic_1.5mPa	0,5431	ns
A_KOREENSIS_Absent_ZnO_UVC_Sem	0,0003	*
A_KOREENSIS_Present_ZnO_UVC_Sem	0,0000	*
Control_Present_ZnO_UVC_Sem	0,0978	ns
A_KOREENSIS_Absent_ZnO_UVC_Osmotic_0.5mPa	0,0401	*
A_KOREENSIS_Present_ZnO_UVC_Osmotic_0.5mPa	0,7978	ns
Control_Present_ZnO_UVC_Osmotic_0.5mPa	0,1376	ns
A_KOREENSIS_Absent_ZnO_UVC_Osmotic_1.5mPa	0,0389	*
A_KOREENSIS_Present_ZnO_UVC_Osmotic_1.5mPa	0,6366	ns
Control_Present_ZnO_UVC_Osmotic_1.5mPa	0,5431	ns
A_KOREENSIS_Absent_ZnO_Environmental_UV_Sem	0,0001	*
A_KOREENSIS_Present_ZnO_Environmental_UV_Sem	0,0210	*
Control_Present_ZnO_Environmental_UV_Sem	0,0978	ns
A_KOREENSIS_Absent_ZnO_Environmental_UV_Osmotic_0.5mPa	0,0805	ns
A_KOREENSIS_Present_ZnO_Environmental_UV_Osmotic_0.5mPa	0,0000	*
Control_Present_ZnO_Environmental_UV_Osmotic_0.5mPa	0,1376	ns
A_KOREENSIS_Absent_ZnO_Environmental_UV_Osmotic_1.5mPa	0,5988	ns
A_KOREENSIS_Present_ZnO_Environmental_UV_Osmotic_1.5mPa	0,0000	*
Control_Present_ZnO_Environmental_UV_Osmotic_1.5mPa	0,5431	ns

Table S26. Dunnett's post hoc test comparing fresh root biomass (g) under osmotic stress

Treatment	*p-value vs. control*	*Significance*
A_KOREENSIS_Absent_ZnO_No_UV_Sem	0,0016	*
A_KOREENSIS_Present_ZnO_No_UV_Sem	0,0165	*
Control_Present_ZnO_No_UV_Sem	0,4941	ns
A_KOREENSIS_Absent_ZnO_No_UV_Osmotic_0.5mPa	0,0000	*
A_KOREENSIS_Present_ZnO_No_UV_Osmotic_0.5mPa	0,8568	ns
Control_Present_ZnO_No_UV_Osmotic_0.5mPa	0,0000	*
A_KOREENSIS_Absent_ZnO_No_UV_Osmotic_1.5mPa	0,0000	*
A_KOREENSIS_Present_ZnO_No_UV_Osmotic_1.5mPa	0,7521	ns
Control_Present_ZnO_No_UV_Osmotic_1.5mPa	0,0000	*
A_KOREENSIS_Absent_ZnO_UVC_Sem	0,1193	ns

A_KOREENSIS_Present_ZnO_UVC_Sem	0,0669	ns
Control_Present_ZnO_UVC_Sem	0,4941	ns
A_KOREENSIS_Absent_ZnO_UVC_Osmotic_0.5mPa	0,8157	ns
A_KOREENSIS_Present_ZnO_UVC_Osmotic_0.5mPa	0,9572	ns
Control_Present_ZnO_UVC_Osmotic_0.5mPa	0,0000	*
A_KOREENSIS_Absent_ZnO_UVC_Osmotic_1.5mPa	0,8686	ns
A_KOREENSIS_Present_ZnO_UVC_Osmotic_1.5mPa	0,4975	ns
Control_Present_ZnO_UVC_Osmotic_1.5mPa	0,0000	*
A_KOREENSIS_Absent_ZnO_Environmental_UV_Sem	0,0149	*
A_KOREENSIS_Present_ZnO_Environmental_UV_Sem	0,0004	*
Control_Present_ZnO_Environmental_UV_Sem	0,4941	ns
A_KOREENSIS_Absent_ZnO_Environmental_UV_Osmotic_0.5mPa	0,8587	ns
A_KOREENSIS_Present_ZnO_Environmental_UV_Osmotic_0.5mPa	0,0316	*
Control_Present_ZnO_Environmental_UV_Osmotic_0.5mPa	0,0000	*
A_KOREENSIS_Absent_ZnO_Environmental_UV_Osmotic_1.5mPa	0,6785	ns
A_KOREENSIS_Present_ZnO_Environmental_UV_Osmotic_1.5mPa	0,9221	ns
Control_Present_ZnO_Environmental_UV_Osmotic_1.5mPa	0,0000	*

Table S27. Dunnett's post hoc test comparing dry shoot biomass (g) under osmotic stress

Treatment	***p-value vs. control***	***Significance***
A_KOREENSIS_Absent_ZnO_No_UV_Sem	0,0008	*
A_KOREENSIS_Present_ZnO_No_UV_Sem	0,2875	ns
Control_Present_ZnO_No_UV_Sem	0,4185	ns
A_KOREENSIS_Absent_ZnO_No_UV_Osmotic_0.5mPa	0,0518	ns
A_KOREENSIS_Present_ZnO_No_UV_Osmotic_0.5mPa	0,0045	*
Control_Present_ZnO_No_UV_Osmotic_0.5mPa	0,0204	*
A_KOREENSIS_Absent_ZnO_No_UV_Osmotic_1.5mPa	0,0696	ns
A_KOREENSIS_Present_ZnO_No_UV_Osmotic_1.5mPa	0,0001	*
Control_Present_ZnO_No_UV_Osmotic_1.5mPa	0,6685	ns
A_KOREENSIS_Absent_ZnO_UVC_Sem	0,3035	ns
A_KOREENSIS_Present_ZnO_UVC_Sem	0,0352	*
Control_Present_ZnO_UVC_Sem	0,4185	ns
A_KOREENSIS_Absent_ZnO_UVC_Osmotic_0.5mPa	0,0063	*
A_KOREENSIS_Present_ZnO_UVC_Osmotic_0.5mPa	0,1126	ns
Control_Present_ZnO_UVC_Osmotic_0.5mPa	0,0204	*
A_KOREENSIS_Absent_ZnO_UVC_Osmotic_1.5mPa	0,0461	*
A_KOREENSIS_Present_ZnO_UVC_Osmotic_1.5mPa	0,4593	ns
Control_Present_ZnO_UVC_Osmotic_1.5mPa	0,6685	ns
A_KOREENSIS_Absent_ZnO_Environmental_UV_Sem	0,0011	*
A_KOREENSIS_Present_ZnO_Environmental_UV_Sem	0,1751	ns
Control_Present_ZnO_Environmental_UV_Sem	0,4185	ns
A_KOREENSIS_Absent_ZnO_Environmental_UV_Osmotic_0.5mPa	0,0764	ns
A_KOREENSIS_Present_ZnO_Environmental_UV_Osmotic_0.5mPa	0,0000	*

Control_Present_ZnO_Environmental_UV_Osmotic_0.5mPa	0,0204	*
A_KOREENSIS_Absent_ZnO_Environmental_UV_Osmotic_1.5mPa	0,4907	ns
A_KOREENSIS_Present_ZnO_Environmental_UV_Osmotic_1.5mPa	0,0050	*
Control_Present_ZnO_Environmental_UV_Osmotic_1.5mPa	0,6685	ns

Table S28. Dunnett's post hoc test comparing dry root biomass (g) under osmotic stress

Treatment	***p-value vs. control***	***Significance***
A_KOREENSIS_Absent_ZnO_No_UV_Sem	0,0020	*
A_KOREENSIS_Present_ZnO_No_UV_Sem	0,4956	ns
Control_Present_ZnO_No_UV_Sem	0,9239	ns
A_KOREENSIS_Absent_ZnO_No_UV_Osmotic_0.5mPa	0,0096	*
A_KOREENSIS_Present_ZnO_No_UV_Osmotic_0.5mPa	0,0133	*
Control_Present_ZnO_No_UV_Osmotic_0.5mPa	0,0000	*
A_KOREENSIS_Absent_ZnO_No_UV_Osmotic_1.5mPa	0,0000	*
A_KOREENSIS_Present_ZnO_No_UV_Osmotic_1.5mPa	0,0375	*
Control_Present_ZnO_No_UV_Osmotic_1.5mPa	0,0000	*
A_KOREENSIS_Absent_ZnO_UVC_Sem	0,2800	ns
A_KOREENSIS_Present_ZnO_UVC_Sem	0,9809	ns
Control_Present_ZnO_UVC_Sem	0,9239	ns
A_KOREENSIS_Absent_ZnO_UVC_Osmotic_0.5mPa	0,2739	ns
A_KOREENSIS_Present_ZnO_UVC_Osmotic_0.5mPa	0,0008	*
Control_Present_ZnO_UVC_Osmotic_0.5mPa	0,0000	*
A_KOREENSIS_Absent_ZnO_UVC_Osmotic_1.5mPa	0,1486	ns
A_KOREENSIS_Present_ZnO_UVC_Osmotic_1.5mPa	0,0441	*
Control_Present_ZnO_UVC_Osmotic_1.5mPa	0,0000	*
A_KOREENSIS_Absent_ZnO_Environmental_UV_Sem	0,0367	*
A_KOREENSIS_Present_ZnO_Environmental_UV_Sem	0,3211	ns
Control_Present_ZnO_Environmental_UV_Sem	0,9239	ns
A_KOREENSIS_Absent_ZnO_Environmental_UV_Osmotic_0.5mPa	0,0545	ns
A_KOREENSIS_Present_ZnO_Environmental_UV_Osmotic_0.5mPa	0,0001	*
Control_Present_ZnO_Environmental_UV_Osmotic_0.5mPa	0,0000	*
A_KOREENSIS_Absent_ZnO_Environmental_UV_Osmotic_1.5mPa	0,3395	ns
A_KOREENSIS_Present_ZnO_Environmental_UV_Osmotic_1.5mPa	0,2476	ns
Control_Present_ZnO_Environmental_UV_Osmotic_1.5mPa	0,0000	*

5 GENERAL CONCLUSIONS

This thesis demonstrates that extremophilic microorganisms isolated from photovoltaic panels constitute a valuable biological resource for enhancing plant performance under abiotic stress conditions. Through a progressive and integrative experimental framework, the results reveal that microbial stress tolerance, seed germination responses, and early seedling growth are strongly influenced by the interaction between microbial identity, stress type and intensity, radiation exposure, and the presence of crystalline zinc oxide.

The initial characterization of microbial UV resistance confirmed a clear stratification among isolates, with *Rhodotorula mucilaginosa* exhibiting superior tolerance to both UV-C and environmental-UV radiation, while bacterial strains displayed variable and generally lower intrinsic resistance under planktonic conditions. These findings indicate that microbial persistence on photovoltaic panels may depend not only on individual resistance mechanisms but also on ecological factors such as biofilm formation and community-level protection.

Subsequent germination assays demonstrated that extremophilic microorganisms can significantly enhance seed germination percentage and germination speed of *Eruca sativa* under saline and osmotic stress. However, these effects were not universal; rather, they were highly strain-specific and stress-dependent. Microbial efficacy was consistently amplified by the presence of ZnO crystals, particularly under severe stress conditions, highlighting a robust synergistic interaction between biological and inorganic components.

Early seedling growth experiments further revealed that microbial inoculation primarily contributed to growth stability and biomass allocation modulation rather than uniform biomass maximization. *Arthrobacter koreensis* promoted improved shoot development and stress tolerance under moderate salinity and osmotic stress, especially when combined with ZnO and non-germicidal radiation regimes. Under severe stress, microbial treatments mitigated growth inhibition but did not fully overcome physiological constraints, underscoring the importance of stress intensity as a limiting factor.

Collectively, the results emphasize that extremophilic microorganisms function as conditional biostimulants, whose effectiveness depends on environmental context rather than exhibiting generalized growth-promoting behavior. The incorporation of ZnO crystals acted as a

functional amplifier of microbial effects, enabling microbial-derived benefits to be expressed more consistently under adverse conditions.

Overall, this thesis advances a conceptual shift from binary evaluations of biostimulant performance toward a context-aware framework that integrates microbial ecology, plant physiology, and material science. The findings support the strategic use of extremophilic microorganisms and inorganic cofactors as sustainable tools to enhance early plant establishment in stress-prone agricultural systems. Future research should extend these approaches and include molecular and biochemical analyses for agronomic applicability.

REFERENCES

Abdelkhalik A, Gyushi MAH, Howladar SM, Kutby AM, Asiri NA, Baeshen AA, Nahari AM, Alsamadany H, Semida WM (2025) Synergistic Effects of Zinc Oxide Nanoparticles and Moringa Leaf Extracts on Drought Tolerance and Productivity of Cucurbita pepo L. Under Saline Conditions. Plants 14(4):544. https://doi.org/10.3390/plants14040544

Abdul Rahman NSN, Abdul Hamid NW, Nadarajah K (2021) Effects of Abiotic Stress on Soil Microbiome. International Journal of Molecular Sciences 22(16):9036. https://doi.org/10.3390/ijms22169036

Adhikari A, Khan MA, Lee K-E, Kang S-M, Dhungana SK, Bhusal N, Lee I-J (2020) The Halotolerant Rhizobacterium—Pseudomonas koreensis MU2 Enhances Inorganic Silicon and Phosphorus Use Efficiency and Augments Salt Stress Tolerance in Soybean (Glycine max L.). Microorganisms 8(9):1256. https://doi.org/10.3390/microorganisms8091256

Ahmad HM, Fiaz S, Hafeez S, Zahra S, Shah AN, Gul B, Aziz O, Mahmood-Ur-Rahman, Fakhar A, Rafique M, Chen Y, Yang SH, Wang X (2022a) Plant Growth-Promoting Rhizobacteria Eliminate the Effect of Drought Stress in Plants: A Review. Front Plant Sci 13. https://doi.org/10.3389/fpls.2022.875774

Ahmad T, Pandey V, Saddam Husain M, Adiba, Munjal S (2022b) Structural and spectroscopic analysis of pure phase hexagonal wurtzite ZnO nanoparticles synthesized by sol-gel. Materials Today: Proceedings 49:1694–1697. https://doi.org/10.1016/j.matpr.2021.07.456

Ahmed M, Decsi K, Tóth Z (2023) Different Tactics of Synthesized Zinc Oxide Nanoparticles, Homeostasis Ions, and Phytohormones as Regulators and Adaptatively Parameters to Alleviate the Adverse Effects of Salinity Stress on Plants. Life 13(1):73. https://doi.org/10.3390/life13010073

Ajijah N, Fiodor A, Pandey AK, Rana A, Pranaw K (2023) Plant Growth-Promoting Bacteria (PGPB) with Biofilm-Forming Ability: A Multifaceted Agent for Sustainable Agriculture. Diversity 15(1):112. https://doi.org/10.3390/d15010112

Akhtar N, Khan S, Rehman SU, Rha ES, Jamil M (2022) Combined Effect of Zinc Oxide Nanoparticles and Bacteria on Osmolytes and Antioxidative Parameters of Rice (Oryza sativa L.) Plant Grown in Heavy Metal-Contaminated Water. Adsorption Science & Technology 2022:4148765. https://doi.org/10.1155/2022/4148765

Albarracín VH, Pathak GP, Douki T, Cadet J, Borsarelli CD, Gärtner W, Farias ME (2012) Extremophilic Acinetobacter Strains from High-Altitude Lakes in Argentinean Puna: Remarkable UV-B Resistance and Efficient DNA Damage Repair. Orig Life Evol Biosph 42(2):201–221. https://doi.org/10.1007/s11084-012-9276-3

Alharbi K, Hafez EM, Omara AE-D, Rashwan E, Alshaal T (2023) Zinc oxide nanoparticles and PGPR strengthen salinity tolerance and productivity of wheat irrigated with saline water in sodic-saline soil. Plant Soil 493(1):475–495. https://doi.org/10.1007/s11104-023-06245-7

Álvarez S, Gómez-Bellot MJ, Castillo M, Bañón S, Sánchez-Blanco MJ (2012) Osmotic and saline effect on growth, water relations, and ion uptake and translocation in *Phlomis purpurea* plants. Environmental and Experimental Botany 78:138–145. https://doi.org/10.1016/j.envexpbot.2011.12.035

Álvarez S, Sánchez-Blanco MJ (2015) Comparison of individual and combined effects of salinity and deficit irrigation on physiological, nutritional and ornamental aspects of tolerance in *Callistemon laevis* plants. Journal of Plant Physiology 185:65–74. https://doi.org/10.1016/j.jplph.2015.07.009

Angelakis GN, Psarologaki C, Pirintsos S, Kotzabasis K (2024) Extremophiles and Extremophilic Behaviour—New Insights and Perspectives. Life 14(11):1425. https://doi.org/10.3390/life14111425

Anwar T, Safdar A, Qureshi H, Siddiqi EH, Ullah N, Naseem MT, Soufan W (2025) Synergistic effects of Vachellia nilotica-derived zinc oxide nanoparticles and melatonin on drought tolerance in Fragaria × ananassa. BMC Plant Biol 25(1):82. https://doi.org/10.1186/s12870-025-06114-8

Balasubramaniyam S, Rathinam T, Srinivasan M, Arulselvan P, Mickymaray S, Alfaiz FA (2025) Green-engineered synthesis of zinc oxide (ZnO) nanoparticles using Musa paradisiaca: evaluation of antioxidant, antimicrobial, anti-inflammatory, and antihyperglycemic activities. 3 Biotech 15(10):358. https://doi.org/10.1007/s13205-025-04526-9

Bao X-G, Chong P-F, He C, Lu X-M, Wang X-Y, Zhang F, Tan B-B, Yang J-L, Gao L-L (2025) Enterobacter-inoculation altered the C, N contents and regulated biomass allocation in Reaumuria soongorica to promote plant growth and improve salt stress tolerance. Front Plant Sci 15. https://doi.org/10.3389/fpls.2024.1502659

Barampuram S, Allen G, Krasnyanski S (2014) Effect of various sterilization procedures on the in vitro germination of cotton seeds. Plant Cell Tiss Organ Cult 118(1):179–185. https://doi.org/10.1007/s11240-014-0472-x

Barcia RA, Pena LB, Zawoznik MS, Benavides MP, Gallego SM (2014) Osmotic adjustment and maintenance of the redox balance in root tissue may be key points to overcome a mild water deficit during the early growth of wheat. Plant Growth Regul 74(2):107–117. https://doi.org/10.1007/s10725-014-9902-3

Bayindir F, Coşkun Y (2022) The effects of irrigation water salinity on the seed germination and seedling growth of rice. Genetika 54(1):255–264

Blake C, Christensen MN, Kovács ÁT (2021) Molecular Aspects of Plant Growth Promotion and Protection by Bacillus subtilis. MPMI 34(1):15–25. https://doi.org/10.1094/MPMI-08-20-0225-CR

Braga CR, Richard KN, Gardner H, Swain G, Hunsucker KZ (2023) Investigating the Impacts of UVC Radiation on Natural and Cultured Biofilms: An assessment of Cell Viability. Microorganisms 11(5):1348. https://doi.org/10.3390/microorganisms11051348

Cardarelli M, Woo SL, Rouphael Y, Colla G (2022) Seed Treatments with Microorganisms Can Have a Biostimulant Effect by Influencing Germination and Seedling Growth of Crops. Plants 11(3):259. https://doi.org/10.3390/plants11030259

Caser M, Percivalle NM, Cauda V (2024) The Application of Micro- and Nano-Sized Zinc Oxide Particles Differently Triggers Seed Germination in Ocimum basilicum L., Lactuca sativa L., and Lepidium sativum L. under Controlled Conditions. Horticulturae 10(6):575. https://doi.org/10.3390/horticulturae10060575

Chandran V, Shaji H, Mathew L (2020) 7 - Endophytic microbial influence on plant stress responses. In: Kumar A, E.k R (eds) Microbial Endophytes. Woodhead Publishing, pp 161–193

Chen C, Zhan J, Du W, Wu S, Li L, Yin C (2025) The mechanisms of plant-associated microbes in regulating plant drought adaptation. J Plant Ecol 18(4):rtaf047. https://doi.org/10.1093/jpe/rtaf047

Chourasia KN, Lal MK, Tiwari RK, Dev D, Kardile HB, Patil VU, Kumar A, Vanishree G, Kumar D, Bhardwaj V, Meena JK, Mangal V, Shelake RM, Kim J-Y, Pramanik D (2021) Salinity Stress in Potato: Understanding Physiological, Biochemical and Molecular Responses. Life 11(6):545. https://doi.org/10.3390/life11060545

Chrunik M, Majchrowski A, Zasada D, Chlanda A, Szala M, Salerno M (2017) Modified Pechini synthesis of Bi2ZnB2O7 nanoparticles. Journal of Alloys and Compounds 725:587–597. https://doi.org/10.1016/j.jallcom.2017.07.172

Cimini S, Gualtieri C, Macovei A, Balestrazzi A, De Gara L, Locato V (2019) Redox Balance-DDR-miRNA Triangle: Relevance in Genome Stability and Stress Responses in Plants. Front Plant Sci 10. https://doi.org/10.3389/fpls.2019.00989

Cushman JC, Denby K, Mittler R (2022) Plant responses and adaptations to a changing climate. The Plant Journal 109(2):319–322. https://doi.org/10.1111/tpj.15641

Dagher D, Taskos D, Mourouzidou S, Monokrousos N (2025) Microbial-Enhanced Abiotic Stress Tolerance in Grapevines: Molecular Mechanisms and Synergistic Effects of Arbuscular Mycorrhizal Fungi, Plant Growth-Promoting Rhizobacteria, and Endophytes. Horticulturae 11(6):592. https://doi.org/10.3390/horticulturae11060592

Das A, Janda T, Sil SK, Adak MK (2025) Exploring regulatory roles of putrescine-doped zinc oxide nanoentities on ethylene signaling, redox imbalance, and programmed cell death in drought-stressed rice (Oryza sativa L.) seedlings. Front Plant Sci 16. https://doi.org/10.3389/fpls.2025.1630837

de Carvalho CCCR (2017) Biofilms: Microbial Strategies for Surviving UV Exposure. Adv Exp Med Biol 996:233–239. https://doi.org/10.1007/978-3-319-56017-5_19

Donia DT, Carbone M (2023a) Seed Priming with Zinc Oxide Nanoparticles to Enhance Crop Tolerance to Environmental Stresses. International Journal of Molecular Sciences 24(24):17612. https://doi.org/10.3390/ijms242417612

Donia DT, Carbone M (2023b) Seed Priming with Zinc Oxide Nanoparticles to Enhance Crop Tolerance to Environmental Stresses. International Journal of Molecular Sciences 24(24):17612. https://doi.org/10.3390/ijms242417612

Dorado-Morales P, Vilanova C, Peretó J, Codoñer FM, Ramón D, Porcar M (2016a) A highly diverse, desert-like microbial biocenosis on solar panels in a Mediterranean city. Sci Rep 6(1):29235. https://doi.org/10.1038/srep29235

Dorado-Morales P, Vilanova C, Peretó J, Codoñer FM, Ramón D, Porcar M (2016b) A highly diverse, desert-like microbial biocenosis on solar panels in a Mediterranean city. Sci Rep 6:29235. https://doi.org/10.1038/srep29235

Dsouza M, Taylor MW, Turner SJ, Aislabie J (2015) Genomic and phenotypic insights into the ecology of Arthrobacter from Antarctic soils. BMC Genomics 16(1):36. https://doi.org/10.1186/s12864-015-1220-2

Eesha A, Sharma R, Chaudhary NS (2023) Effect of PEG-6000 Osmoticum on Seed Germination and Seedling Growth of Lentil (Lens culinaris Medik.) Genotypes. IJARe. https://doi.org/10.18805/IJARe.A-6078

Ellington AJ, Schult TJ, Reisch CR, Christner BC (2025) The Genetic Determinants of Extreme UV Radiation and Desiccation Tolerance in a Bacterium Recovered from the Stratosphere. Microorganisms 13(4):756. https://doi.org/10.3390/microorganisms13040756

El-Shazoly RM, Othman AA, Zaheer MS, Al-Hossainy AF, Abdel-Wahab DA (2025) Zinc oxide seed priming enhances drought tolerance in wheat seedlings by improving antioxidant activity and osmoprotection. Sci Rep 15(1):3863. https://doi.org/10.1038/s41598-025-86824-z

Fang D, Li C, Wang N, Li P, Yao P (2013) Structural and optical properties of Mg-doped ZnO thin films prepared by a modified Pechini method. Crystal Research and Technology 48(5):265–272. https://doi.org/10.1002/crat.201200437

Fernández-González AJ, Martínez-Hidalgo P, Cobo-Díaz JF, Villadas PJ, Martínez-Molina E, Toro N, Tringe SG, Fernández-López M (2017) The rhizosphere microbiome of burned holm-oak: potential role of the genus Arthrobacter in the recovery of burned soils. Sci Rep 7(1):6008. https://doi.org/10.1038/s41598-017-06112-3

Fiodor A, Ajijah N, Dziewit L, Pranaw K (2023) Biopriming of seed with plant growth-promoting bacteria for improved germination and seedling growth. Front Microbiol 14. https://doi.org/10.3389/fmicb.2023.1142966

Fouad N, El-Zayat EM, Amr D, El-Khishin DA, Abd-Elhalim HM, Hafez A, Radwan KH, Hamwieh A, Tadesse W (2025) Characterizing Wheat Rhizosphere Bacterial Microbiome

Dynamics Under Salinity Stress: Insights from 16S rRNA Metagenomics for Enhancing Stress Tolerance. Plants 14(7):1033. https://doi.org/10.3390/plants14071033

Garbeles D, Milan M, Palmiano D (2024) Effects of Ultraviolet-C (UV-C) radiation on germination, seedling growth, and abiotic stress response in waxy corn (Zea mays L.). Academia Journal of Biology 46(4):35–46. https://doi.org/10.15625/2615-9023/21074

Garcia-Cortes A, Garcia-Vásquez JA, Aranguren Y, Ramirez-Castrillon M (2021) Pigment Production Improvement in Rhodotorula mucilaginosa AJB01 Using Design of Experiments. Microorganisms 9(2):387. https://doi.org/10.3390/microorganisms9020387

Ghaffari Yaichi Z, Hassanpouraghdam MB, Rasouli F, Aazami MA, Vojodi Mehrabani L, Jabbari SF, Asadi M, Esfandiari E, Jimenez-Becker S (2025) Zinc oxide nanoparticles foliar use and arbuscular mycorrhiza inoculation retrieved salinity tolerance in Dracocephalum moldavica L. by modulating growth responses and essential oil constituents. Sci Rep 15(1):492. https://doi.org/10.1038/s41598-024-84198-2

Gloster TM, Toksoy Öner E (2025) Microbial exopolysaccharide production by polyextremophiles in the adaptation to multiple extremes. FEBS Letters 599(23):3417–3443. https://doi.org/10.1002/1873-3468.70138

González-García Y, Escobar-Hernández DI, Benavides-Mendoza A, Morales-Díaz AB, Olivares-Sáenz E, Juárez-Maldonado A (2023) UV-A Radiation Stimulates Tolerance against Fusarium oxysporum f. sp. lycopersici in Tomato Plants. Horticulturae 9(4):499. https://doi.org/10.3390/horticulturae9040499

Guesmi S, Pujic P, Nouioui I, Dubost A, Najjari A, Ghedira K, Igual JM, Miotello G, Cherif A, Armengaud J, Klenk H-P, Normand P, Sghaier H (2021) Ionizing-radiation-resistant Kocuria rhizophila PT10 isolated from the Tunisian Sahara xerophyte Panicum turgidum: Polyphasic characterization and proteogenomic arsenal. Genomics 113(1 Pt 1):317–330. https://doi.org/10.1016/j.ygeno.2020.11.029

Guijarro-Real C, Navarro A, Esposito S, Festa G, Macellaro R, Di Cesare C, Fita A, Rodríguez-Burruezo A, Cardi T, Prohens J, Tripodi P (2020) Large scale phenotyping and molecular analysis in a germplasm collection of rocket salad (Eruca vesicaria) reveal a differentiation of the gene pool by geographical origin. Euphytica 216(3):53. https://doi.org/10.1007/s10681-020-02586-x

Hammami SBM, Chaari S, Baazaoui N, Drira R, Drira N, Aounallah K, Maazoun A, Antar Z, Jorrín Novo JV, Bettaieb T, Rapoport HF, Sghaier-Hammami B (2022) The Regulation of Ion Homeostasis, Growth, and Biomass Allocation in Date Palm Ex Vitro Plants Depends on the Level of Water Salinity. Sustainability 14(19):12676. https://doi.org/10.3390/su141912676

Hanin M, Ebel C, Ngom M, Laplaze L, Masmoudi K (2016) New Insights on Plant Salt Tolerance Mechanisms and Their Potential Use for Breeding. Front Plant Sci 7. https://doi.org/10.3389/fpls.2016.01787

Hasanuzzaman M, Parvin K, Bardhan K, Nahar K, Anee TI, Masud AAC, Fotopoulos V (2021) Biostimulants for the Regulation of Reactive Oxygen Species Metabolism in Plants under Abiotic Stress. Cells 10(10):2537. https://doi.org/10.3390/cells10102537

Hernández-Fernández G, Galán B, Carmona M, Castro L, García JL (2022) Transcriptional response of the xerotolerant Arthrobacter sp. Helios strain to PEG-induced drought stress. Front Microbiol 13. https://doi.org/10.3389/fmicb.2022.1009068

Hosseinpour A, Haliloglu K, Tolga Cinisli K, Ozkan G, Ozturk HI, Pour-Aboughadareh A, Poczai P (2020) Application of Zinc Oxide Nanoparticles and Plant Growth Promoting Bacteria Reduces Genetic Impairment under Salt Stress in Tomato (Solanum lycopersicum L. 'Linda'). Agriculture 10(11):521. https://doi.org/10.3390/agriculture10110521

Ianculescu AC, Vasilescu CA, Crisan M, Raileanu M, Vasile BS, Calugaru M, Crisan D, Dragan N, Curecheriu L, Mitoseriu L (2015) Formation mechanism and characteristics of lanthanum-doped BaTiO3 powders and ceramics prepared by the sol–gel process. Materials Characterization 106:195–207. https://doi.org/10.1016/j.matchar.2015.05.022

Janah I, Elhasnaoui A, Laouane RB, Ait-El-Mokhtar M, Anli M (2025) Exploring Seed Priming as a Strategy for Enhancing Abiotic Stress Tolerance in Cereal Crops. Stresses 5(2):39. https://doi.org/10.3390/stresses5020039

Jayachandran A, T.r. A, Nair AS (2021) Green synthesis and characterization of zinc oxide nanoparticles using Cayratia pedata leaf extract. Biochemistry and Biophysics Reports 26:100995. https://doi.org/10.1016/j.bbrep.2021.100995

Jones DL, Baxter BK (2017) DNA Repair and Photoprotection: Mechanisms of Overcoming Environmental Ultraviolet Radiation Exposure in Halophilic Archaea. Front Microbiol 8. https://doi.org/10.3389/fmicb.2017.01882

Jovović M, Tunguz V, Mirosavljević M, Pržulj N (2018) Effect of salinity and drought stress on germination and early seedlings growth of bread wheat (Triticum aestivum L.). Genetika 50(1):285–298

Kajla M, Yadav VK, Khokhar J, Singh S, Chhokar RS, Meena RP, Sharma RK (2015) Increase in wheat production through management of abiotic stresses : A review. Journal of Applied and Natural Science 7(2):1070–1080. https://doi.org/10.31018/jans.v7i2.733

Kalleku JN, Ihsan S, Al-Azzawi TNI, Khan M, Hussain A, Chebitok F, Das AK, Moon Y-S, Mun B-G, Lee I-J, Ali S, Yun B-W (2024) Halotolerant Pseudomonas koreensis S4T10 mitigate salt and drought stress in Arabidopsis thaliana. Physiologia Plantarum 176(2):e14258. https://doi.org/10.1111/ppl.14258

Karentz D (2015) Beyond Xeroderma Pigmentosum: DNA Damage and Repair in an Ecological Context. A Tribute to James E. Cleaver. Photochemistry and Photobiology 91(2):460–474. https://doi.org/10.1111/php.12388

Khan N, Ali S, Tariq H, Latif S, Yasmin H, Mehmood A, Shahid MA (2020) Water Conservation and Plant Survival Strategies of Rhizobacteria under Drought Stress. Agronomy 10(11):1683. https://doi.org/10.3390/agronomy10111683

Koza NA, Adedayo AA, Babalola OO, Kappo AP (2022) Microorganisms in Plant Growth and Development: Roles in Abiotic Stress Tolerance and Secondary Metabolites Secretion. Microorganisms 10(8):1528. https://doi.org/10.3390/microorganisms10081528

Kumar SM, Yadav S, Choudhary R, Anumantharaj A, Yadav A, Hussain Z, Singh PK, Singh SP, Mandal A, Singh N, Sushkova S, Ercisli S, Sarker U, Yadav SK (2025) Nanopriming with zinc oxide nanoparticle boosts seed vigour, photosynthesis, osmolytes accumulation and antioxidant activity in tomato. Sci Rep 15(1):37375. https://doi.org/10.1038/s41598-025-09269-4

Labadie M, Marchal F, Merbahi N, Girbal-Neuhauser E, Fontagné-Faucher C, Marcato-Romain C-E (2024) Cell density and extracellular matrix composition mitigate bacterial biofilm sensitivity to UV-C LED irradiation. Appl Microbiol Biotechnol 108(1):286. https://doi.org/10.1007/s00253-024-13123-4

Lastochkina O, Garshina D, Ivanov S, Yuldashev R, Khafizova R, Allagulova C, Fedorova K, Avalbaev A, Maslennikova D, Bosacchi M (2020) Seed Priming with Endophytic Bacillus subtilis Modulates Physiological Responses of Two Different Triticum aestivum L. Cultivars under Drought Stress. Plants 9(12):1810. https://doi.org/10.3390/plants9121810

Lee K, An SK, Ku K-M, Kim J (2024) The Optimum Substrate Moisture Level to Enhance the Growth and Quality of Arugula (Eruca sativa). Horticulturae 10(5):483. https://doi.org/10.3390/horticulturae10050483

Lei C, Bagavathiannan M, Wang H, Sharpe SM, Meng W, Yu J (2021) Osmopriming with Polyethylene Glycol (PEG) for Abiotic Stress Tolerance in Germinating Crop Seeds: A Review. Agronomy 11(11):2194. https://doi.org/10.3390/agronomy11112194

Li H, Duijts K, Pasini C, van Santen JE, Lamers J, de Zeeuw T, Verstappen F, Wang N, Zeeman SC, Santelia D, Zhang Y, Testerink C (2023) Effective root responses to salinity stress include maintained cell expansion and carbon allocation. New Phytologist 238(5):1942–1956. https://doi.org/10.1111/nph.18873

Li Z, Li C, Cheng P, Yu G (2022) Rhodotorula mucilaginosa—alternative sources of natural carotenoids, lipids, and enzymes for industrial use. Heliyon 8(11):e11505. https://doi.org/10.1016/j.heliyon.2022.e11505

Libkind D, Moliné M, Sampaio JP, van Broock M (2009) Yeasts from high-altitude lakes: influence of UV radiation. FEMS Microbiol Ecol 69(3):353–362. https://doi.org/10.1111/j.1574-6941.2009.00728.x

Liu F, Ma H, Liu B, Du Z, Ma B, Jing D (2023) Effects of Plant Growth-Promoting Rhizobacteria on the Physioecological Characteristics and Growth of Walnut Seedlings under Drought Stress. Agronomy 13(2):290. https://doi.org/10.3390/agronomy13020290

Lopes MJ dos S, Dias-Filho MB, Gurgel ESC (2021) Successful Plant Growth-Promoting Microbes: Inoculation Methods and Abiotic Factors. Front Sustain Food Syst 5. https://doi.org/10.3389/fsufs.2021.606454

Louis N, Dhankher OP, Puthur JT (2023) Seed priming can enhance and retain stress tolerance in ensuing generations by inducing epigenetic changes and trans-generational memory. Physiologia Plantarum 175(2):e13881. https://doi.org/10.1111/ppl.13881

Mahamuni PP, Patil PM, Dhanavade MJ, Badiger MV, Shadija PG, Lokhande AC, Bohara RA (2019) Synthesis and characterization of zinc oxide nanoparticles by using polyol chemistry for their antimicrobial and antibiofilm activity. Biochemistry and Biophysics Reports 17:71–80. https://doi.org/10.1016/j.bbrep.2018.11.007

Mahmood MZ, Odeibat HA, Ahmad R, Gatasheh MK, Shahzad M, Abbasi AM (2024) Low apoplastic Na+ and intracellular ionic homeostasis confer salinity tolerance upon Ca2SiO4 chemigation in Zea mays L. under salt stress. Front Plant Sci 14. https://doi.org/10.3389/fpls.2023.1268750

Maldonade IR, Rodriguez-Amaya DB, Scamparini ARP (2012) Statistical optimisation of cell growth and carotenoid production by rhodotorula mucilaginosa. Braz J Microbiol 43(1):109–115. https://doi.org/10.1590/S1517-838220120001000012

Manzanera M, Narváez-Reinaldo JJ, García-Fontana C, Vílchez JI, González-López J (2015) Genome Sequence of Arthrobacter koreensis 5J12A, a Plant Growth-Promoting and Desiccation-Tolerant Strain. Genome Announcements 3(3):10.1128/genomea.00648-15. https://doi.org/10.1128/genomea.00648-15

Marzban G, Tesei D (2025) The Extremophiles: Adaptation Mechanisms and Biotechnological Applications. Biology 14(4):412. https://doi.org/10.3390/biology14040412

Masmoudi F, Alsafran M, Jabri HA, Hosseini H, Trigui M, Sayadi S, Tounsi S, Saadaoui I (2023) Halobacteria-Based Biofertilizers: A Promising Alternative for Enhancing Soil Fertility and Crop Productivity under Biotic and Abiotic Stresses—A Review. Microorganisms 11(5):1248. https://doi.org/10.3390/microorganisms11051248

Maucieri C, Caruso C, Bona S, Borin M, Barbera AC, Cavallaro V (2018) Influence of salinity and osmotic stress on germination process in an old sicilian landrace and a modern cultivar of Triticum Durum Desf. Cereal Research Communications 46(2):253–262. https://doi.org/10.1556/0806.46.2018.07

Mazhar MW, Ishtiaq M, Hussain I, Parveen A, Bhatti KH, Azeem M, Thind S, Ajaib M, Maqbool M, Sardar T, Muzammil K, Nasir N (2022) Seed nano-priming with Zinc Oxide nanoparticles in rice mitigates drought and enhances agronomic profile. PLOS ONE 17(3):e0264967. https://doi.org/10.1371/journal.pone.0264967

Meza C, Valenzuela F, Echeverría-Vega A, Gomez A, Sarkar S, Cabeza RA, Arencibia AD, Quiroz K, Carrasco B, Banerjee A (2022) Plant-growth-promoting bacteria from rhizosphere of Chilean common bean ecotype (Phaseolus vulgaris L.) supporting seed germination and growth against salinity stress. Front Plant Sci 13. https://doi.org/10.3389/fpls.2022.1052263

Minton KW (1994) DNA repair in the extremely radioresistant bacterium Deinococcus radiodurans. Mol Microbiol 13(1):9–15. https://doi.org/10.1111/j.1365-2958.1994.tb00397.x

Miranda RDQ, Correia RM, de Almeida-Cortez JS, Pompelli MF (2014) Germination of Prosopis juliflora (Sw.) D.C. seeds at different osmotic potentials and temperatures. Plant Species Biology 29(3):E9–E20. https://doi.org/10.1111/1442-1984.12025

Mishra D, Chitara MK, Negi S, Pal singh J, Kumar R, Chaturvedi P (2023) Biosynthesis of Zinc Oxide Nanoparticles via Leaf Extracts of Catharanthus roseus (L.) G. Don and Their Application in Improving Seed Germination Potential and Seedling Vigor of Eleusine coracana (L.) Gaertn. Advances in Agriculture 2023(1):7412714. https://doi.org/10.1155/2023/7412714

Moliné M, Flores MR, Libkind D, Diéguez M del C, Farías ME, Broock M van (2010) Photoprotection by carotenoid pigments in the yeast Rhodotorula mucilaginosa: the role of torularhodin. Photochem Photobiol Sci 9(8):1145–1151. https://doi.org/10.1039/C0PP00009D

Mondal S, Bose B, Mondal S, Bose B (2021) Seed Priming: An Interlinking Technology between Seeds, Seed Germination and Seedling Establishment. In: Plant Reproductive Ecology - Recent Advances. IntechOpen

Mongodin EF, Shapir N, Daugherty SC, DeBoy RT, Emerson JB, Shvartzbeyn A, Radune D, Vamathevan J, Riggs F, Grinberg V, Khouri H, Wackett LP, Nelson KE, Sadowsky MJ (2006) Secrets of Soil Survival Revealed by the Genome Sequence of Arthrobacter aurescens TC1. PLOS Genetics 2(12):e214. https://doi.org/10.1371/journal.pgen.0020214

Moradtalab N, Ahmed A, Geistlinger J, Walker F, Höglinger B, Ludewig U, Neumann G (2020) Synergisms of Microbial Consortia, N Forms, and Micronutrients Alleviate Oxidative Damage and Stimulate Hormonal Cold Stress Adaptations in Maize. Front Plant Sci 11. https://doi.org/10.3389/fpls.2020.00396

Moura JB, Delforno TP, do Prado PF, Duarte IC (2021) Extremophilic taxa predominate in a microbial community of photovoltaic panels in a tropical region. FEMS Microbiology Letters 368(16):fnab105. https://doi.org/10.1093/femsle/fnab105

Muhae-Ud-Din G, Abid R, Ghorbani A, Atta S, Yong W (2025) Bacillus velezensis and Zinc Oxide Nanoparticles in Suppressing Colletotrichum capsici-Induced Anthracnose Disease in Chili: Mechanistic Insights Into Antioxidant System and Plant Growth. Physiologia Plantarum 177(3):e70330. https://doi.org/10.1111/ppl.70330

Muhammad A, Kong X, Zheng S, Bai N, Li L, Khan MHU, Fiaz S, Zhang Z (2024) Exploring plant-microbe interactions in adapting to abiotic stress under climate change: a review. Front Plant Sci 15. https://doi.org/10.3389/fpls.2024.1482739

Mushtaq NU, Alghamdi KM, Saleem S, Tahir I, Bahieldin A, Henrissat B, Alghamdi MK, Rehman RU, Hakeem KR (2023) Exogenous zinc mitigates salinity stress by stimulating proline metabolism in proso millet (Panicum miliaceum L.). Front Plant Sci 14. https://doi.org/10.3389/fpls.2023.1053869

Muthukrishanan G, Munisamy J, Gopalasubramaniam SK, Subramanian KS, Dharmaraj R, Nath DJ, Dutta P, Devarajan AK (2024) Impact of foliar application of phyllosphere yeast strains combined with soil fertilizer application on rice growth and yield. Environmental Microbiome 19(1):102. https://doi.org/10.1186/s40793-024-00635-9

Mutungi PM, Wekesa VW, Onguso J, Kanga E, Baleba SBS, Boga HI (2022) Culturable Bacterial Endophytes Associated With Shrubs Growing Along the Draw-Down Zone of Lake Bogoria, Kenya: Assessment of Antifungal Potential Against Fusarium solani and Induction of Bean Root Rot Protection. Front Plant Sci 12. https://doi.org/10.3389/fpls.2021.796847

Nowicki M, Nowakowska M, Nowak K, Szczechura W, Kaminski P (2025) Seed priming and abiotic stress tolerance in carrot: Unraveling the mechanisms of improved germination. PLOS ONE 20(2):e0318753. https://doi.org/10.1371/journal.pone.0318753

Núñez M, Naciff A, Cuadros F, Rojas C, Carvallo G, Yáñez C (2025) Adapting to UV: Integrative Genomic and Structural Analysis in Bacteria from Chilean Extreme Environments. International Journal of Molecular Sciences 26(12):5842. https://doi.org/10.3390/ijms26125842

O'Callaghan M (2016) Microbial inoculation of seed for improved crop performance: issues and opportunities. Appl Microbiol Biotechnol 100(13):5729–5746. https://doi.org/10.1007/s00253-016-7590-9

Ochoa-Chaparro EH, Patiño-Cruz JJ, Anchondo-Páez JC, Pérez-Álvarez S, Chávez-Mendoza C, Castruita-Esparza LU, Márquez EM, Sánchez E (2025) Seed Nanopriming with ZnO and SiO2 Enhances Germination, Seedling Vigor, and Antioxidant Defense Under Drought Stress. Plants 14(11):1726. https://doi.org/10.3390/plants14111726

Okabe S, Kamizono A, Zhang L, Kawasaki S, Kobayashi K, Oshiki M (2024) Salinity Tolerance and Osmoadaptation Strategies in Four Genera of Anammox Bacteria: Brocadia, Jettenia, Kuenenia, and Scalindua. Environ Sci Technol 58(12):5357–5371. https://doi.org/10.1021/acs.est.3c07324

Okon OG (2025) Mitigating plant environmental stressors: Exploring sustainable and eco-friendly solutions. Journal of Plant Stress Physiology :19–25. https://doi.org/10.25081/jpsp.2025.v11.9126

Oren A, Gunde-Cimerman N (2007) Mycosporines and mycosporine-like amino acids: UV protectants or multipurpose secondary metabolites? FEMS Microbiol Lett 269(1):1–10. https://doi.org/10.1111/j.1574-6968.2007.00650.x

Pereira A (2016) Plant Abiotic Stress Challenges from the Changing Environment. Front Plant Sci 7. https://doi.org/10.3389/fpls.2016.01123

Pereira MF, Silva-Neta AR, Farias AFF, Souza AG, Fonseca MG, Pontes LFBL, Santos IMG (2017) Pure and Al-doped ZnO obtained by the modified Pechini method applied in ethanolic transesterification of cottonseed oil. Cerâmica 63:82–89. https://doi.org/10.1590/0366-69132017633652066

Pérez V, Hengst M, Kurte L, Dorador C, Jeffrey WH, Wattiez R, Molina V, Matallana-Surget S (2017) Bacterial Survival under Extreme UV Radiation: A Comparative Proteomics Study of Rhodobacter sp., Isolated from High Altitude Wetlands in Chile. Front Microbiol 8. https://doi.org/10.3389/fmicb.2017.01173

Pezzoni M, Pizarro RA, Costa CS (2018) Exposure to low doses of UVA increases biofilm formation in Pseudomonas aeruginosa. Biofouling 34(6):673–684. https://doi.org/10.1080/08927014.2018.1480758

Porcar M, Louie KB, Kosina SM, Van Goethem MW, Bowen BP, Tanner K, Northen TR (2018) Microbial Ecology on Solar Panels in Berkeley, CA, United States. Front Microbiol 9. https://doi.org/10.3389/fmicb.2018.03043

Prisa D, Fresco R, Spagnuolo D (2023) Microbial Biofertilisers in Plant Production and Resistance: A Review. Agriculture 13(9):1666. https://doi.org/10.3390/agriculture13091666

Pulschen AA, Rodrigues F, Duarte RTD, Araujo GG, Santiago IF, Paulino-Lima IG, Rosa CA, Kato MJ, Pellizari VH, Galante D (2015a) UV-resistant yeasts isolated from a high-altitude volcanic area on the Atacama Desert as eukaryotic models for astrobiology. MicrobiologyOpen 4(4):574–588. https://doi.org/10.1002/mbo3.262

Pulschen AA, Rodrigues F, Duarte RTD, Araujo GG, Santiago IF, Paulino-Lima IG, Rosa CA, Kato MJ, Pellizari VH, Galante D (2015b) UV-resistant yeasts isolated from a high-altitude volcanic area on the Atacama Desert as eukaryotic models for astrobiology. Microbiologyopen 4(4):574–588. https://doi.org/10.1002/mbo3.262

Raklami A, Babalola OO, Jemo M, Nafis A (2024) Unlocking the plant growth-promoting potential of yeast spp.: exploring species from the Moroccan extremophilic environment for enhanced plant growth and sustainable farming. FEMS Microbiol Lett 371:fnae015. https://doi.org/10.1093/femsle/fnae015

Ramijan K, Ultee E, Willemse J, Zhang Z, Wondergem JAJ, van der Meij A, Heinrich D, Briegel A, van Wezel GP, Claessen D (2018) Stress-induced formation of cell wall-deficient cells in filamentous actinomycetes. Nat Commun 9(1):5164. https://doi.org/10.1038/s41467-018-07560-9

Ramos LTS, Borges SS, Cunha S, Mesquita PRR, Nascimento MM, Silva LA (2025) Green Synthesis of Zinc Oxide Using Oil Palm Leaf Extract for the Photocatalytic Degradation of Amoxicillin. Waste Biomass Valor. https://doi.org/10.1007/s12649-025-03427-5

Ramzan M, Parveen M, Naz G, Sharif HMA, Nazim M, Aslam S, Hussain A, Rahimi M, Alamer KH (2024) Enhancing physio-biochemical characteristics in okra genotypes through seed priming with biogenic zinc oxide nanoparticles synthesized from halophytic plant extracts. Sci Rep 14(1):23753. https://doi.org/10.1038/s41598-024-74129-6

Rawashdeh RY, Harb AM, AlHasan AM (2020) Biological interaction levels of zinc oxide nanoparticles; lettuce seeds as case study. Heliyon 6(5):e03983. https://doi.org/10.1016/j.heliyon.2020.e03983

Raza SH, Shahzadi A, Iqbal M, Shafiq F, Mahmood A, Anwar S, Ashraf M (2022) Foliar application of nano-zinc oxide crystals improved zinc biofortification in cauliflower (Brassica oleracea L. var. botrytis). Appl Nanosci 12(6):1803–1813. https://doi.org/10.1007/s13204-022-02455-0

Rebelo Romão I, Rodrigues dos Santos AS, Velasco L, Martínez-Ferri E, Vilchez JI, Manzanera M (2022) Seed-Encapsulation of Desiccation-Tolerant Microorganisms for the Protection of Maize from Drought: Phenotyping Effects of a New Dry Bioformulation. Plants 11(8):1024. https://doi.org/10.3390/plants11081024

Rhaman MS (2025) Seed Priming Before the Sprout: Revisiting an Established Technique for Stress-Resilient Germination. Seeds 4(3):29. https://doi.org/10.3390/seeds4030029

Rizk R, Ahmed M, Abdul-Hamid D, Zedan M, Tóth Z, Decsi K (2025) Resulting Key Physiological Changes in Triticum aestivum L. Plants Under Drought Conditions After Priming the Seeds with Conventional Fertilizer and Greenly Synthesized Zinc Oxide Nanoparticles from Corn Wastes. Agronomy 15(1):211. https://doi.org/10.3390/agronomy15010211

Rodrigues ES, Silva MS, Azevedo WM, Feitosa SS, Stingl A, Farias PMA (2019) ZnO nanoparticles with tunable bandgap obtained by modified Pechini method. Appl Phys A 125(8):504. https://doi.org/10.1007/s00339-019-2805-4

Safaeipour M, Kalat M, Shahverdi M (2023) Assessing the impact of seed priming by nanomaterials on stevia germination and biochemical attributes under drought stress. Fundam Appl Agric 8(3):615. https://doi.org/10.5455/faa.160768

Saravanan M, Gopinath V, Chaurasia MK, Syed A, Ameen F, Purushothaman N (2018) Green synthesis of anisotropic zinc oxide nanoparticles with antibacterial and cytofriendly properties. Microbial Pathogenesis 115:57–63. https://doi.org/10.1016/j.micpath.2017.12.039

Selim S, Hassan YM, Saleh AM, Habeeb TH, AbdElgawad H (2019) Actinobacterium isolated from a semi-arid environment improves the drought tolerance in maize (*Zea mays* L.). Plant Physiology and Biochemistry 142:15–21. https://doi.org/10.1016/j.plaphy.2019.06.029

Sen D, Paul K, Saha C, Mukherjee G, Nag M, Ghosh S, Das A, Seal A, Tripathy S (2019) A unique life-strategy of an endophytic yeast Rhodotorula mucilaginosa JGTA-S1—a comparative genomics viewpoint. DNA Res 26(2):131–146. https://doi.org/10.1093/dnares/dsy044

Sena EMN de, Silva FFS da, Silva J de J, Gomes RA, Pelacani CR, Dantas BF (2023) Germination niche of a neotropical dry forest species: seed osmotic stress and recovery. J Seed Sci 45:e202345028. https://doi.org/10.1590/2317-1545v45272288

Sghayar S, Debez A, Lucchini G, Abruzzese A, Zorrig W, Negrini N, Morgutti S, Abdelly C, Sacchi GA, Pecchioni N, Vaccino P (2023) Seed priming mitigates high salinity impact on germination of bread wheat (Triticum aestivum L.) by improving carbohydrate and protein mobilization. Plant Direct 7(6):e497. https://doi.org/10.1002/pld3.497

Shafiq T, Yasmin H, Shah ZA, Nosheen A, Ahmad P, Kaushik P, Ahmad A (2022) Titanium Oxide and Zinc Oxide Nanoparticles in Combination with Cadmium Tolerant Bacillus pumilus Ameliorates the Cadmium Toxicity in Maize. Antioxidants 11(11):2156. https://doi.org/10.3390/antiox11112156

Sharma V, Sharma JK, Kansay V, Sharma VD, Sharma A, Kumar S, Sharma AK, Bera MK (2023) The effect of calcination temperatures on the structural and optical properties of zinc oxide nanoparticles and their influence on the photocatalytic degradation of leather dye. Chemical Physics Impact 6:100196. https://doi.org/10.1016/j.chphi.2023.100196

Sherzad Z, Nawakht NA, Sherzad F (2025) Plant growth-promoting endophytic bacteria: a sustainable solution for climate change and environmental stresses in agriculture. Discov Appl Sci 7(8):894. https://doi.org/10.1007/s42452-025-07123-w

Shoukat A, Maryam U, Pitann B, Zafar MM, Nawaz A, Hassan W, Seleiman MF, Saqib ZA, Mühling KH (2025) Efficacy of Nano and Conventional Zinc and Silicon Fertilizers for Nutrient Use Efficiency and Yield Benefits in Maize Under Saline Field Conditions. Plants 14(5):673. https://doi.org/10.3390/plants14050673

Sibanda T, Selvarajan R, Reinhold-Hurek B (2024) Enhancing Crop Resilience to Drought and Salinity: the Potential Role of Extremophiles in Mitigating Food Insecurity in Sub-Saharan Africa. Journal of Crop Health 77(1):17. https://doi.org/10.1007/s10343-024-01090-9

Silva MF da, Araújo EF, Silva LJ da, Amaro HTR, Dias LA dos S, Dias DCF dos S (2019) Tolerance of crambe (*Crambe abyssinica* Hochst) to salinity and water stress during seed germination and initial seedling growth. Ciênc agrotec 43:e025418. https://doi.org/10.1590/1413-7054201943025418

Singh A, Rajput VD, Lalotra S, Agrawal S, Ghazaryan K, Singh J, Minkina T, Rajput P, Mandzhieva S, Alexiou A (2024) Zinc oxide nanoparticles influence on plant tolerance to salinity stress: insights into physiological, biochemical, and molecular responses. Environ Geochem Health 46(5):148. https://doi.org/10.1007/s10653-024-01921-8

Singh A, Sengar RS, Rajput VD, Minkina T, Singh RK (2022) Zinc Oxide Nanoparticles Improve Salt Tolerance in Rice Seedlings by Improving Physiological and Biochemical Indices. Agriculture 12(7):1014. https://doi.org/10.3390/agriculture12071014

Singh P, Vaishnav A, Liu H, Xiong C, Singh HB, Singh BK (2023) Seed biopriming for sustainable agriculture and ecosystem restoration. Microbial Biotechnology 16(12):2212–2222. https://doi.org/10.1111/1751-7915.14322

Soni R, Prakash G, Sharma S, Sinha D, Mishra R (2023) Role of microbes in alleviating abiotic stress in plants. Plant Science Today 10(3):160–187. https://doi.org/10.14719/pst.2215

Srinivasan S (2024) Radiation-Tolerant Fibrivirga spp. from Rhizosphere Soil: Genome Insights and Potential in Agriculture. Genes 15(8):1048. https://doi.org/10.3390/genes15081048

Straková D, Sánchez-Porro C, de la Haba RR, Ventosa A (2025) Strategies of Environmental Adaptation in the Haloarchaeal Genera Haloarcula and Natrinema. Microorganisms 13(4):761. https://doi.org/10.3390/microorganisms13040761

Strekalovskaya EI, Perfileva AI, Krutovsky KV (2024) Zinc Oxide Nanoparticles in the "Soil–Bacterial Community–Plant" System: Impact on the Stability of Soil Ecosystems. Agronomy 14(7):1588. https://doi.org/10.3390/agronomy14071588

Suneja Y, Gupta AK, Bains NS (2019) Stress Adaptive Plasticity: Aegilops tauschii and Triticum dicoccoides as Potential Donors of Drought Associated Morpho-Physiological Traits in Wheat. Front Plant Sci 10. https://doi.org/10.3389/fpls.2019.00211

Tanner K, Martí JM, Belliure J, Fernández-Méndez M, Molina-Menor E, Peretó J, Porcar M (2018) Polar solar panels: Arctic and Antarctic microbiomes display similar taxonomic profiles. Environmental Microbiology Reports 10(1):75–79. https://doi.org/10.1111/1758-2229.12608

Tanner K, Martorell P, Genovés S, Ramón D, Zacarías L, Rodrigo MJ, Peretó J, Porcar M (2019) Bioprospecting the Solar Panel Microbiome: High-Throughput Screening for Antioxidant Bacteria in a Caenorhabditis elegans Model. Front Microbiol 10:986. https://doi.org/10.3389/fmicb.2019.00986

Tanner K, Molina-Menor E, Latorre-Pérez A, Vidal-Verdú À, Vilanova C, Peretó J, Porcar M (2020) Extremophilic microbial communities on photovoltaic panel surfaces: a two-year study. Microbial Biotechnology 13(6):1819–1830. https://doi.org/10.1111/1751-7915.13620

Tao Q, Xing J, Meng F, Zhang Y, Liu X, Guo S, Shan Y, Zhong S, Sun J, Zhao Y (2024) Siberian Wildrye (Elymus sibiricus) Seed Vigor Estimation for the Prediction of Emergence Performance under Diverse Environmental Conditions. Agronomy 14(1):173. https://doi.org/10.3390/agronomy14010173

Teiba II, El-Bilawy EH, Elsheery NI, Rastogi A (2024) Microbial Allies in Agriculture: Harnessing Plant Growth-Promoting Microorganisms as Guardians against Biotic and Abiotic Stresses. Horticulturae 10(1):12. https://doi.org/10.3390/horticulturae10010012

Tkáčová J, Čaplová J, Klempová T, Čertík M (2017) Correlation between lipid and carotenoid synthesis in torularhodin-producing Rhodotorula glutinis. Ann Microbiol 67(8):541–551. https://doi.org/10.1007/s13213-017-1284-0

Tokarz B, Wójtowicz T, Makowski W, Jędrzejczyk RJ, Tokarz KM (2020) What is the Difference between the Response of Grass Pea (Lathyrus sativus L.) to Salinity and Drought Stress?—A Physiological Study. Agronomy 10(6):833. https://doi.org/10.3390/agronomy10060833

Torkzadeh H, Zodrow KR, Bridges WC, Cates EL (2021) Quantification and modeling of the response of surface biofilm growth to continuous low intensity UVC irradiation. Water Res 193:116895. https://doi.org/10.1016/j.watres.2021.116895

Tripathi JM, Khan BR, Gaur R, Yadav D, Verma KK, Gupta R (2025) Gibberellic Acid Improves Photosynthetic Electron Transport and Stomatal Function in Crops That Are Adversely Affected by Salinity Exposure. Plants 14(21):3388. https://doi.org/10.3390/plants14213388

Trzcińska-Wencel J, Wypij M, Terzyk AP, Rai M, Golińska P (2023) Biofabrication of novel silver and zinc oxide nanoparticles from Fusarium solani IOR 825 and their potential application in agriculture as biocontrol agents of phytopathogens, and seed germination and seedling growth promoters. Front Chem 11. https://doi.org/10.3389/fchem.2023.1235437

Uçarlı C (2020) Effects of Salinity on Seed Germination and Early Seedling Stage. In: Abiotic Stress in Plants. IntechOpen

Valliere JM, Wong WS, Nevill PG, Zhong H, Dixon KW (2020) Preparing for the worst: Utilizing stress-tolerant soil microbial communities to aid ecological restoration in the Anthropocene. Ecological Solutions and Evidence 1(2):e12027. https://doi.org/10.1002/2688-8319.12027

Verma KK, Joshi A, Song X-P, Singh S, Kumari A, Arora J, Singh SK, Solanki MK, Seth CS, Li Y-R (2024) Synergistic interactions of nanoparticles and plant growth promoting rhizobacteria enhancing soil-plant systems: a multigenerational perspective. Front Plant Sci 15. https://doi.org/10.3389/fpls.2024.1376214

Vílchez JI, García-Fontana C, Román-Naranjo D, González-López J, Manzanera M (2016) Plant Drought Tolerance Enhancement by Trehalose Production of Desiccation-Tolerant Microorganisms. Front Microbiol 7. https://doi.org/10.3389/fmicb.2016.01577

Villarreal P, Carrasco M, Barahona S, Alcaíno J, Cifuentes V, Baeza M (2016) Tolerance to Ultraviolet Radiation of Psychrotolerant Yeasts and Analysis of Their Carotenoid, Mycosporine, and Ergosterol Content. Curr Microbiol 72(1):94–101. https://doi.org/10.1007/s00284-015-0928-1

Wang Y, Jie W, Peng X, Hua X, Yan X, Zhou Z, Lin J (2019) Physiological Adaptive Strategies of Oil Seed Crop Ricinus communis Early Seedlings (Cotyledon vs. True Leaf) Under Salt and Alkali Stresses: From the Growth, Photosynthesis and Chlorophyll Fluorescence. Front Plant Sci 9. https://doi.org/10.3389/fpls.2018.01939

Wang Z, Wang S, Ma T, Liang Y, Huo Z, Yang F (2023) Synthesis of Zinc Oxide Nanoparticles and Their Applications in Enhancing Plant Stress Resistance: A Review. Agronomy 13(12):3060. https://doi.org/10.3390/agronomy13123060

Wankhade A, Wilkinson E, Britt DW, Kaundal A (2025) A Review of Plant–Microbe Interactions in the Rhizosphere and the Role of Root Exudates in Microbiome Engineering. Applied Sciences 15(13):7127. https://doi.org/10.3390/app15137127

Weissman J, Fagan WF, Johnson PLF (2019) Linking high GC content to the repair of double strand breaks in prokaryotic genomes. PLoS Genet 15(11):e1008493. https://doi.org/10.1371/journal.pgen.1008493

Win PP, Park H-H, Kuk Y-I (2025) Integrated Approach of Using Biostimulants for Improving Growth, Physiological Traits, and Tolerance to Abiotic Stressors in Rice and Soybean. Agronomy 15(10):2265. https://doi.org/10.3390/agronomy15102265

Wu H, Zhang Z, Hu S, Yu J (2012) On the molecular mechanism of GC content variation among eubacterial genomes. Biol Direct 7:2. https://doi.org/10.1186/1745-6150-7-2

Yarzábal Rodríguez LA, Álvarez Gutiérrez PE, Gunde-Cimerman N, Ciancas Jiménez JC, Gutiérrez-Cepeda A, Ocaña AMF, Batista-García RA (2024) Exploring extremophilic fungi in soil mycobiome for sustainable agriculture amid global change. Nat Commun 15(1):6951. https://doi.org/10.1038/s41467-024-51223-x

Yin W, Wang Y, Liu L, He J (2019) Biofilms: The Microbial "Protective Clothing" in Extreme Environments. Int J Mol Sci 20(14):3423. https://doi.org/10.3390/ijms20143423

Zahra S, Bukhari H, Qaisar S, Sheikh A, Amin A (2022) Synthesis of nanosize zinc oxide through aqueous sol–gel route in polyol medium. BMC Chemistry 16(1):104. https://doi.org/10.1186/s13065-022-00900-3

Zannier F, Portero LR, Douki T, Gärtner W, Farías ME, Albarracín VH (2022) Proteomic Signatures of Microbial Adaptation to the Highest Ultraviolet-Irradiation on Earth: Lessons From a Soil Actinobacterium. Front Microbiol 13. https://doi.org/10.3389/fmicb.2022.791714

Zenteno-Alegría CO, Yarzábal Rodríguez LA, Ciancas Jiménez J, Álvarez Gutiérrez PE, Gunde-Cimerman N, Batista-García RA (2024) Fungi beyond limits: The agricultural promise of extremophiles. Microbial Biotechnology 17(3):e14439. https://doi.org/10.1111/1751-7915.14439

Zhai J, Xian X, Zhang Z, Wang Y (2025) Nano-Zinc Oxide Can Enhance the Tolerance of Apple Rootstock M9-T337 Seedlings to Saline Alkali Stress by Initiating a Variety of

Physiological and Biochemical Pathways. Plants 14(2):233. https://doi.org/10.3390/plants14020233

Zhang Y, Ren H, Zhang G (2014) Microbacterium hydrothermale sp. nov., an actinobacterium isolated from hydrothermal sediment. International Journal of Systematic and Evolutionary Microbiology 64(Pt_10):3508–3512. https://doi.org/10.1099/ijs.0.061697-0

Zhang Z, Tariq A, Zeng F, Graciano C, Zhang B (2020) Nitrogen application mitigates drought-induced metabolic changes in *Alhagi sparsifolia* seedlings by regulating nutrient and biomass allocation patterns. Plant Physiology and Biochemistry 155:828–841. https://doi.org/10.1016/j.plaphy.2020.08.036